RELAY FEEDBACK METHOD FOR PROCESS MODELLING

UTKAL V. MEHTA

DEPARTMENT OF ELECTRONICS AND ELECTRICAL ENGINEERING

INDIAN INSTITUTE OF TECHNOLOGY GUWAHATI

GUWAHATI - 781039, ASSAM, INDIA

RELAY FEEDBACK METHOD FOR PROCESS MODELLING

A

Thesis Submitted

in Partial Fulfilment of the Requirements

for the Degree of

DOCTOR OF PHILOSOPHY

By

UTKAL V. MEHTA

Department of Electronics and Electrical Engineering

Indian Institute of Technology Guwahati

Guwahati - 781 039, INDIA.

August, 2011

Certificate

This is to certify that the thesis entitled "**RELAY FEEDBACK METHOD FOR PROCESS MODELLING**", submitted by **Utkal V. Mehta** (08610210), a research scholar in the *Department of Electronics & Electrical Engineering, Indian Institute of Technology Guwahati*, for the award of the degree of **Doctor of Philosophy**, is a record of an original research work carried out by him under my supervision and guidance. The thesis has fulfilled all requirements as per the regulations of the institute and in my opinion has reached the standard needed for submission. The results embodied in this thesis have not been submitted to any other University or Institute for the award of any degree or diploma.

Dated:

Guwahati.

Prof. Somanath Majhi
Dept. of Electronics & Electrical Engg.
Indian Institute of Technology Guwahati
Guwahati - 781039, Assam, India.

Acknowledgements

I would like to express my sincere gratitude to my supervisor, Prof. Somanath Majhi, for his excellent guidance and support throughout the course for this work. My heartfelt thanks to him for the unlimited support and patience shown to me. I would particularly like to thank for all his help in patiently and carefully correcting all my manuscripts.

I would like to thank my doctoral committee members Dr. C. Mahanta, Dr. H. B. Nemade and Prof. S. K. Dwivedy for sparing their precious time to evaluate the progress of my work. Their suggestions have been valuable. I would also like to thank other faculty members for their kind help carried out during my academic studies. My special thanks to Mr. Sanjib, Mr. Sidananda, Mr. Goswami and all the members of the Control & Instrumentation Laboratory for maintaining an excellent computing facility and providing various resources useful for the research work.

I had a great time with my many friends at IITG, including (but not limited to) Sanjoy, Dola, Shyam, Maheto, Rupaban and Narasimhamurthy. I thank them for their support and encouragement. The company of my friend Ali at IITG proved to be a great asset which helped me stay relaxed during throughout my research. The energetic company of Senthil helped me tackle several problems.

Among those deserving of a special mention is my wife Dr. Yogi, who had extended their wholeheartedly support to bring this work into existence. She has been able to take care of my daughter extremely well. I thank my daughter Aastha for keeping me energetic and reducing my worries. Again, I am grateful to my parents, in-laws, sisters and brothers, whose love and encouragement made this research possible.

I also grateful acknowledge AICTE, Govt. of India for financing my studies under QIP scheme at IIT Guwahati. Finally, I would like to thank the Almighty God for bestowing me this opportunity and showering his blessings on me to come out successful against all odds.

(Utkal V. Mehta)

Abstract

From a practical and simplicity point of views, the relay feedback identification is extended to the various fields of process control industries. The proposed techniques yield significantly improved accuracy over the conventional relay feedback method by deriving the explicit expressions for unknown process model parameters in terms of the output limit cycle data. A relay with hysteresis instead of an ideal relay is used in all the identification procedures to make the resultant system less sensitive to measurement noise. Next, the applicability of the relay feedback is shown by identifying nonlinear processes with static nonlinearities. On-line identification and tuning are major design objectives to achieve for certain critical applications. The modification is done by adding a relay in parallel to the controller to induce a limit cycle oscillation without breaking the closed-loop control. Based on half limit cycle data, a systematic procedure is developed to estimate a low order transfer function model. To obtain the optimum control input variations, the controller tuning rules are derived from the time weighted integral performance criteria. In addition, the necessary condition for the existence of the limit cycle for unstable processes are obtained for first and second order process models. Finally, a simple control strategy is given to induce a sustained limit cycle oscillation where the conventional relay feedback fails for unstable processes with large time delay. All the above benefits are achieved at no significant incremental costs in terms of implementation resources and application complexities. Both simulation examples and laboratory tests are furnished to illustrate the effectiveness of the proposed approaches.

CONTENTS

LIST OF FIGURES

LIST OF TABLES

NOMENCLATURE

DFA	Describing function approximation
FOPDT	First order plus time delay process model
FPAA	Field programmable analog array
ISE	Integral of error squared
ISTE	Integral of time error squared
ITAE	Integral of time weighted absolute error
PCS	Process Control Simulator
PD	Proportional derivative controller
PID	Proportional integral derivative controller
PI-PD	Proportional integral - proportional derivative controller
SG	Saviztky-Golay filter
SOPDT	Second order plus time delay process model

MATHEMATICAL NOTATIONS

k	Steady state gain of a process
θ	Time delay of a process
θ_n	Normalised dead time of a process
τ, τ_1, τ_2	Time constants of a process model transfer function
K_c	Proportional gain
K_i	Integral gain
K_d	Derivative gain
T_i	Integral time constant
T_d	Derivative time constant
h	Amplitude of a relay
ε	Hysteresis of a relay
A_1, A_2	Peak amplitude of limit cycle output
T	Half period of symmetrical limit cycle output
T_p	Time period of limit cycle oscillation
t_p	Time at which peak amplitude of limit cycle occurs after zero crossing
a_u	Area of the process input signal over one time period
$y(t)$	Output signal
$u(t)$	Control input
$r(t)$	Set-point / reference input
$e(t)$	Error signal
L	Static load disturbance at the input of a process
N	Measurement noise introduced by a sensor

t	Time
$G_p(s)$	Transfer function of a process
$C(s)$	Transfer function of a controller
$f(*)$	Static nonlinear function
D_r	Describing function of the relay

LIST OF PUBLICATIONS

Journal Publications

1. Mehta U. and Majhi S., "On-line relay test for automatic tuning of PI controllers for stable processes, *Trans. Inst. Meas. Control*, Ref. No.: TIMC-11-0073, (accepted)

2. Mehta U. and Majhi S., "On-line identification of cascade control systems based on half limit cycle data", *ISA Transactions, Elsevier*, vol. 50(3), 473-478, 2011

3. Mehta U. and Majhi S., "Identification of a class of Wiener and Hammerstein-type non-linear processes with monotonic static gains", *ISA Transactions, Elsevier*, vol. 49(4), 501-509, 2010.

4. Mehta U. and Majhi S., "Estimation of process model parameters based on half limit cycle data", *Journal of Systems Science and Engineering*, vol. 17(2), 13-21, 2008.

Conference Publications

1. Mehta, U. and Majhi, S.,"On-line identification and control methods for PID controllers", *IEEE ICARCV 2010*, Singapore, 2010.

2. Mehta, U. and Majhi, S.,"An online relay feedback scheme for cascade control systems", *34th NSC*, Surathkal, India, 2010.

3. Mehta, U. and Majhi, S.,"Modeling and control of nonlinear systems with input monotonic gains", *IEEE INDICON*, Kolkata, India, 2010

4. Mehta, U. and Majhi, S.,"Autotuning of PI controller for an unstable FOPDT process", *CERA09*, IIT Roorkee, India, 2010

5. Mehta U. and Majhi S., "Identification of a class of nonminimum phase processes using relay feedback", *Joint Int. Conf. on Applied Systems Research and NSC*, Agra, India, 2009.

6. Mehta U. and Majhi S., "Adaptive relay based identification and control of Hammerstein-type nonlinear processes", *IEEE INDICON*, IIT Kanpur, India, 2008.

7. Mehta U. and Majhi S., "Identification and control of Wiener-type nonlinear processes", *NSC*, IIT Roorkee, India, 2008.

CHAPTER 1

INTRODUCTION

1.1 Research Background

Relay feedback techniques are very appealing to perform identification of processes for control purposes; being fast and easy to use, they can be frequently repeated for all the situations where there is lack of knowledge about a process to build a mathematical model. Various aspects of the relay feedback are discussed in [1–3]. Some of the distinct advantages of the relay feedback are given below:

1. It identifies process information around the important frequency, the ultimate frequency (the frequency where the phase angle is $-\pi$).

2. It is a closed-loop test; therefore, the process will not drift away from the nominal operating point.

3. For processes with a long time constant, it is a more time-efficient method than conventional step or pulse testing. The experimental time is roughly equal to two to four times the ultimate period.

This method has been subject of much interests in recent years and it has been field tested in a wide range of applications.

A. Process identification

In the early eighties, Åström and Hägglund [4] proposed the use of relay feedback combined with a describing function approximation (DFA) as a simple means to determine the ultimate gain and ultimate frequency. The key idea behind this work was that the relay experiment can be used as a mean to automatically excite a process at its critical frequency. When combined with the DFA, the relay proved to be a very efficient way to obtain process information that could be directly applied to proportional-integral-derivative (PID) controller design. Since 1984, many variations and refinements to the original method have been developed and used in a number of applications, including auto-tuning of PID and process identification. Based on the frequency domain describing function approach, many methods have been reported [5–13] with improved accuracy to estimate process transfer function models. The literature on relay feedback applications relies almost exclusively upon the use of the DFA, which estimates a single frequency response point based on the assumption that the relay data has a dominant first harmonic component. A direct consequence of this limited information is that applications have been restricted to certain control strategies (eg. PID tuning using specified gain/phase margins). Moreover, the frequency response at the single point, the ultimate frequency, is insufficient to determine transfer function model with three or more parameters.

While many of the relay auto-tuning methods use the DFA to a relay in their analysis, a very few have applied the exact relay feedback expressions in time-domain analysis. Wang et al. [14] used a time-domain approach to obtain the exact expressions for the limit cycle waveform for a first order plus dead time (FOPDT) transfer function model. Wang et al. [15] proposed a mechanism to combine a relay plus integrator to generate a multifrequency excitation signal based on which a step response model was identified. But, some additional test or prior knowledge of the system is needed to enable and complete the modelling. Majhi and Atherton [16] and Majhi [17, 18] developed relay identification algorithms for the general model structure using a state-space approach. Another improved identification algorithms using the Fourier or Laplace transform for the relay response have been reported by Ramakrishnan and Chidambaram [9]

and Vivek and Chidambaram [19]. Panda and Yu [20, 21] have improved auto-tuning using shape factor of relay feedback response to estimate unknown process model parameters, but requires to solve simultaneous set of equations. The enhance identification performance using integrals of the relay response instead of the point data has been achieved in [22]. However, the method is not only iterative but also requires more data measurements for identification. Recently in [23, 24], based on Fourier/Laplace transform of the relay response, a frequency response algorithm is developed for estimating the multiple frequency response points of the process with the help of the iterative method and suitable initial guesses.

B. Extension to nonlinear processes

When nonlinearities in processes are so severe that their linear approximations are not acceptable, nonlinear models should be considered to describe the nonlinear dynamics. For this, block-oriented nonlinear models that consist of linear dynamic subsystem and memoryless nonlinear static functions such as Wiener, Hammerstein and Hammerstein-Wiener models have been often used because of their simple structure [25]. These particular types of nonlinear models can describe the nonlinear dynamics of many chemical, electrical and biological processes. Most relay based reported methods show significant improvements in identification of the linear process models but not the nonlinear process models. Some researchers have exerted efforts in developing relay based nonlinear process identification methods to overcome the limitations of the linear approaches.

In [26, 27], repetitive relay tests were developed with different relay heights and dynamic elements inserted in the control loop to determine the Hammerstein-type process. Huang et al. [28] proposed an optimizing algorithm using optimal parameter vectors to estimate the static nonlinearity in the Wiener-type process models. Basic conventional approach to classify and identify nonlinear processes using two consecutive relay tests has been proposed by Huang et al. [29]. An optimization procedure to obtain symmetric limit cycle output [27] and a nonlinear control strategy to compensate the nonlinear dynamics [30], were presented based on a relay

feedback test. Park et al. [31] proposed identification of Hammerstein-type processes using a triangular input signal. Lee et al. [32] identified nonlinear process via an iterative procedure with use of an adjustable PI controller. Sung [33] proposed an estimation method for nonlinear static gains using a random binary signal that deactivate the effects of nonlinear gains. Jeng et al.'s [34] method used a systematic approach to identify nonlinear processes with an integrator in the loop. Recently, a new relay feedback method [35], has been proposed to guarantee symmetric responses under static nonlinearity and static disturbances. It can be successfully applied to identify nonlinear processes. A method based on least squares optimization [36] was reported to estimate the static nonlinearity in the Wiener-type process using two step inputs with different widths and amplitudes. The enhanced activation method [37] gave the nonlinear process model parameters in an optimal way by solving a constrained nonlinear optimization procedure.

For noisy environments, all previous methods [27–35, 37, 38] suffer from a relay chattering since they use an ideal relay instead of a relay with hysteresis thereby limiting the practical applicability of their techniques. Moreover, the methods require either special test signals or iterative optimization procedures or a set of approximations to estimate the nonlinear process model parameters.

C. On-line automatic tuning of controllers

One of the main features of the relay auto-tuning method, which probably accounts for its success more than any other associated features, is that it is a closed-loop method [39]. However, the problem has not been fully solved that the loop must be opened and the process must be disturbed to conduct the relay test [40]. The basic conventional relay feedback has several important practical constraints, first, it has a sensitivity problem in the presence of disturbance signals, or equivalent ones arising from varying process dynamics, nonlinearities and uncertainties present in the process. An iterative solution [35, 41] has been proposed for small and constant disturbances by adjusting the relay bias until symmetrical limit cycle oscillations are

obtained. Secondly, the conventional relay feedback is an off-line tuning method, i.e. some information on the process is first extracted with the process under relay feedback and detached from the controller. The information is subsequently used to commission the controller. Off-line tuning affects the operational process regulation which may not be acceptable for certain critical applications. Indeed, in certain key process control areas such as vacuum control, environment control, it may be too expensive or dangerous for the control loop to be broken for tuning purposes. Therefore, the tuning under tight continuous closed-loop control (on-line) is necessary.

In [42], an on-line iterative approach was reported for closed-loop automatic tuning of the PID. But it has long experiment time, which may not be acceptable practically. The on-line tuning methods [40, 43] have been proposed to make them more effective than the basic relay auto-tuning method. The identification procedure in [40] is not straightforward and one needs to have prior knowledge about the system to decide about the suitable frequency response prototypes. Ho et al. [44] have presented relay auto-tuning of PID compensator for desired phase and bandwidth. The complexity of the method is apparent from computing the gradient of the quadratic criterion. The exact analytical method [45] has been proposed in which a relay is connected in series with a controller. Recently, on-line computing rules [46] were developed by introducing a relay with a pure time lag to find new PI and lead compensators based on specified gain and phase margins.

Through the past decades, numerous tuning methods have been proposed for standard controllers and processes modelled as a first order transfer function [47]. A recent survey [48] shows that the ratio of applications of PID control, conventional advanced control (feed forward, override, valve position control, gain-scheduled PID, etc.) and model predictive control is about 100 : 10 : 1. In addition, the vast majority of the PID controllers do not use derivative action. Even though the PI controller only has two adjustable parameters, it is not simple to find good settings and many controllers are poorly tuned. In [49], the approach has been given to look the quality of the control actions to preserve actuators from untimely attrition. In a real plant the controlled variables must be limited both in its amplitude (saturation bounds)

and in its dynamics (finite bandwidth of the actuators). In this context, less attention has been paid, although in [50, 51] the index has been introduced to measure the variations in the control signal and the criteria are presented, to give an excellent trade-off between robustness and performance.

D. Extension to cascade control systems

Cascade control is one of the most popular complex control structures that can be found in the process industries, implemented in order to improve the disturbance rejection properties of the controlled system [52]. The introduction and use of an additional sensor that allows for a separation of the fast and slow dynamics of the process results in a nested loop configuration. Each loop has associated with its corresponding PI/PID controller. The standard conventional approach of tuning these cascade controllers is often ineffective because it ignores strong interaction between the two loops. Therefore the tuning of a cascade control system in the conventional way is a fairly cumbersome and time consuming task. In view of its wide spread application, it would be very useful to realize the auto-tuning procedure which estimates both inner and outer process dynamics simultaneously.

In order to provide users with an effective aid in the design of the cascade control system, a relay feedback auto-tuning technique has been proposed in [53]. It basically consists of applying the typical relay feedback based auto-tuning to the two loops, sequentially as in the conventional approach. Thus, the procedure is time consuming. In order to avoid the sequential nature of the tuning procedure, a simultaneous on-line automatic tuning technique has been proposed in [54]. However, the experiment requires prior information of the process and the ultimate frequency used for outer loop design is based on initial ultimate frequency without considering changes in inner loop control parameters. Some reported methods [55, 56] for auto-tuning of cascade control are still based on an off-line relay test. Again the tuning methodology in [56] remains the sequential in nature. In [57], the tuning rules have been proposed to tune the primary and secondary controllers, but it has not been specified how the procedure can be

automated. An automatic tuning method in [58] for the cascade system requires an open-loop step test for estimation of process dynamics and command signal generator for setpoint tracking. An iterative method based on genetic algorithm [59] has been proposed for tuning cascade controllers, however the on-line experiment time is very long which may not be acceptable in practice. Recently, two-degrees of freedom design approach for a cascade control configuration [60] is reported by introducing additional parameters that need to be tuned appropriately. Tuning rules for parallel cascade control have been discussed in [61, 62] with prior information about the process dynamics in form of FOPDT models.

E. Relay feedback for unstable processes

The relay auto-tuning method is not applicable to certain class of processes which are not relay stabilizable, such as unstable processes and processes with more than one integrator [39,63]. For these processes, relay feedback does not induce a stable limit cycle sometimes. Again, the conventional relay feedback test for unstable FOPDT process produces limit cycle when the ratio of time delay to unstable time constant is less than 0.693 [64]. Although the relay auto-tuning methods have been improved by several authors [8, 65, 66], the improvements do not overcome the constraints of an ideal relay test. In [9], a modified asymmetrical relay feedback method was given to get improved estimates of the parameters of the FOPDT model. A step response based identification method [67] has been provided for unstable processes using the PID controller. This work has been further extended in the recent paper [68] by using peak values of the closed-loop step response. The constraint of a relay feedback for unstable processes was relaxed up to one by providing an inner feedback proportional controller during the auto-tuning test [66, 69]. This method was further extended in [13] for identification of a unstable FOPDT model based on the describing function analysis. The improved analytical method [70] under relay feedback and fitting conditions of the limit cycle was reported for unstable processes with the help of an iterative numerical algorithm.

1.2 Motivation

While the relay feedback experiment yields sufficiently accurate results for many of the processes encountered in the process control industry, there are some potential problems associated with such techniques. These arise as a result of the approximations used in the development of the procedures. Several modified relay feedback methods were reported with the improved accuracy of identification, though one needs to solve simultaneously a set of nonlinear equations or iterative algorithms. Furthermore, most reported methods are successful in identifying the linear process models accurately but not the nonlinear process models. This motivated the researchers to propose the extended method of relay feedback such that the static nonlinearity along with linear process is accurately identified. An attempt has been made on similar lines to derive explicit expressions for identifying cascade processes using a single relay experiment. It would be very useful to tune the cascade control system in one experiment to reduce the time of tedious sequential approach. The relay feedback fails to induce limit cycle oscillations when an unstable process has long time delay. This can be overcome by using an inner PD controller such that overall relay control is stabilized during the process identification. On the other hand, it may be advantageous to use a relay with hysteresis so that the resultant system is less sensitive to measurement noise.

1.3 Contributions of this Thesis

Although relay auto-tuning has been widely accepted, some problems remain open and their solutions are sought. The thesis has investigated and contributed to the following areas.

I. Identification of linear processes using the half limit cycle data

This thesis provides, an exact analytical method for identifying a class of stable and unstable processes using a single symmetrical relay test. The exact analytical expressions for a half limit cycle waveform induced from a relay with hysteresis test are derived. Since a relay with hysteresis instead of an ideal relay is used for the identification, the resultant system is less sensitive to measurement noise. The method achieves improved estimation accuracy by providing

explicit expressions in terms of a half limit cycle data. Models with up to four parameters are identified by means of a single relay experiment without solving any nonlinear equations. The procedure to estimate the process model parameters is non-iterative and also does not present any convergence problem.

II. Identification of nonlinear processes with monotonic static gains

The analytical method presented earlier aimed at identification of linear process models accurately. The method is extended to identify nonlinear process models. These nonlinear models are composed of linear dynamics and nonlinear static functions as blocks in series. A single symmetrical relay test is conducted to determine the structure and then the parameters of the block-oriented nonlinear model. The static nonlinearity block is represented by a memoryless and monotonic function while the linear process model by a stable transfer function. The proposed identification technique is simple and gives better performance than previous methods for processes with static nonlinearity. A real-time experimental study is also included to prove the efficacy of the procedure.

III. On-line relay auto-tuning for stable processes

The applicability of the basic relay tuning method is extended to an on-line method to tune the controllers without breaking the closed-loop control. A relay is connected in parallel to the controller to induce selfoscillation and then simple measurements are made only on the half period of limit cycle output. The process dynamics is first identified by a low order transfer function, regardless of initial conditions or possible load disturbances affecting the control loop during identification. Aim is to achieve the optimum control signal variations without compromising the overall performance. From the well-known integral squared time error (ISTE) index, a new constraint is derived. Two real time experimental studies of the proposed method, one using a process simulator and second using the DC servo position control system, are demonstrated in this thesis.

IV. On-line identification of cascade control systems based on half limit cycle data

An on-line identification procedure is given for the cascade control system in which both inner and outer loop process dynamics are modelled simultaneously by performing a single

relay experiment. The relay feedback induces limit cycle oscillations without detaching the main loop controllers. The closed-form formulas for the unknown parameters of the process model are derived in terms of the half cycle data. Departing from the standard conventional approach for tuning these cascade controllers, the proposed method completes the entire tuning process in one experiment.

V. Extension of relay feedback technique for unstable processes with large time delay

The applicability of the relay feedback test is extended for unstable processes with large time delay. The necessary conditions for existence of limit cycle oscillation are derived when a symmetrical relay with hysteresis test is performed. Further analysis is carried out for choosing a suitable PD controller such that a sustained oscillation (limit cycle) is obtained for an extended value of the normalize time delay. Based on the relay induced half limit cycle signal the unknown process model parameters are estimated accurately. All the above benefits are achieved at no further significant complexities over the conventional relay method.

1.4 Thesis Organization

The thesis is organized as follows.

Chapter 2 presents an exact analytical method to estimate the stable and unstable process models. The time-domain expressions of limit cycle waveforms for different types of process models are developed using a state space approach. The technique proposed in this chapter improves the accuracy by deriving the explicit expressions of the unknown process model parameters. Suitability of the non-iterative method in the presence of measurement noise is also discussed and the performance is demonstrated with different examples.

Chapter 3 discusses the extended relay feedback method for modelling of nonlinear processes which are mainly represented by Wiener or Hammerstein types. The nonlinear model structure and its parameters are obtained from a single symmetrical relay test. Simulation examples and results from a real-time experiment show the effectiveness and assessment accuracy of the proposed approach.

Chapter 4 proposes the on-line relay feedback approach to re-tune PI controller without breaking the closed-loop control. The approach uses a relay in parallel to the controller to provide oscillations within tolerance of process variable swing. From these oscillations, only half period of limit cycle data is used to obtain the FOPDT model of process dynamics. Following the identification, the chapter also proposes the design of the PI controller to preserve the actuator from the large variation of control signals. Simulation and real-time experiment for a DC servo position control system are presented using the proposed scheme.

Chapter 5 is focused on the development of the simple on-line procedure for auto-tuning of cascade control systems. The method estimates both inner and outer loop process dynamics simultaneously by performing a single relay experiment. The relay test is performed with the controllers in the loop and then process model parameters are obtained from appropriate explicit expressions. Simulation examples are included to demonstrate the effectiveness of the proposed method.

In chapter 6, the limitation of relay feedback test for obtaining a sustained limit cycle output for unstable processes is addressed. The proposed control strategy extends the relay feedback for unstable processes by providing a suitable inner loop PD controller.

Finally in Chapter 7, general conclusions and suggestions for further work are documented.

CHAPTER 2

IDENTIFICATION OF LINEAR PROCESSES USING THE HALF LIMIT CYCLE DATA

2.1 Introduction

Relay based auto-tuning proposed by Åström and Hägglund [4] was one of the first to be commercialized for the purpose of identification and automatic tuning and has remained attractive owing to its simplicity and robustness. A number of relay based identification methods have been proposed in the literature to obtain process models in terms of transfer functions. Several authors [5–12, 71] have used the approximate describing function (DF) method with or without involving modified relays for estimating process transfer function models.

While many of the auto-tuning methods use the DF of a relay in their analysis, a very few have applied the exact relay feedback expressions but involving more complexities. Wang et al. [14] presented the time domain approach to estimate parameters of a stable first order plus dead time (FOPDT) process model by identifying multiple points of the Nyquist curve from a single relay test. Majhi and Atherton [16] proposed state space based exact analytical expressions for the identification of a first and second order plus dead time (SOPDT) models by asymmetrical relay tests. Luyben [72] proposed shape factor technique to identify stable and unstable FOPDT systems using a single relay feedback test. Relay based identification algorithm to improve the frequency response has been explored in [73] for an overdamped SOPDT model. Vivek and Chidambaram [19] presented the improved FOPDT and SOPDT identification algorithms using the fitting conditions established from the Fourier or Laplace transform of

the relay response. Auto-tuning method using shape factor of relay feedback response has been reported by Panda and Yu [20, 21] to estimate unknown process model parameters by solving simultaneous a set of equations. Their closed form solutions can easily be obtained from the general analytical expressions proposed by Majhi and Atherton [16]. Lee et al. [22] used integrals of the relay response instead of the point data to enhance identification performances. However, their method is not only iterative but also requires to handle lots of data for estimating the SOPDT model parameters. Majhi [17] has proposed simple analytical expressions using the amplitude, peak time and second derivative of the symmetrical limit cycle output for process identification. Liu and Gao [70] and Liu et al. [23] proposed identification methods based on biased/unbiased relay feedback test and using some iterative methods and suitable initial guesses. However, the improved accuracy is achieved by considering several exact relay responses and solving simultaneously a set of nonlinear equations for estimating the process model parameters. Problems may arise in that convergence may take place to a false solution if poor initial estimates are used while solving simultaneously the set of nonlinear equations.

This chapter presents identification methods for stable and unstable processes using a single symmetrical relay test. The accuracy of the relay experiment is adversely affected when there is measurement noise present in the system output and spurious switching of the relay is experienced. Therefore, a relay with hysteresis is used and a half cycle of the sustained oscillatory output data is measured for estimating process model parameters. Next, explicit expressions for the unknown parameters of the process model where the model can be a stable/unstable FOPDT or SOPDT or integrating SOPDT transfer function, are derived in terms of a few critical points of the half cycle data and its first and second derivatives. Models with up to four parameters can be identified from the half limit cycle data without solving the set of nonlinear equations. Illustrative examples are given to demonstrate the effectiveness and merits of the proposed identification methods.

2.2 Analytical expressions for the limit cycle waveform

A general relay feedback system, that induces limit cycle oscillation is shown in Fig. 2.1. In the figure, r is the reference or setpoint input and e and u are the relay input and output signal, respectively. It is assumed that the static load disturbance L and the random measurement noise N appear at the process input and output, respectively.

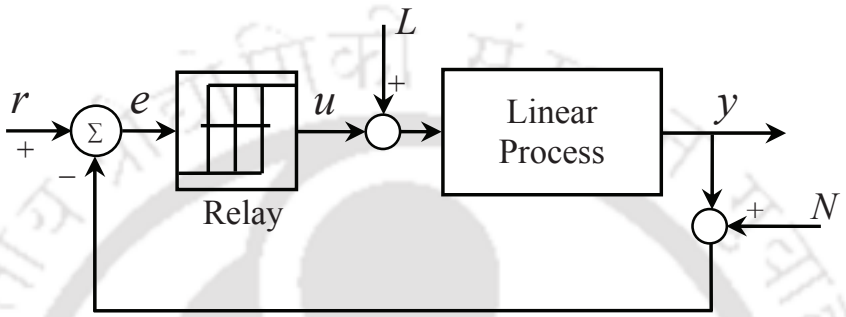

Figure 2.1: Relay feedback system for identification

Conventional relay experiment using an ideal relay induces chattering in the presence of noise which is usually considered undesirable from a practical point of view [2]. In order to minimize correlation with high frequency noise, the relay is typically implemented with a hysteresis of width ε, which is generally set to be about two times the estimated standard deviation of the noise. Therefore, to trigger a switch, the feedback error must move beyond the zero crossing by a significant amount relative to the noise level. Fig. 2.2 shows the relay responses to process output for ideal relay and relay with hysteresis, where $\pm h$ is the relay amplitudes and $\pm\varepsilon$ is the hysteresis widths.

Analytical expressions in time domain are developed to represent relay responses produced by different process models. The state-space representation of the system when the process contains a time delay θ, is

$$\dot{\mathbf{x}}(t) = \mathbf{A}\mathbf{x}(t) + \mathbf{b}u(t-\theta) \tag{2.1}$$

$$y(t) = \mathbf{c}\mathbf{x}(t) \tag{2.2}$$

where $\mathbf{A}$ is an $n \times n$ square matrix, $\mathbf{b}$ is an $n \times 1$ column vector and $\mathbf{c}$ is a row vector of dimension

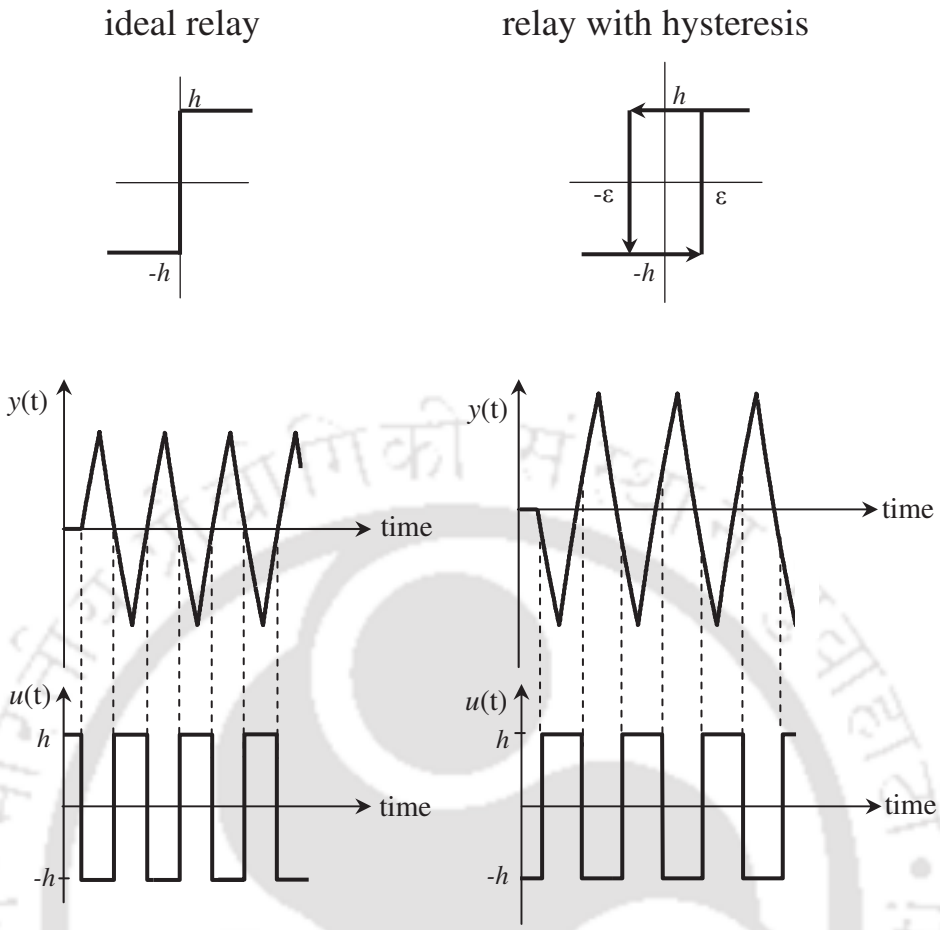

Figure 2.2: System output and input signals for ideal relay and relay with hysteresis

$1 \times n$. Assume that there exists a symmetrical limit cycle output with half period T as shown in Fig. 2.3 that is obtained with the initial condition $\mathbf{x}(t_0)$. Although, the relay switches from h to $-h$ at time $t = t_0$, the delayed relay output signal in Fig. 2.3 has two different piecewise constant input signals during a positive or negative half period of the process output. The solution of (2.1) for the time range $t_0 \leq t \leq t_1$ becomes

$$\mathbf{x}(t) = e^{\mathbf{A}(t-t_0)}\mathbf{x}(t_0) + \mathbf{A}^{-1}(e^{\mathbf{A}(t-t_0)} - \mathbf{I})\mathbf{b}h \tag{2.3}$$

where $\mathbf{I}$ is an identity matrix of the order of $\mathbf{A}$. Then for the time range $t_1 < t \leq (T + t_0)$ where $u(t) = -h$, the expression for the states becomes

$$\mathbf{x}(t) = e^{\mathbf{A}(t-t_1)}\mathbf{x}(t_1) - \mathbf{A}^{-1}(e^{\mathbf{A}(t-t_1)} - \mathbf{I})\mathbf{b}h \tag{2.4}$$

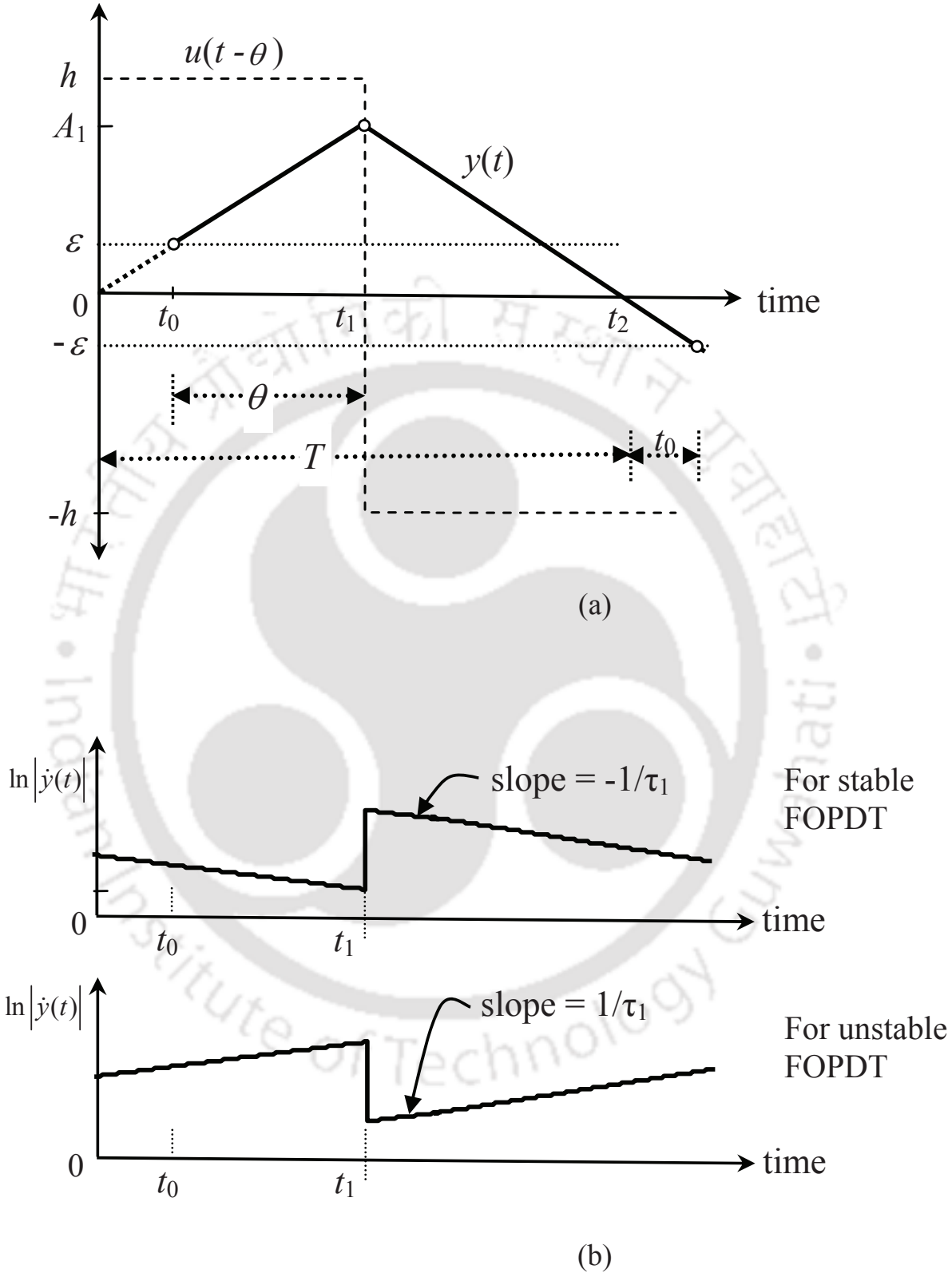

Figure 2.3: (a) Process input $u(t)$ and output $y(t)$ waveforms for the FOPDT model under relay feedback, (b) plots of $\ln|\dot{y}(t)|$ data

Since the limit cycle is symmetrical, it follows that $\mathbf{x}(T+t_0) = -\mathbf{x}(t_0)$. Thus, substituting $t = t_0$ in (2.3) and substituting $t = T + t_0$ in (2.4), one obtains the initial value of the state

$$\mathbf{x}(t_0) = (\mathbf{I} + e^{\mathbf{A}T})^{-1}\mathbf{A}^{-1}(2e^{\mathbf{A}(T-\theta)} - e^{\mathbf{A}T} - \mathbf{I})\mathbf{b}h \tag{2.5}$$

where $\theta = t_1 - t_0$. The necessary conditions for a limit cycle using a relay with hysteresis are:

$$y(t_0) = \mathbf{c}\mathbf{x}(t_0) = \varepsilon; \;\; \dot{y}(t_0) = \mathbf{c}\dot{\mathbf{x}}(t_0) > 0 \tag{2.6}$$

Finally, the limit cycle output $y(t)$ for the time range $t_0 \leq t \leq t_1$ can be expressed as

$$y(t) = \mathbf{c}e^{\mathbf{A}(t-t_0)}\mathbf{x}(t_0) + \mathbf{c}\mathbf{A}^{-1}(e^{\mathbf{A}(t-t_0)} - \mathbf{I})\mathbf{b}h \tag{2.7}$$

and for the time range $t_1 < t \leq (T + t_0)$

$$y(t) = \mathbf{c}e^{\mathbf{A}(t-t_1)}\mathbf{x}(t_1) - \mathbf{c}\mathbf{A}^{-1}(e^{\mathbf{A}(t-t_1)} - \mathbf{I})\mathbf{b}h \tag{2.8}$$

One obtains the expression for $\mathbf{x}(t_1)$ by substituting (2.5) in (2.3) and then setting $t = t_1$. Using $\mathbf{x}(t_1)$ a simple expression for $y(t)$ for the time range $t_1 < t \leq (T + t_0)$ can be rewritten as

$$y(t) = \mathbf{c}\mathbf{A}^{-1}\mathbf{b}h - 2\mathbf{c}e^{\mathbf{A}(t-t_1)}\mathbf{A}^{-1}(\mathbf{I} + e^{\mathbf{A}T})^{-1}\mathbf{b}h \tag{2.9}$$

It is to be noted that since $t_0 = 0$ when $\varepsilon = 0$, therefore the expressions (2.6), (2.7) and (2.9) can also be used for the case of an ideal symmetrical relay.

2.3 Process identification

This section describes the procedure of finding the process model parameters from the limit cycle waveform obtained from a single symmetrical relay test. It is assumed that the test obtains a symmetrical process output and supplies half limit cycle output data. In order to avoid misleading results caused by the transient oscillating behaviour, half cycle data measurements are made after two stabilized cycles have elapsed. Typical transfer function models in process control are often assumed to be the stable and unstable FOPDT, SOPDT or integrating SOPDT models for the dynamics of a major class of processes with time delay. Therefore, the above types of models are considered below for the development of identification procedures.

Type 1: FOPDT Process Model

Consider a stable or unstable FOPDT process model transfer function

$$G_p(s) = \frac{ke^{-\theta s}}{\tau_1 s \pm 1} \tag{2.10}$$

where k, τ_1 and θ are the steady state gain, time constant and time delay of the process model, respectively. Fig. 2.3 shows waveforms of the process input and output signals when identification test is conducted with a symmetrical relay. When the FOPDT model transfer function is expressed in the state space form, its state equation constants become

$$\mathbf{A} = \frac{\mp 1}{\tau_1}; \qquad \mathbf{b} = \frac{k}{\tau_1}; \qquad \mathbf{c} = 1 \tag{2.11}$$

Since a limit cycle condition $y(t_0) = \mathbf{c}\mathbf{x}(t_0) = \varepsilon$, it implies that $\mathbf{x}(t_0) = \varepsilon$ because $\mathbf{c} = 1$. Then substituting $\mathbf{x}(t_0) = \varepsilon$ and the constants of (2.11) in (2.7), the expression of $y(t)$ becomes

$$y(t) = \varepsilon e^{\mp \frac{t-t_0}{\tau_1}} \pm kh(1 - e^{\mp \frac{t-t_0}{\tau_1}}) \tag{2.12}$$

during the time range $t_0 \leq t \leq t_1$. The first derivative of $y(t)$ in (2.12) with respect to t is

$$\dot{y}(t) = \left(\frac{kh \mp \varepsilon}{\tau_1}\right) e^{\mp \frac{t-t_0}{\tau_1}} \tag{2.13}$$

Since the derivatives of $y(t)$ are discontinuous at time $t = t_1 = t_0 + \theta$, its first derivative shall have a large magnitude at that time. Therefore, taking natural logarithm of (2.13) one obtains

$$\ln|\dot{y}(t)| = \ln\left|\frac{kh \mp \varepsilon}{\tau_1}\right| \mp \frac{t-t_0}{\tau_1} \tag{2.14}$$

At time $t = t_0$, (2.14) becomes

$$\ln|\dot{y}(t_0)| = \ln\left|\frac{kh \mp \varepsilon}{\tau_1}\right| \tag{2.15}$$

Fig. 2.3(b) shows the plot of $\ln|\dot{y}(t)|$ for the time range $t_0 \leq t \leq (T + t_0)$. Initially, the time constant τ_1 of the FOPDT model is obtained from the slope of this plot. The time delay $\theta = (t_1 - t_0)$ is estimated from the measurements of t_0 and t_1 of $y(t)$ and $\ln|\dot{y}(t)|$, respectively. Next the steady state gain k is estimated with the help of (2.15) which can be expressed as

$$k = \frac{\tau_1 \, e^{(\ln|\dot{y}(t_0)|)} \pm \varepsilon}{h} \tag{2.16}$$

This shows how simply one can obtain (k, τ_1, θ) from the relay response data without solving any nonlinear equations.

Type 2: SOPDT Process Model

Consider a stable or unstable SOPDT process model transfer function

$$G_p(s) = \frac{ke^{-\theta s}}{(\tau_1 s \pm 1)(\tau_2 s + 1)} \tag{2.17}$$

assuming that $\tau_1 > \tau_2$. When it is expressed in the Jordan canonical state space form, its state and output equation constants can be given as

$$\mathbf{A} = \begin{bmatrix} \mp\frac{1}{\tau_1} & 0 \\ 0 & -\frac{1}{\tau_2} \end{bmatrix}; \quad \mathbf{b} = \begin{bmatrix} 1 \\ 1 \end{bmatrix}; \quad \mathbf{c} = \frac{k}{\tau_1 \mp \tau_2}[1 \quad -1] \tag{2.18}$$

Substitution of the above constants in (2.9), the expression for limit cycle output for the SOPDT process model during time range $t_1 < t \leq t_2$ becomes

$$y(t) = \mp kh(1 - c_1\, a\, e^{\mp\frac{(t-t_1)}{\tau_1}} + c_2\, b\, e^{-\frac{(t-t_1)}{\tau_2}}) \tag{2.19}$$

where $c_1 = 2(1+e^{\mp\frac{T}{\tau_1}})^{-1}$, $c_2 = 2(1+e^{\frac{-T}{\tau_2}})^{-1}$, $a = \frac{\tau_1}{\tau_1 \mp \tau_2}$ and $b = \frac{\pm\tau_2}{\tau_1 \mp \tau_2}$.

The first and second derivative of $y(t)$ in (2.19) with respect to t are

$$\dot{y}(t) = kh(\frac{-c_1 a e^{\mp\frac{(t-t_1)}{\tau_1}}}{\tau_1} \pm \frac{c_2 b e^{-\frac{(t-t_1)}{\tau_2}}}{\tau_2}) \tag{2.20}$$

$$\ddot{y}(t) = kh(\frac{\pm c_1 a e^{\mp\frac{(t-t_1)}{\tau_1}}}{\tau_1^2} \mp \frac{c_2 b e^{-\frac{(t-t_1)}{\tau_2}}}{\tau_2^2}) \tag{2.21}$$

Fig. 2.4 shows a typical half limit cycle data of $y(t)$, its first derivative $\dot{y}(t)$ and second derivative $\ddot{y}(t)$ plots for the SOPDT model given in (2.17). For this process model, $\dot{y}(t)$ and $\ddot{y}(t)$ plots of the half cycle data show an appreciable change at time $t = t_0 + \theta = t_1$. This can easily be detected from the second derivative of the half cycle data and thus the time delay parameter of the process model can be obtained from $\ddot{y}(t)$ as $\theta = (t_1 - t_0)$. It may be noted that $y(t_0) = \varepsilon$.

Now the expressions of $y(t)$, $\dot{y}(t)$ and $\ddot{y}(t)$ at time $t = t_1$ become

$$y(t_1) \quad = \quad \mp kh(1 - c_1\, a + c_2\, b) \tag{2.22}$$

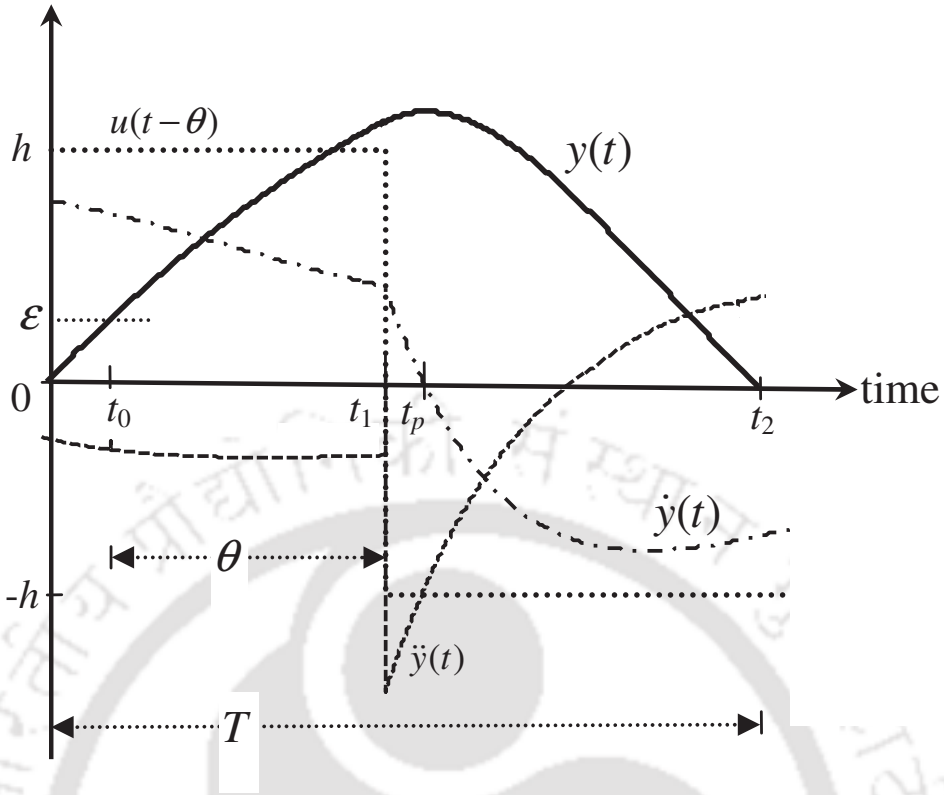

Figure 2.4: Half cycle output and its derivatives for the SOPDT model

$$\dot{y}(t_1) = \frac{kh}{\tau_1 \mp \tau_2}(-c_1 + c_2) \tag{2.23}$$

$$\ddot{y}(t_1) = \frac{kh}{\tau_1 \mp \tau_2}\left(\frac{\pm c_1}{\tau_1} - \frac{c_2}{\tau_2}\right) \tag{2.24}$$

(2.23) can be expressed as

$$c_1 = c_2 - \dot{y}(t_1)\left(\frac{\tau_1 \mp \tau_2}{kh}\right) \tag{2.25}$$

Substitution of (2.25) in (2.24) results in

$$\ddot{y}(t_1) = \mp kh\left(\frac{\pm c_2}{\tau_1\tau_2} + \frac{\dot{y}(t_1)}{kh\tau_1}\right) \tag{2.26}$$

The above expression can be written as

$$c_2 = \frac{\tau_1\tau_2}{kh}\left(-\ddot{y}(t_1) \mp \frac{\dot{y}(t_1)}{\tau_1}\right) \tag{2.27}$$

Substituting the expressions for c_1 and c_2 in (2.22) one obtains

$$y(t_1) = \mp(kh + \dot{y}(t_1)(\tau_1 \pm \tau_2) + \ddot{y}(t_1)(\tau_1\tau_2)) \tag{2.28}$$

If t_p is the time instant at which the positive peak output of the process occurs and $t_p \geq t_1$, then (2.20) can be used to obtain the ratio

$$\frac{c_1}{c_2} = \frac{e^{-(t_p - t_1)/\tau_2}}{e^{\mp(t_p - t_1)/\tau_1}} \tag{2.29}$$

since $\dot{y}(t_p) = 0$. Now, multiplying both sides of (2.20) by $e^{(t-t_1)/\tau_2}$, it is easy to obtain

$$\begin{aligned} \dot{y}(t)e^{\frac{(t-t_1)}{\tau_2}} &= kh\left(\frac{-c_1 a e^{\mp\frac{(t-t_1)}{\tau_1}}}{\tau_1} \pm \frac{c_2 b e^{-\frac{(t-t_1)}{\tau_2}}}{\tau_2}\right) e^{\frac{(t-t_1)}{\tau_2}} \\ &= \frac{kh}{\tau_1 \mp \tau_2}\left(-c_1\, e^{\mp\frac{(t-t_1)}{\tau_1}} e^{\frac{(t-t_1)}{\tau_2}} \pm c_2\right) \end{aligned} \tag{2.30}$$

Then, differentiating (2.30) with respect to time, one gets

$$\ddot{y}(t)e^{\frac{(t-t_1)}{\tau_2}} + \frac{\dot{y}(t)}{\tau_2}e^{\frac{(t-t_1)}{\tau_2}} = \frac{kh}{\tau_1 \mp \tau_2}\left(-c_1\, e^{\mp\frac{(t-t_1)}{\tau_1}} e^{\frac{(t-t_1)}{\tau_2}}(\mp\frac{1}{\tau_1} + \frac{1}{\tau_2})\right) \tag{2.31}$$

The above equation at time $t = t_p$ becomes,

$$\ddot{y}(t_p) = -\frac{kh}{\tau_1 \tau_2} c_1 e^{\mp(t_p - t_1)/\tau_1} \tag{2.32}$$

Now, (2.19) at time $t = t_p$ becomes

$$y(t_p) = \mp kh(1 - c_1\, a\, e^{\mp(t_p - t_1)/\tau_1} + c_2\, b\, e^{-(t_p - t_1)/\tau_2}) \tag{2.33}$$

Substituting a and b in (2.33) and using (2.29, 2.32), it is easy to get a linear equation of the form

$$kh = \mp y(t_p) - \ddot{y}(t_p)\tau_1\tau_2 \tag{2.34}$$

which can be rewritten as

$$\tau_1\tau_2 = -\frac{kh \pm y(t_p)}{\ddot{y}(t_p)} \tag{2.35}$$

As shown in Fig. 2.4, at time $t = t_2$ the limit cycle output $y(t_2) = 0$. Thus (2.19) at time $t = t_2$ becomes

$$y(t_2) = \mp kh(1 - c_1\, a\, e^{\mp(t_2 - t_1)/\tau_1} + c_2\, b\, e^{-(t_2 - t_1)/\tau_2}) = 0 \tag{2.36}$$

Further simplification of (2.36) gives

$$c_2\, e^{-(t_2 - t_1)/\tau_2} = \mp\left(\frac{\tau_1 \mp \tau_2}{\tau_2}\right) \pm \frac{c_1\, \tau_1\, e^{\mp(t_2 - t_1)/\tau_1}}{\tau_2} \tag{2.37}$$

(2.20) can be expressed using (2.37) as

$$\dot{y}(t_2) = \frac{kh}{\tau_2}(\pm c_1\, e^{\mp(t_2-t_1)/\tau_1} \mp 1) \tag{2.38}$$

The above equation can be rewritten as

$$c_1\, e^{\mp(t_2-t_1)/\tau_1} = 1 \pm \left(\frac{\tau_2}{kh}\right)\dot{y}(t_2) \tag{2.39}$$

Next, substitution of (2.39) and (2.37) in (2.21) for time $t = t_2$ gives

$$kh = \mp(\tau_1 \pm \tau_2)\dot{y}(t_2) - \tau_1\tau_2\ddot{y}(t_2) \tag{2.40}$$

Putting the expression for $\tau_1\tau_2$ of (2.35) in (2.40), one obtains a second linear equation of the form

$$\tau_1 \pm \tau_2 = -kh\left(\frac{\ddot{y}(t_p) - \ddot{y}(t_2)}{\ddot{y}(t_p)\dot{y}(t_2)}\right) \pm \left(\frac{y(t_p)\ddot{y}(t_2)}{\ddot{y}(t_p)\dot{y}(t_2)}\right) \tag{2.41}$$

Finally, substituting (2.35) and (2.41) in (2.28) and rearranging the equation, the expression for the steady state gain becomes

$$k = \frac{y(t_1) + \dot{y}(t_1)\left(\frac{y(t_p)\ddot{y}(t_2)}{\ddot{y}(t_p)\dot{y}(t_2)}\right) - \left(\frac{\ddot{y}(t_1)y(t_p)}{\ddot{y}(t_p)}\right)}{\mp h\left[1 - \dot{y}(t_1)\left(\frac{\ddot{y}(t_p)-\ddot{y}(t_2)}{\ddot{y}(t_p)\dot{y}(t_2)}\right) - \frac{\ddot{y}(t_1)}{\ddot{y}(t_p)}\right]} \tag{2.42}$$

The process time delay θ is estimated from the second derivative of the relay response curve that shows an abrupt change in slope at time $t = t_1$ (time is measured from the beginning of the positive half cycle $y(t)$) due to non-monotonic characteristics of the limit cycle data. Since the relay switches at time $t = t_0$, the time delay is calculated by $\theta = t_1 - t_0$. The steady state gain k of the process model is obtained from (2.42) and the remaining parameters (τ_1, τ_2) of the stable or unstable process model are estimated using the expressions (2.41) and (2.35). Thus, all the unknown model parameters in (2.17) are obtained using the half limit cycle data.

Type 3: Integrating SOPDT Process Model

For an integrating SOPDT transfer function

$$G_p(s) = \frac{ke^{-\theta s}}{s(\tau_1 s \pm 1)} \tag{2.43}$$

Here the model has three parameters (k, τ_1, θ) and its state equation constants can be obtained by assuming $\frac{1}{\tau_2} << 1$ in (2.18) of the SOPDT model. After following similar steps as that for the SOPDT model, the expression of $y(t)$ for an integrating SOPDT process model is obtained for time range $t_1 < t \leq t_2$ as

$$y(t) = \mp kh \left[t - t_1 - 0.5T - \tau_1 (1 - c_1 \, e^{\mp \frac{(t-t_1)}{\tau_1}}) \right] \tag{2.44}$$

where, $c_1 = 2(1 + e^{\mp \frac{T}{\tau_1}})^{-1}$. The first derivative of $y(t)$ in (2.44) with respect to t is

$$\dot{y}(t) = \mp kh (1 - c_1 e^{\mp \frac{(t-t_1)}{\tau_1}}) \tag{2.45}$$

Since $\dot{y}(t_p) = 0$ at time $t = t_p$, the above expression gives

$$c_1 = e^{\pm \frac{(t_p - t_1)}{\tau_1}} \tag{2.46}$$

Substituting c_1 in (2.44) at time $t = t_p$, one obtains a simple expression for the steady state gain

$$k = \mp \frac{y(t_p)}{h(t_p - t_1 - 0.5T)} \tag{2.47}$$

From similar analysis at time $t = t_1$ for $y(t)$ and $\dot{y}(t)$, it is easy to show the relations

$$y(t_1) = \mp kh(-\tau_1 - 0.5T + \tau_1 c_1) \tag{2.48}$$

and

$$c_1 = \left(1 \pm \frac{\dot{y}(t_1)}{kh} \right) \tag{2.49}$$

Substituting c_1 of (2.49) in (2.48) and then simplifying gives

$$\tau_1 = \left(\frac{\pm khT - 2y(t_1)}{2\dot{y}(t_1)} \right) \tag{2.50}$$

The explicit expressions for estimating unknown parameters of process models (other than the time delay θ) in Type-1, 2 and 3 are summarized in Table 2.1. It is to be noted that the half cycle data of higher order processes often assumes the form of the half cycle relay response curve as shown in Fig. 2.4. Therefore the third or high order processes with or without time delay are often identified by SOPDT models with an effective time delay [17]. The time delay θ is estimated from the second derivative of $y(t)$ that shows a discontinuity in output at the time $t_1 = t_0 + \theta$, due to non-monotonic characteristics of the limit cycle waveform. But, we know

that $y(t)=\varepsilon$ at time t_0. Thus, $\theta=t_1-t_0$ is obtained from the measurements of t_0 and t_1 of $y(t)$ and $\ddot{y}(t)$, respectively.

Table. 2.1: Identification procedures for unknown parameters

Model	Equations/ Plot	Procedures
$\frac{ke^{-\theta s}}{\tau_1 s\pm 1}$	Slope of plot of $\ln\lvert\dot{y}(t)\rvert$	Estimate τ_1
	$k=\frac{\tau_1\, e^{(\ln\lvert\dot{y}(t_0)\rvert)}+\varepsilon}{h}$	Estimate k
$\frac{ke^{-\theta s}}{(\tau_1 s\pm 1)(\tau_2 s+1)}$	$k=\frac{y(t_1)+\dot{y}(t_1)\left(\frac{y(t_p)\ddot{y}(t_2)}{\ddot{y}(t_p)\dot{y}(t_2)}\right)-\left(\frac{\ddot{y}(t_1)y(t_p)}{\ddot{y}(t_p)}\right)}{\mp h\left[1-\dot{y}(t_1)\left(\frac{\ddot{y}(t_p)-\ddot{y}(t_2)}{\ddot{y}(t_p)\dot{y}(t_2)}\right)-\frac{\ddot{y}(t_1)}{\ddot{y}(t_p)}\right]}$	Estimate k
	$\tau_1\pm\tau_2=-kh\left(\frac{\ddot{y}(t_p)-\ddot{y}(t_2)}{\ddot{y}(t_p)\dot{y}(t_2)}\right)\pm\left(\frac{y(t_p)\ddot{y}(t_2)}{\ddot{y}(t_p)\dot{y}(t_2)}\right)$ $\tau_1\tau_2=-\frac{kh\pm y(t_p)}{\ddot{y}(t_p)}$	Estimate τ_1, τ_2
$\frac{ke^{-\theta s}}{s(\tau_1 s\pm 1)}$	$k=\mp\frac{y(t_p)}{h(t_p-t_1-0.5T)}$	Estimate k
	$\tau_1=\left(\frac{\pm khT-2y(t_1)}{2\dot{y}(t_1)}\right)$	Estimate τ_1

2.4 Issue of load disturbance and measurement noise

2.4.1 Presence of load disturbance

In the presence of a static load disturbance of magnitude L at the process input, a symmetrical relay feedback test obtains an asymmetrical process output. In this situation, the magnitude of L can be obtained accurately from the measurements of the area of the process input over a period

$$a_u=\int_0^{T_p}u(t)\mathrm{d}t=(h+L)T_p+2hT_+ \tag{2.51}$$

where T_+ and T_p are the time period for the positive output of the relay and the period of the relay output, respectively. Then, the load disturbance can be estimated as

$$\hat{L} = -h + \frac{a_u + 2hT_+}{T_p} \tag{2.52}$$

A bias of $\hat{L}$ may be added to the relay height to restore the symmetry in limit cycle output.

2.4.2 Measurement noise

In process control systems, the noises come from measuring devices, control valves, or the process itself. In relay feedback experiments, the amplitude of the limit cycle is often corrupted with noises which can possibly fail the test. To overcome the possible failure, a relay with hysteresis is considered in the proposed identification method. Generally, the width of the hysteresis is kept atleast twice of the standard deviation of the noise [1]. Again, the effect of measurement noise on the identified model parameters can be investigated in simulations by introducing a normally distributed random additive noise with zero mean and varying variance, $(0, \sigma_N^2)$, at the output of the process during the relay test thus making the oscillations noisy. The noise power is quantified by SNR (Signal to Noise Ratio) in decibel (dB) which is defined as $\text{SNR} = 10\log(\sigma_y^2/\sigma_N^2)$, where σ_y^2 is the variance of the output signal and σ_N^2 is the variance of the noise. Then, the least squares polynomial based low-pass filter known as the Saviztky-Golay (SG) filter [74] can be used to measure the limit cycle parameters. This is well-adapted for data smoothing and suitable for de-noising the noisy limit cycle. The advantage of this filtering technique is that it tends to preserve features of the data such as peak height and width. The SG filter can be represented by

$$\tilde{y}_i(t) = \sum_{n=-n_L}^{n_R} d_n \, y_{i+n} \tag{2.53}$$

where n_L is the number of points used to the left of a i^{th} data point, n_R is the number of points used to the right and $\tilde{y}(t)$ is the denoised output. The filter coefficients, d_n, are given by:

$$d_n = \left[(\mathbf{Q}^T\mathbf{Q})^{-1}\mathbf{Q}^T\right]_{0,n+n_L} \tag{2.54}$$

where,

$$\mathbf{Q} = \begin{bmatrix} 1 & \cdots & 0 & \cdots & 1 \\ -n_L & \cdots & 0 & \cdots & n_R \\ \vdots & & \vdots & & \vdots \\ (-n_L)^{r+1} & \cdots & 0 & \cdots & (n_R)^{r+1} \end{bmatrix} \tag{2.55}$$

Eqs. (2.53) and (2.54) help to compute a smooth de-noised signal for some specified degree of the polynomial r and number of data points (span) n, where $r < n$. This enables one to accurately calculate instantaneous amplitudes from the noisy output signal. Also, instead of numerical derivative, the required data $(\dot{y}$ and $\ddot{y})$ can also be computed by modifying the filter in (2.53) [75]. For example, the filtered first derivative is the convolution (2.53) divided by the stepsize (Δt). The derivative coefficient now in (2.54) is multiplied by $m!$, where $m =$ order of derivative. The smoothed data and the smoothed differentiation are effectively obtained from the noisy output signal using the SG filtering technique and the results are presented in Fig. 2.5.

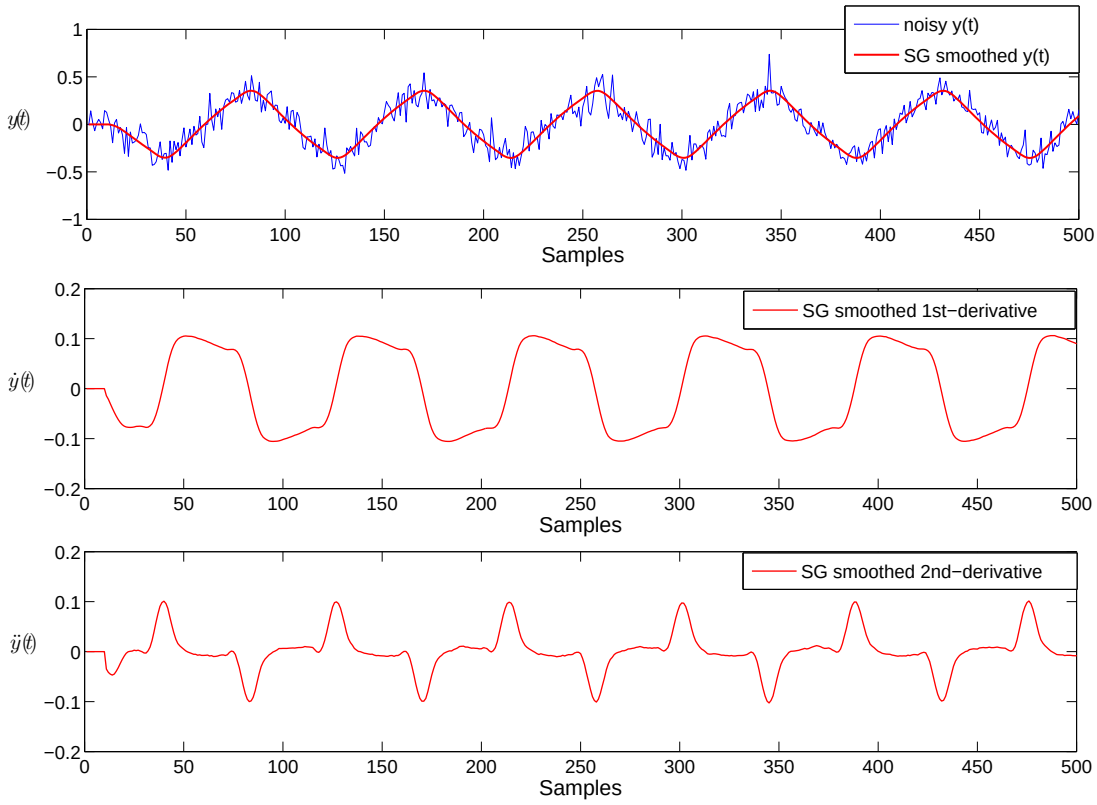

Figure 2.5: Results from the SG filter

2.5 Simulation study

Six examples studied in the recent literature are considered here to illustrate the effectiveness and accuracy of the proposed identification method. To overcome the undesirable relay chattering caused by noisy signals, the width of the hysteresis of the relay is set to twice the standard deviation of the noise. To show that the proposed scheme can be applied to the higher order processes, a fifth order plus delay transfer function is considered in the last example. The first and third examples show that the expected results are achievable irrespective of the presence of measurement noise during the relay experiments.

Example 1:

Consider a first order process $G_1(s) = \frac{e^{-2s}}{(10s+1)}$. A relay with $h = 1$ and $\varepsilon = 0.1$ in the absence of measurement noise induces a sustained process output as shown in Fig. 2.6.

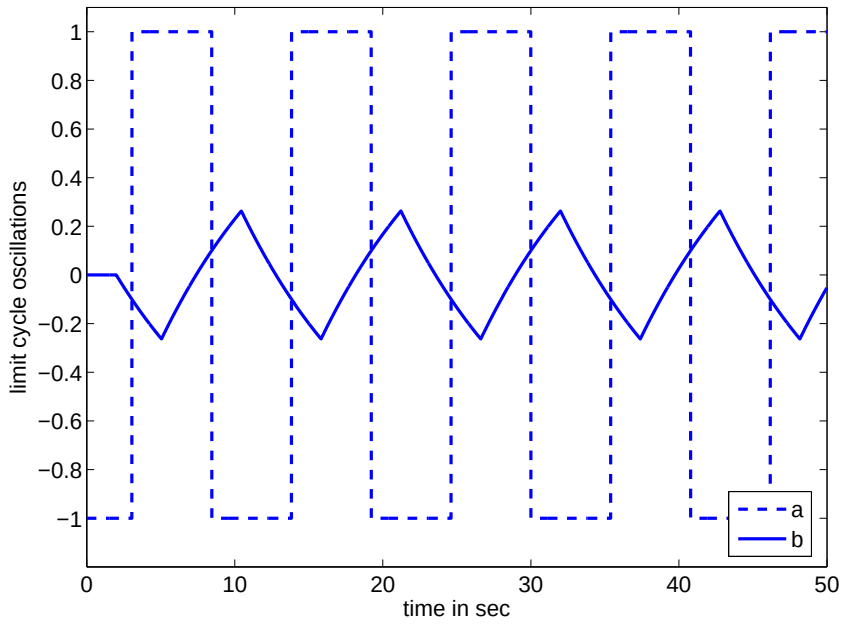

Figure 2.6: Typical limit cycle waveforms, (a) $u(t)$ and (b) $y(t)$ for Example 1

From the half limit cycle data in Fig. 2.7, the required values are obtained as: $t_0 = 1.053$, $t_1 = 3.053$, $\ln|\dot{y}(t_0)| = -2.4078$ and slop of $\ln|\dot{y}(t)| = -0.1$. The explicit expressions given in Table 2.1 gives $\tau_1 = 10$, $k = 1.0$ and $\theta = t_1 - t_0 = 2.0$ to within 10^{-4}. For the same process, Li et al.'s [71] method with an ideal relay gave $k = 0.988$, $\tau_1 = 8.02$ and $\theta = 2.0$, Srinivasan

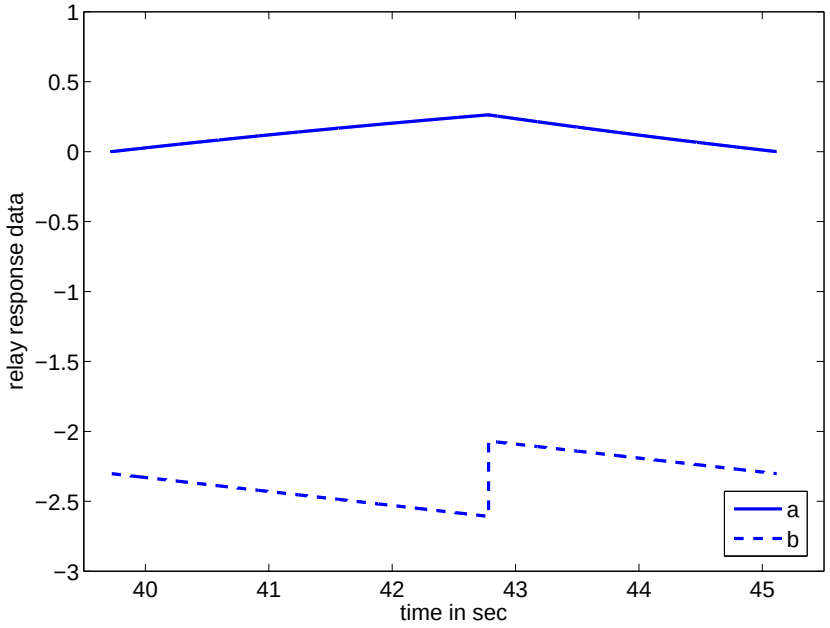

Figure 2.7: Simulation results for Example 1: (a) $y(t)$ and (b) $\ln|\dot{y}(t)|$

and Chidambaram's [9] method with an asymmetrical relay estimated $k = 1.03$, $\tau_1 = 10.3$ and $\theta = 2.3$, whereas the method by Vivek and Chidambaram [19] gave $k = 0.9467$, $\tau_1 = 9.5028$ and $\theta = 2.0$ after solving linear algebraic equations. Thus, the proposed identification technique is found to be superior in terms of accuracy in estimation of the model parameters.

To verify the usefulness of the method under realistic conditions, the process model parameters are estimated in the face of measurement noise. Let the process output be corrupted by Gaussian distributed random noise of several σ_N^2 such that the SNR varies from 10 dB to 25 dB. Noise reduction using the SG filter gives a smooth half cycle data without attenuation of data features, as shown in Fig. 2.8. The measured quantities from the denoised signal are used to estimate the model parameters and percentage errors in these parameters due to the noise are given in Table 2.2. Interestingly, the estimated values under observation noise of various σ_N^2 become close to the actual values in almost all the cases.

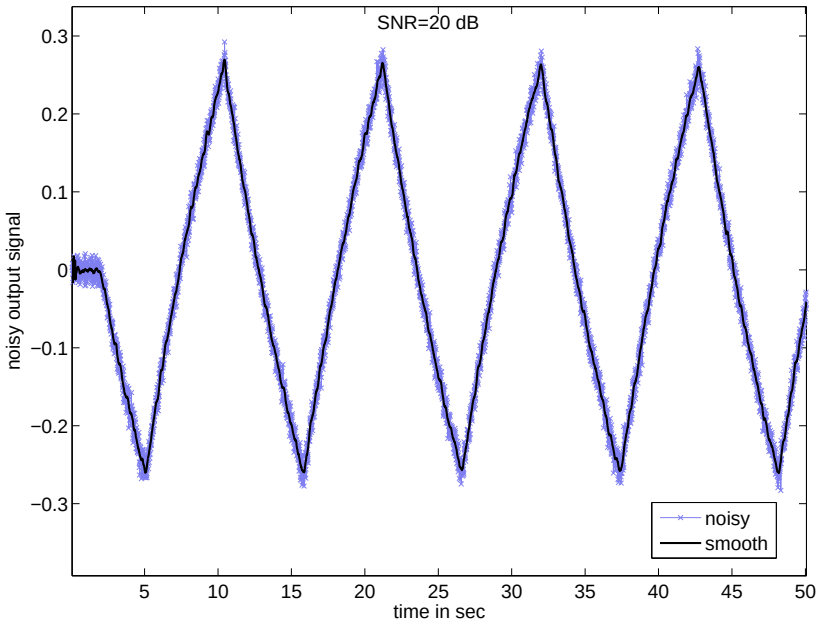

Figure 2.8: Noisy and denoised output signals

Table. 2.2: Effects of measurement noise for Example 1

SNR (dB)	% Error in				
	$\ln\lvert\dot{y}(t_0)\rvert$	slope of $\ln\lvert\dot{y}(t)\rvert$	θ	k	τ_1
10	0.830	0.604	5.502	−0.530	−0.578
15	−1.249	0.400	3.522	−0.310	−0.376
20	0.041	0.200	3.012	−0.140	−0.148
25	0.021	0.110	0.502	−0.050	−0.054

Example 2:

Consider an unstable process $G_2(s) = \frac{e^{-0.4s}}{(s-1)}$. Based on two different relay tests, Marchetti et al. [8] have obtained the FOPDT model with $k = 0.928$, $\tau_1 = 0.757$ and $\theta = 0.392$ and using a biased relay test, Liu and Gao [70] have identified the FOPDT model with $k = 1.0001$, $\tau_1 = 0.9954$ and $\theta = 0.4$. Now, relay experiment is conducted and only a half period of limit cycle output for $G_2(s)$ is obtained with relay setting $(h, \varepsilon) = (1, 0)$. From the data plotted in Fig. 2.9, the required values are obtained as: $t_0 = 0, t_1 = 0.4$, $\ln|\dot{y}(t_0)| = 0.0001$ and slop of $\ln|\dot{y}(t)| = 1.0$. The parameters $k = 1.0$, $\tau_1 = 1.0$ and $\theta = 0.4$ are estimated again to within 10^{-4}. Here, it is observed that the same steps are applicable to an ideal relay $(\varepsilon = 0)$ without modifying

the identification procedure. Moreover, the identification procedure requires significantly less information (analysis of half cycle data only) for obtaining accurate model parameters.

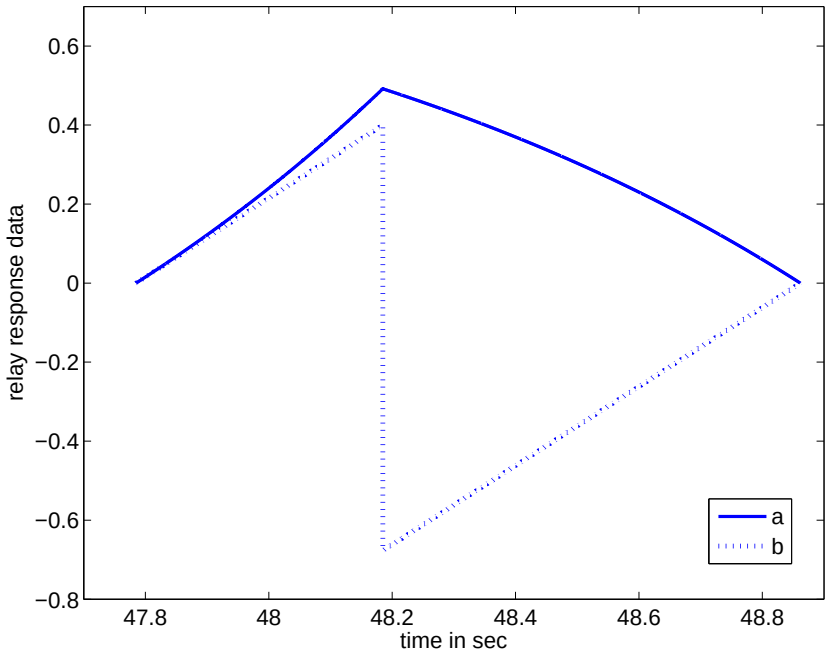

Figure 2.9: Simulation results for Example 2: (a) $y(t)$ and (b) $\ln|\dot{y}(t)|$

Table. 2.3: Half limit cycle data for Examples 3-6

Process	$y(t_1)$	$\dot{y}(t_1)$	$\ddot{y}(t_1)$	$y(t_p)$	$\ddot{y}(t_p)$	$\dot{y}(t_2)$	$\ddot{y}(t_2)$
G_3	0.3448	0.0654	−0.2065	0.3566	−0.1357	−0.0977	0.0075
G_4	0.5410	0.7701	−1.6143	0.8570	−0.1430	−0.5000	−0.2500
G_5	8.1638	0.8508	–	12.8671	–	–	–
G_6	0.7563	−0.0345	−0.0568	0.7668	−0.1861	−0.1781	0.0091

Example 3:

This example considers the overdamped SOPDT process widely studied in the literature [23, 71, 73] as $G_3(s) = \frac{e^{-2s}}{(10s+1)(s+1)}$. The parameters identified by Li et al. [71] were $k = 0.853$, $\theta = 2$, $\tau_1 = 7.416$, $\tau_2 = 1.15$ by following the two relay tests. The method proposed by Ramakrishnan and Chidambaram [73] using a single asymmetric relay feedback test gave $k = 1.05$, $\theta = 1.814$, $\tau_1 = 9.766$, $\tau_2 = 1.271$. By nonlinear programming iterative algorithm, Liu et al. [23] estimated

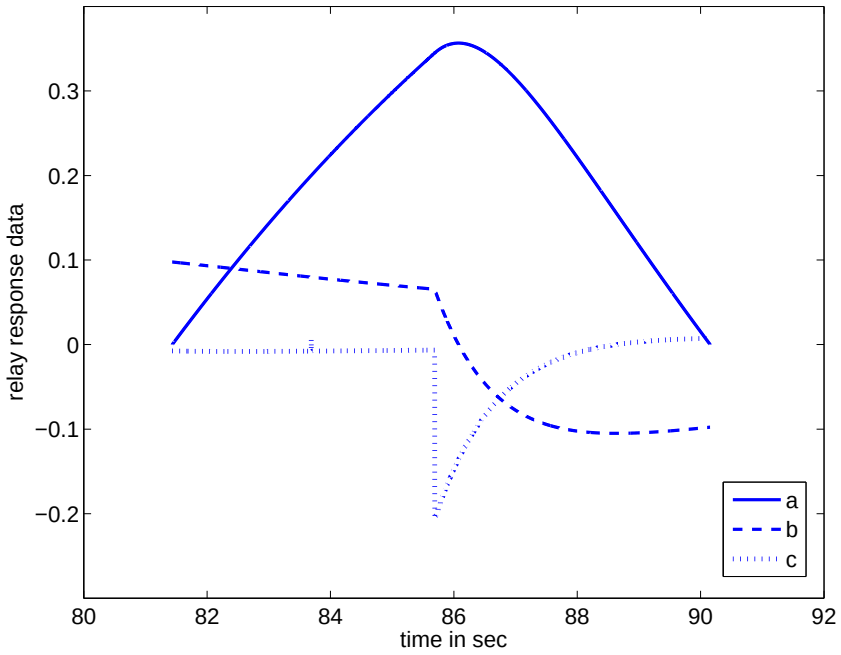

Figure 2.10: Simulation results for Example 3: (a) $y(t)$, (b) $\dot{y}(t)$ and (c) $\ddot{y}(t)$

$k = 1.0122$, $\theta = 2.0037$, $\tau_1 = 10.1178$, $\tau_2 = 0.992$ from an unbiased relay test. Employing a relay with parameters $(h, \varepsilon) = (1, 0.2)$, the half limit cycle data are measured by the proposed method for estimating an SOPDT model parameters and tabulated in Table 2.3. Exact process model with $k = 1.0$, $\tau_1 = 10.0$, $\tau_2 = 1.0$ and $\theta = (t_1 - t_0) = (4.2525 - 2.2525) = 2.0$ are calculated to within 10^{-3} of these values given in $G_3(s)$ using equations listed in Table 2.1. This clearly indicates that the proposed method gives better parameter estimation.

Like the previous studies, the identification is conducted with additive noise of various amplitudes. The modelling errors after using the SG smoothing technique are given in Table 2.4. Nyquist plots for the original process and the identified models are shown in Fig. 2.11 . It is observed from the Nyquist plots in Fig. 2.11 that the presented analytical method for identification computes more accurate models as compared to the methods reported in [23, 71, 73].

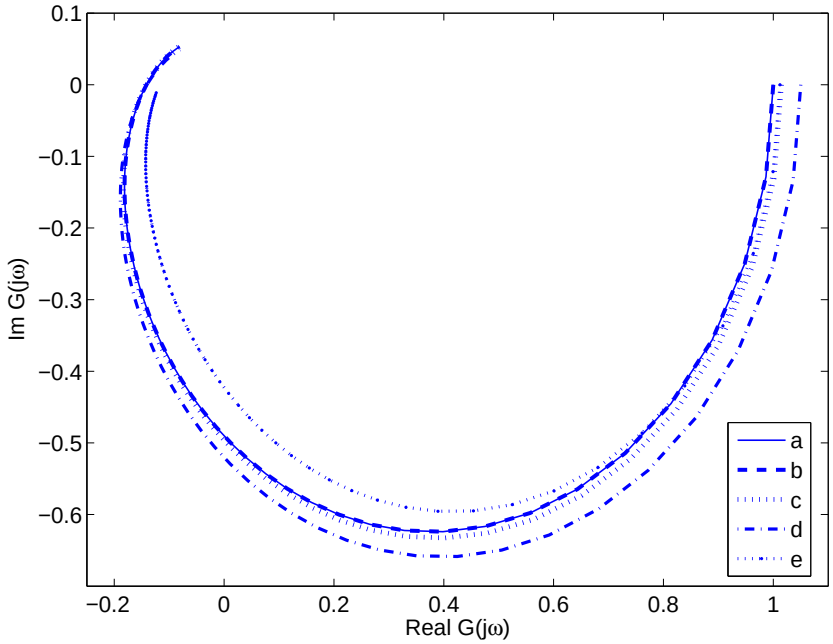

Figure 2.11: Nyquist plots for Example 3: (a) actual process, identified model by the (b) proposed method with no noise, (c) proposed method with SNR 10%, (d) Ramakrishnan et al.'s method and (e) Liu et al.'s method

Table. 2.4: Effects of measurement noise for Example 3

SNR (dB)	% Error in			
	k	θ	τ_1	τ_2
10	0.450	−0.015	0.530	−0.930
15	−0.390	0.081	−0.500	0.150
20	0.780	0.310	0.900	−0.130
25	−0.018	0.070	0.120	−0.060

Example 4:

In this example, an unstable process $G_4(s) = \frac{e^{-0.5s}}{(2s-1)(0.5s+1)}$ studied in [70, 73] is considered. The relay test is conducted with amplitudes $(h, \varepsilon) = (1, 0.2)$ and the measured values on the half cycle waveform and its derivatives are shown in Fig. 2.12 and Table 2.3. Following the identification procedure, the estimated parameters are $k = 1.0$, $\theta = 0.5$, $\tau_1 = 2.0$ and $\tau_2 = 0.5$ to within 10^{-3}. Here, the time delay parameters θ is obtained by subtracting $t_0 = 0.365$ from $t_1 = 0.865$ due to hysteresis in the relay. Ramakrishnan and Chidambaram [73]'s asymmetric relay test method estimated $k = 1.00$, $\theta = 0.52$, $\tau_1 = 1.9999$ and $\tau_2 = 0.4837$. From a biased

relay feedback test, Liu and Gao [70] estimated $k = 1.0001$, $\theta = 0.5051$, $\tau_1 = 1.9975$ and $\tau_2 = 0.4988$ using an iterative algorithm. This shows that the proposed method can identify an unstable process model from relatively less amount of data without compromising accuracy and also without any iteration.

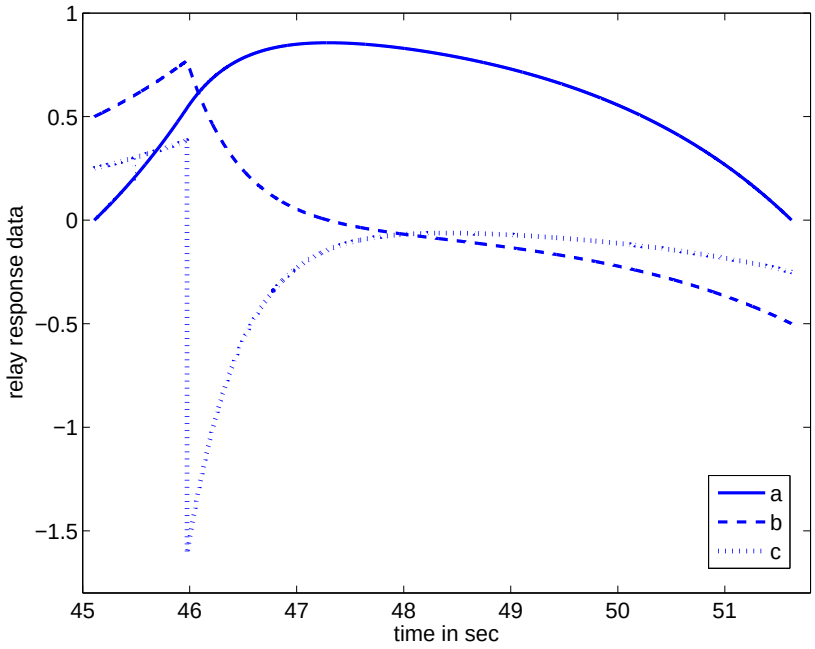

Figure 2.12: Simulation results for Example 4: (a) $y(t)$, (b) $\dot{y}(t)$ and (c) $\ddot{y}(t)$

Example 5:

Consider the SOPDT integrating process studied by Liu and Gao [70] and Kaya [11] $G_5(s) = \frac{e^{-10s}}{s(20s+1)}$. Liu and Gao [70] estimated $k = 0.9983$, $\theta = 10.027$ and $\tau_1 = 19.9443$ using the Newton–Raphson iteration method and for the same process Kaya [11] derived an almost exact SOPDT model with each parameter error within 0.1%. However, Kaya's method requires one to solve nonlinear equations with suitable initial guesses. By performing a symmetrical relay test with $h = 1$ and $\varepsilon = 0.1$, the limit cycle data $t_0 = 0.1323$, $t_1 = 10.1325$ and $t_p = 22.4448$ are obtained alongwith the set of data for $G_5(s)$ as listed in Table 2.3. The proposed method yields the exact process model, $k = 1.0$, $\theta = (t_1 - t_0) = 10.0$, $\tau_1 = 20.0$ to within 10^{-3}, indicating good identification accuracy. It also shows the proposed identification method can obtain accurate process model without solving any nonlinear equations and initial guesses.

Example 6: Consider the higher order process $G_6(s) = \frac{e^{-2s}}{(2s+1)^5}$ studied by Kaya and Atherton [10] and Boiko [76]. Performing a symmetrical relay test, the quantities as shown in Table 2.3 are measured with the relay setting of $h = 1$ and $\varepsilon = 0.3$. Using the identification procedure for the SOPDT process model, the estimated parameters of the process model are $k = 1.0$, $\theta = (t_1 - t_0) = (5.754 - 0.577) = 5.177$, $\tau_1 = 3.082$ and $\tau_2 = 3.081$. For the same $G_6(s)$, Kaya and Atherton [10] 's asymmetrical relay test estimated $k = 1.0$, $\theta = 5.422$ and $\tau_1 = \tau_2 = 3.723$ after solving two nonlinear equations. Boiko [76] has identified the FOPDT model giving $k = 1.0$, $\theta = 7.675$ and $\tau_1 = 6.641$ using a piece-wise linear approximation method. Fig. 2.13 shows the Nyquist plots of the actual process and the identified model which again indicates a good agreement near to the critical point.

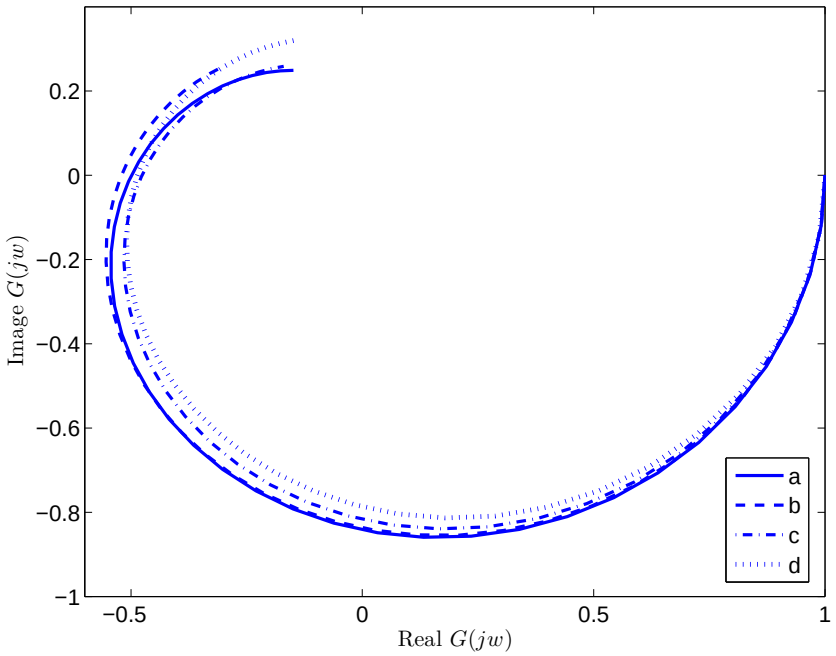

Figure 2.13: Nyquist plots for Example 6: (a) actual process, identified model by the (b) proposed method, (c) Boiko's method and (d) Kaya and Atherton's method

2.6 Summary

It is shown that how simple analysis of half limit cycle data can be used for identification of a class of processes with time delay. Models with up to four parameters can be identified by

means of a single symmetrical relay experiment, thus allowing one to acquire more information about the process dynamics from reasonably less amount of limit cycle data. The procedure can be used to estimate parameters of low order process models without solving any nonlinear equations and so it is free from any convergence problem unlike many relay based exact identification methods reported in the literature. To prevent the system from oscillating at high frequency and relay switching at wrong instants, relay hysteresis is adopted. Simulation examples illustrate the potential advantages of the proposed method.

CHAPTER 3

IDENTIFICATION OF NONLINEAR PROCESSES WITH MONOTONIC STATIC GAINS

3.1 Introduction

Recently, identification method for nonlinear processes has received much attentions since most physical systems are inherently nonlinear although in some cases they can be represented by linear models over a restricted operating range. A wide class of nonlinear processes, called block-oriented systems, can be modelled by interconnected memoryless nonlinear gains and linear subsystems [34]. Nonlinearities may enter the system in different ways: either at the input or at the output end or in the feedback path. A model in which the nonlinear static block is followed by the linear dynamic block is referred to as the Hammerstein model. The Wiener model uses the reverse order in that the nonlinear static block follows the linear dynamic block.

A number of relay feedback based methods have been reported in the literature for the process identification [77]. Improved relay feedback methods that used a saturation relay, a preload relay, an asymmetrical relay with state space approach and integral of the relay response are given in [7, 12, 16, 22]. These methods are successful in identifying the linear process models accurately but not the nonlinear process models. Luyben and Eskinat [26] proposed a relay based nonlinear auto-tuning variation test to determine nonlinear process models. Huang et al. [28] suggested the use of relays to estimate the Wiener-type process models. Although

their approach is simple, one needs to solve an optimizing algorithm for the optimal parameter vector which is used for estimating the static nonlinearity. Huang et al. [29] suggested a method to classify and identify nonlinear processes using two consecutive relay tests. Lee and Huang [27] adopted an optimization procedure to obtain a symmetric limit cycle output for Hammerstein-type processes. Sung and Lee [30] used a nonlinear control strategy to compensate the nonlinear dynamics of the Wiener type process using a relay feedback test. However, their method employs an approximate sinusoidal input before carrying out the test. Park et al. [31] proposed identification of Hammerstein-type processes using a relay feedback and a triangular input signal. Lee et al. [32] identified nonlinear process via an optimization procedure using an adjustable proportional-integral (PI) controller. Sung [33] proposed an estimation method for nonlinear static gains using a random binary signal that deactivate the effects of nonlinear gains. Yoneya [38] presented a method to identify the linear part of a process using fractional harmonic components from a limit cycle test. Jeng et al. [34] proposed a systematic approach to identify nonlinear processes using a set of relay settings and with an integrator in the loop. Sung and Lee [35] used the approximated sinusoidal test signal to manipulate the output nonlinearity and static disturbances by setting different time length of the relay output. Park and Lee [36] have suggested a simple identification method to estimate the nonlinear static function of the Wiener model using two step inputs with different widths and amplitudes and a least squares optimization. The enhanced activation method reported by Je et al. [37] estimates the process model parameters in an optimal way by solving a constrained nonlinear optimization procedure.

Most of the above methods reported in the literature [27–35,37,38] use an ideal relay instead of a relay with hysteresis thereby limiting the practical applicability of their techniques. Moreover, their methods require either special test signals or iterative optimization procedures or a set of approximations to estimate the nonlinear process model parameters. To overcome these limitations, a non-iterative approach to identifying Wiener and Hammerstein models, including model structure and parameters, is proposed. A single symmetrical relay test is conducted to determine the structure and then the parameters of the block-oriented nonlinear model pos-

sessing a static nonlinearity and a linear process in cascade. No other explicit input signal is required. A relay with hysteresis is used to prevent spurious switching of relay in the event of output measurement noise. The method is simple and gives improved performance than several identification methods for processes with static nonlinearity.

3.2 Modelling of nonlinear processes

Nonlinear processes are often represented in block-oriented forms as Wiener or Hammerstein types, as shown in Fig. 3.1 (a) and (b).

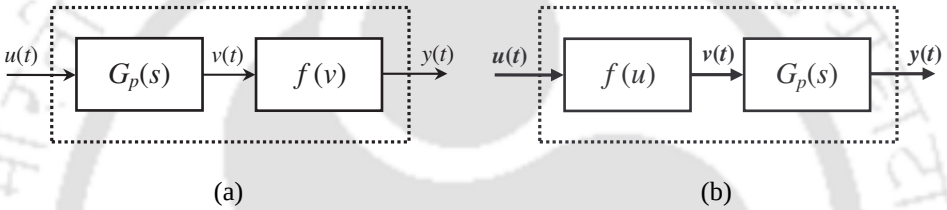

Figure 3.1: Nonlinear process models: (a) Wiener-type and (b) Hammerstein-type

Let the process input $u(t)$ and output $y(t)$ are measurable while the internal variable $v(t)$ is unmeasurable. Both the process models consist of a static nonlinear function denoted by $f(*)$ and a linear subsystem $G_p(s)$. It is assumed that $G_p(s)$ is a stable process and the static nonlinear function $f(*)$ is monotonic and crossing at the origin. The aim of this research is to estimate parameters of the linear subsystem and the static nonlinearity by reconstructing the internal variable from the available input-output data. A block diagram of relay feedback identification of nonlinear processes is shown in Fig. 3.2.

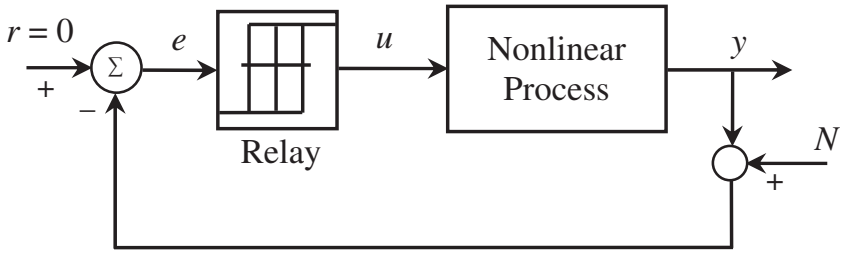

Figure 3.2: Structure for identification of the nonlinear process

Huang et al. [29] presented a strategy for selecting a feasible model structure via features of observed output from an ideal symmetrical relay test. They decided the model configuration based on the positive duration, T_+ and the negative duration, T_- of a period of limit cycle output. When $T_+ = T_-$, the nonlinear process is the Wiener-type otherwise it is of the Hammerstein-type. But, an ideal relay without hysteresis may cause a relay chattering problem due to measurement noise and lead to difficulties in determining the period of a stable limit cycle accurately. To overcome this problem, a relay with hysteresis is used in this work. In the following, a criterion for deciding the structure of a nonlinear process model is introduced.

Let the relay amplitudes be $\pm h$ during a relay feedback test. Then, the area of the process input signal a_u over the last stable period T_p can be expressed as

$$a_u = \int_{t_0}^{t_0+T_p} u(t)\mathrm{dt} = |h|(T_+ - T_-) \tag{3.1}$$

The ideal relay yields a signal with $T_+ = T_-$ at the output of a nonlinear process that can be represented by Wiener-type models. However, when the relay possesses hysteresis with widths $\pm\varepsilon$, a_u becomes nonzero due to the relay switchings at $\pm\varepsilon$. As shown in Fig. 3.3, let Δ_+ and Δ_- are time elapsed for the output to range from 0 to $\pm\varepsilon$ and T'_+ and T'_- are time duration of positive and negative waveforms when the output goes from ε to 0, respectively. Also the positive and negative peak amplitudes of the output are A_1 and A_2, respectively.

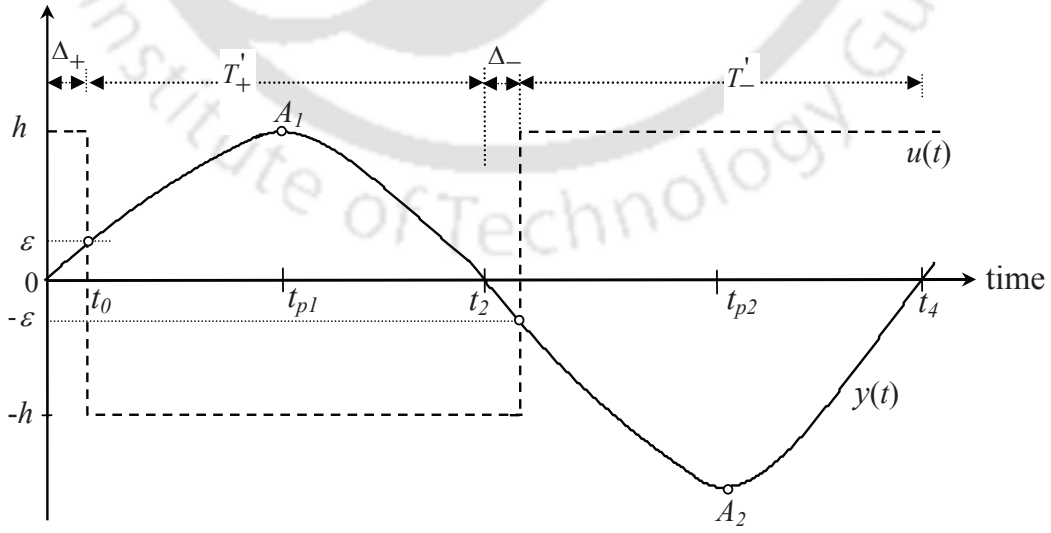

Figure 3.3: Typical relay feedback responses under a symmetrical relay with hysteresis test

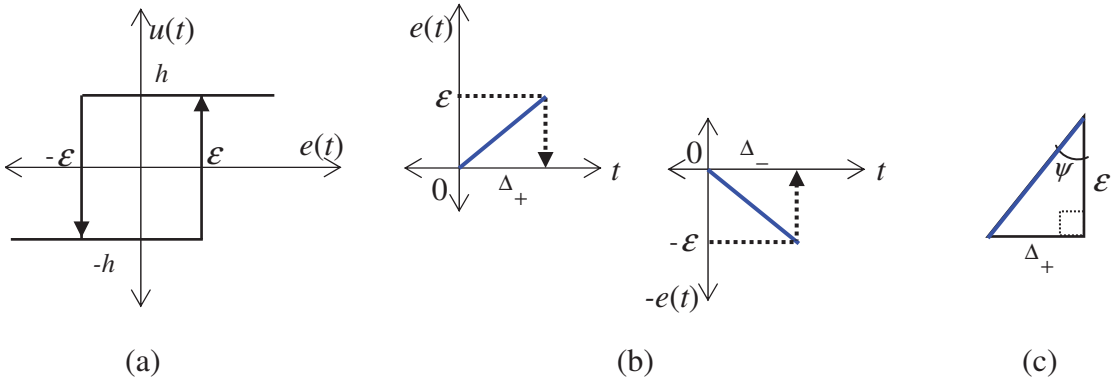

Figure 3.4: A symmetrical relay with hysteresis and its contributed area

Obviously due to the characteristics of a symmetrical relay, the output shows $T'_+ = T'_-$ and therefore (3.1) can be written as,

$$\begin{aligned} a_u &= |h|(T'_+ + \Delta_+ - T'_- - \Delta_-) \\ &= |h|(\Delta_+ - \Delta_-) \\ &< |h|\Delta_+ \quad , \quad \forall\ \Delta_+ > 0, \Delta_- > 0 \text{ and } (\Delta_+ - \Delta_-) < \Delta_+ \end{aligned} \tag{3.2}$$

Fig. 3.4 shows a symmetrical relay with hysteresis and its contributed area. Solving right triangles using trigonometry, it is found that an angle of $\psi = 45^\circ$ yields an optimum area of the triangle. Considering the optimum condition, (3.2) is expressed in terms of the relay parameters as

$$a_u < |h||\varepsilon| \tag{3.3}$$

which gives

$$\frac{a_u}{|h|} < |\varepsilon| \tag{3.4}$$

When the above condition is not satisfied then the nonlinear process is of Hammerstein-type. Thus, a relay with hysteresis test is conducted and (3.4) is used to determine the structure of a block-oriented nonlinear model. Table 3.1 summarizes the important features of the limit cycle data from a symmetrical relay with hysteresis test for structure identification under ideal operating condition.

Table. 3.1: Rules for selecting a feasible model structure

	Linear model	Wiener model	Hammerstein model
Peak Amplitudes	$A_1 = A_2$	$A_1 \neq A_2$	$A_1 \neq A_2$
Input area	$a_u = 0$	$\frac{a_u}{\lvert h \rvert} < \lvert \varepsilon \rvert$	$\frac{a_u}{\lvert h \rvert} > \lvert \varepsilon \rvert$

The linear subsystem $G_p(s)$ in both types of nonlinear models is assumed to have the transfer function

$$G_p(s) = \frac{e^{-\theta s}}{(\tau_1 s + 1)^2} \tag{3.5}$$

where θ and τ_1 denote the time delay and time constant, respectively. As illustrated by Panda and Yu [21] by quantitative classification of different model structures, the model (3.5) covers largest parameters space for the systems studied by them especially compared to a first order model structure that is widely practiced. Further, it is obvious that the high order processes having multi-repetitive poles can be represented by the second order model (3.5) with less estimation error and efforts. Here the hypothesis of unitary gain of G_p is not restrictive at all, since the static gain of a nonlinear process model is determined by the static nonlinearity, the gain of the linear subsystem is redundant and can be normalized to 1 [78, 79].

3.3 Estimation of Wiener model parameters

Let the process dynamics for Wiener-type model expressed in the time domain controllable canonical form has the state and output equations

$$\dot{\mathbf{x}}(t) = \mathbf{A}\mathbf{x}(t) + \mathbf{b}u(t-\theta) \tag{3.6}$$

$$v(t) = \mathbf{c}\mathbf{x}(t) \tag{3.7}$$

$$y(t) = f(v(t)) \tag{3.8}$$

where **A** is an 2×2 square matrix, **b** is an 2×1 column vector and **c** is a row vector of dimension 1×2. Also, let the static nonlinear function is approximated by a finite polynomial of the form

$$f(v(t)) = \sum_{j=1}^{m} \alpha_j v^j(t) \tag{3.9}$$

where α_j are constants and m is the order of the polynomial.

In Wiener-type model, the linear subsystem output $v(t)$ becomes symmetrical for a symmetrical relay input $u(t)$. The typical activated process input and output signal corresponding to a symmetrical relay with hysteresis test is shown in Fig. 3.5.

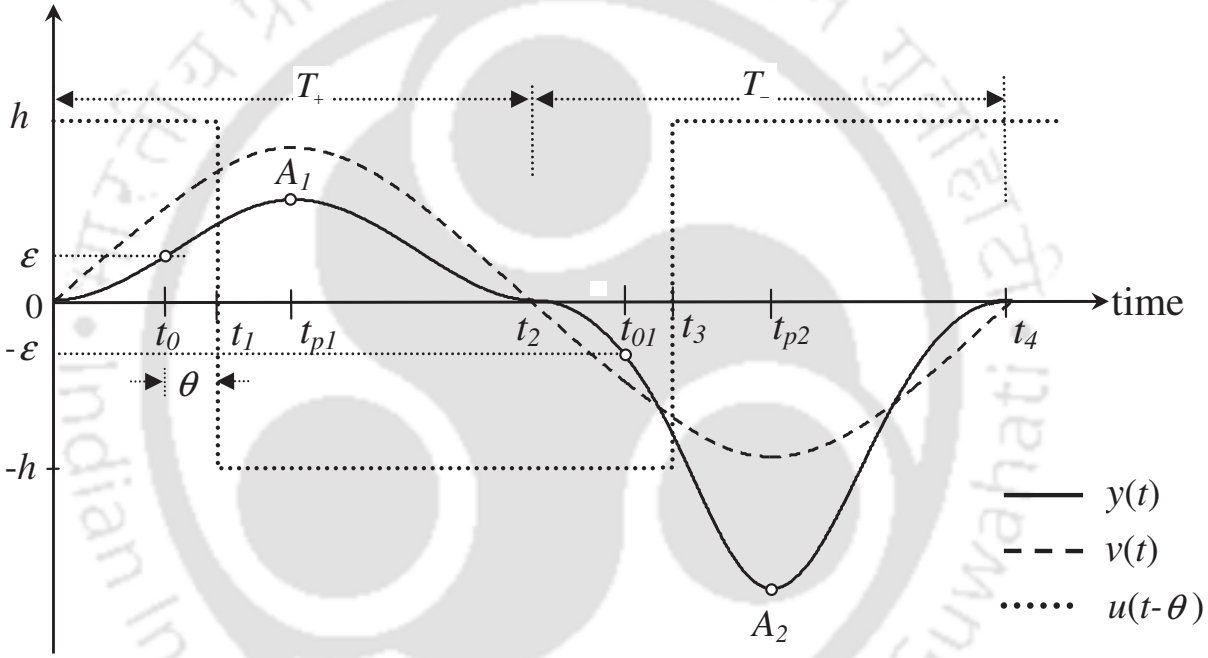

Figure 3.5: Input and output signals of the Wiener model under relay control

When the model transfer function (3.5) is expressed in the state space form, its state equation constants become

$$\mathbf{A} = \begin{bmatrix} -\frac{1}{\tau_1} & 1 \\ 0 & -\frac{1}{\tau_1} \end{bmatrix}; \quad \mathbf{b} = \begin{bmatrix} 0 \\ 1 \end{bmatrix}; \quad \mathbf{c} = \begin{bmatrix} -\frac{1}{\tau_1^2} & 0 \end{bmatrix} \tag{3.10}$$

Then it is easy to obtain the analytical expression for $v(t)$ waveform by substituting the above state equation constants in the expression of (2.9) in section 2.2. It gives the explicit relay

response waveform of $v(t)$ for time range $t_1 < t \leq t_{01}$ as

$$v(t) = -h\left(1 - c_1\, c_2\, e^{-\frac{(t-t_1)}{\tau_1}} - \frac{c_1}{\tau_1}\,(t-t_1)\, e^{-\frac{(t-t_1)}{\tau_1}}\right) \tag{3.11}$$

where $c_1 = 2(1+e^{-\frac{T_+}{\tau_1}})^{-1}$ and $c_2 = 1 - \frac{c_1\, T_+}{2\,\tau_1}\, e^{-\frac{T_+}{\tau_1}}$.

The first derivative of $v(t)$ in (3.11) with respect to t is

$$\dot{v}(t) = -h\left(\frac{c_1\, c_2}{\tau_1}\, e^{-\frac{(t-t_1)}{\tau_1}} + \left(\frac{t-t_1}{\tau_1} - 1\right)\frac{c_1}{\tau_1}\, e^{-\frac{(t-t_1)}{\tau_1}}\right) \tag{3.12}$$

3.3.1 Identification of the linear subsystem

First the time delay θ is obtained from the second derivative of $y(t)$ that shows a discontinuity in output at the time $t_1 = t_0 + \theta$, from its zero crossing due to non-monotonic characteristics of the limit cycle data [17]. But, we know that $y(t) = \varepsilon$ at time t_0. Thus, $\theta = t_1 - t_0$ is estimated from the measurements of t_0 and t_1 of $y(t)$ and $\ddot{y}(t)$, respectively.

Again for Wiener-type processes of which the static nonlinear gain is monotonic, the zero crossing points of the activated process output $y(t)$ and linear block output $v(t)$ are always symmetric in terms of time. Therefore, the time taken to reach from zero to peak amplitude will be the same for both $y(t)$ and $v(t)$ as shown in Fig. 3.5. Since $\dot{v}(t_{p1}) = \dot{y}(t_{p1}) = 0$ at time $t = t_{p1}$, then from (3.12) it is easy to obtain

$$c_2 + \left(\frac{t_{p1} - t_1}{\tau_1} - 1\right) = 0 \tag{3.13}$$

$$1 - \frac{c_1\, T_+}{2\,\tau_1}\, e^{-\frac{T_+}{\tau_1}} = 1 - \left(\frac{t_{p1} - t_1}{\tau_1}\right) \tag{3.14}$$

Substitution of c_1 in the above equation gives the expression

$$\tau_1 = \frac{T_+}{\ln\left(\frac{T_+}{t_{p1}-t_1} - 1\right)} \tag{3.15}$$

Thus the time constant τ_1 can be estimated using (3.15) and the measurements T_+, t_1 and t_{p1} made on the limit cycle output signal $y(t)$.

3.3.2 Identification of the static nonlinear gain

As shown in Fig. 3.5, the outputs at t_{p1}, t_{p2}, t_0 and t_{01} are A_1, A_2, ε and $-\varepsilon$, respectively. It is now straightforward to estimate four corresponding input values using (3.11) at the above times. These input-output pairs are fitted to estimate the order of polynomial m as well as the constants $\alpha_j, (j = 1,..,m)$ of the nonlinear function described in (3.9). To decide the order of polynomial, one needs to know the shape characteristic of $f(v)$. Here, the shape approximation is done through the simplified graphical method in which the secant lines between each estimated point $(p_1(v_1,y_1),....,p_4(v_4,y_4))$ estimate minimum orders of polynomial. The detailed justification of this method is given in Appendix A.2. The steps are:

1. Mark the estimated input-output pairs namely, p_1, p_2, p_3 and p_4 for the time instants t_{p1}, t_{p2}, t_0 and t_{01} respectively.
2. Draw the secant line connecting each point as shown in Fig. 3.6.
3. If a line crosses from Side-1 to Side-2 (or vice-versa), take a minimum order of polynomial $m = 4$ otherwise $m = 2$.

Finally, the steps for determining parameters of the Wiener-type process model are summarized below.

Step 1. Obtain the limit cycle data [T_+, T_-, t_0, t_1, t_{p1}] as shown in Fig. 3.5. Find its second derivative and estimate the time delay θ.

Step 2. Estimate the time constant τ_1 of a linear subsystem using (3.15).

Step 3. Calculate magnitudes of the internal signal $v(t)$ at the time instants $(t_{p1}, t_{p2}, t_0, t_{01})$ using (3.11).

Step 4. Obtain the static nonlinear function $f(v(t))$ by fitting the calculated values of $v(t)$ and the process limit cycle output $y(t)$ at the above time instances.

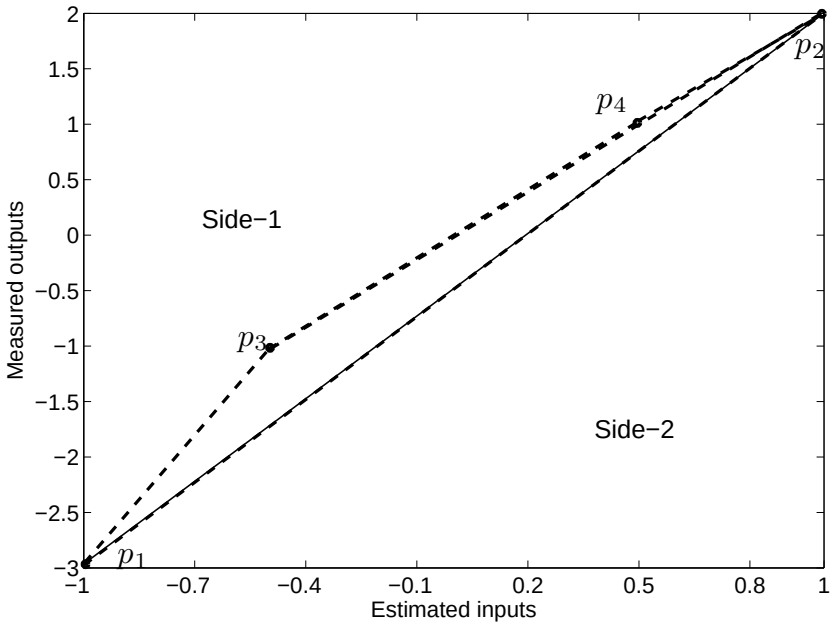

(a)

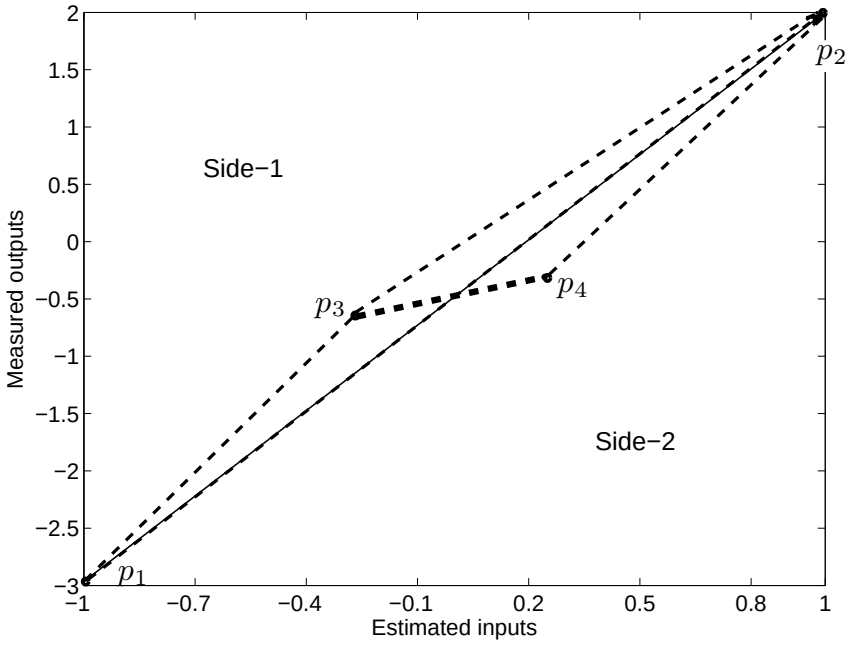

(b)

Figure 3.6: A graphical method to estimate value of m: (a) Order of polynomial $m \geq 2$ and (b) Order of polynomial $m \geq 4$

3.4 Estimation of Hammerstein model parameters

Similar to the Wiener-type, the Hammerstein-type process is expressed in the Jordan canonical state space form as

$$v(t) = f(u(t)) = \sum_{j=1}^{m} \alpha_j u^j(t) \tag{3.16}$$

$$\dot{\mathbf{x}}(t) = \mathbf{A}\mathbf{x}(t) + \mathbf{b}v(t-\theta) \tag{3.17}$$

$$y(t) = \mathbf{c}\mathbf{x}(t) \tag{3.18}$$

The constant matrix / vectors are of the form given in (3.10). Performing a symmetrical relay test, the output of the Hammerstein-type process becomes an asymmetrical where $A_1 \neq A_2$ and $T_+ \neq T_-$ as shown in Fig. 3.7. Although the process input is symmetrical, the linear subsystem is essentially activated by an asymmetric relay signal, say v_1 and $-v_2$ due to combine effect of the relay and the static nonlinear gain. One has to estimate these internal variables (v_1 and v_2) for ease in obtaining the model parameters. Typical waveforms of the internal signal $v(t)$ and the process output $y(t)$ obtained from the Hammerstein-type processes under the relay feedback are shown in Fig. 3.7.

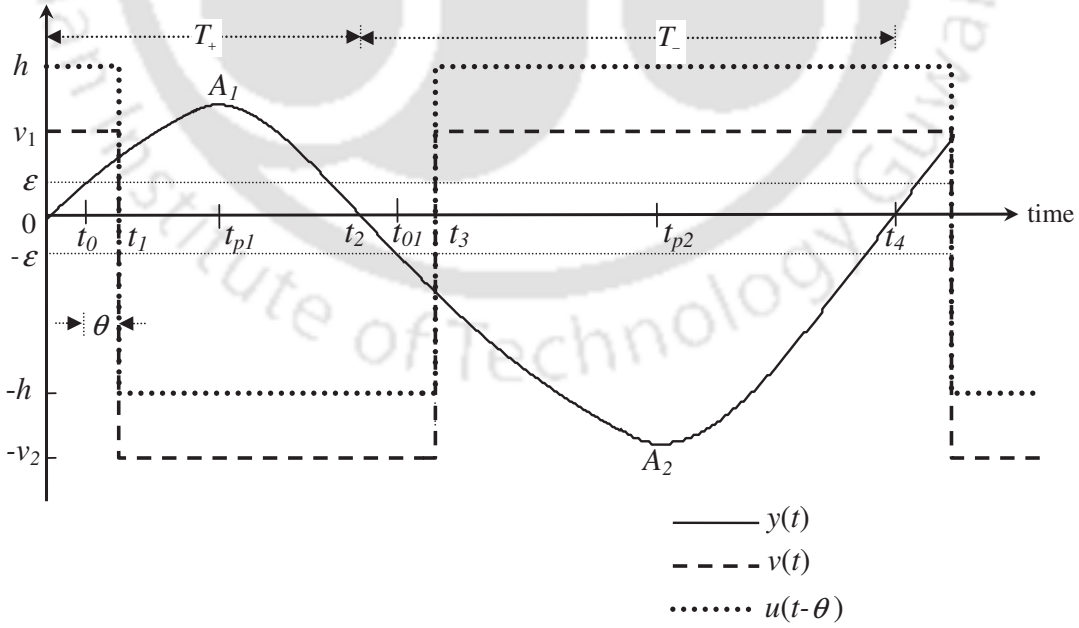

Figure 3.7: Input and output signals of the Hammerstein model under relay control

The expression for an asymmetrical limit cycle output during $t_1 < t \leq t_{01}$ when input is $-v_2$ becomes

$$y(t) = (v_1 + v_2)\, e^{-\frac{(t-t_1)}{\tau_1}} \left(d_1 + \frac{d_1(t-t_1)}{\tau_1} + \frac{d_2}{\tau_1} \right) - v_2 \tag{3.19}$$

where $d_1 = \frac{1-e^{-\frac{T_p-T_+}{\tau_1}}}{1-e^{-\frac{T_p}{\tau_1}}}$, $d_2 = \frac{T_p\, e^{-\frac{T_p}{\tau_1}}\, (1-e^{-\frac{T_p-T_+}{\tau_1}})}{(1-e^{-\frac{T_p}{\tau_1}})^2} - \frac{(T_p-T_+)\, e^{-\frac{T_p-T_+}{\tau_1}}}{(1-e^{-\frac{T_p}{\tau_1}})}$ and $T_p = T_+ + T_-$.

The proof of the above expression is given in the Appendix A.1. The first and second derivative of $y(t)$ in (3.19) with respect to t are

$$\dot{y}(t) = -\frac{v_1 + v_2}{\tau_1^2}\, e^{-\frac{(t-t_1)}{\tau_1}} (d_1(t-t_1) + d_2) \tag{3.20}$$

$$\ddot{y}(t) = -\frac{v_1 + v_2}{\tau_1^2}\, e^{-\frac{(t-t_1)}{\tau_1}} (d_1 - \frac{d_1(t-t_1)}{\tau_1} - \frac{d_2}{\tau_1}) \tag{3.21}$$

Since $\dot{y}(t_{p1}) = 0$ when $y(t)$ is maximum, (3.20) gives

$$d_1\, (t_{p1} - t_1) = -d_2 \tag{3.22}$$

By using (3.22) in (3.21) at $t = t_{p1}$, it is easy to obtain

$$\ddot{y}(t_{p1}) = -\frac{v_1 + v_2}{\tau_1^2} d_1 e^{-(t_{p1}-t_1)/\tau_1} \tag{3.23}$$

Combining (3.19) and (3.23) at $t = t_{p1}$ and using (3.22),

$$\tau_1^2 = -\frac{v_2 + y(t_{p1})}{\ddot{y}(t_{p1})} \tag{3.24}$$

A similar relation can be obtained for the negative values of the process output (when input is v_1) as

$$\tau_1^2 = \frac{v_1 - y(t_{p2})}{\ddot{y}(t_{p2})} \tag{3.25}$$

Taking the ratio of (3.24) and (3.25) and further simplification gives

$$v_1 + v_2 \left(\frac{\ddot{y}(t_{p2})}{\ddot{y}(t_{p1})} \right) = y(t_{p2}) - y(t_{p1}) \left(\frac{\ddot{y}(t_{p2})}{\ddot{y}(t_{p1})} \right) \tag{3.26}$$

Likewise, the process output at time t_2 is zero as shown in Fig. 3.7. The expression (3.19) at time $t = t_2$ gives

$$(v_1+v_2)\,e^{-\frac{(t_2-t_1)}{\tau_1}}(d_1+\frac{d_1(t_2-t_1)}{\tau_1}+\frac{d_2}{\tau_1})=v_2 \tag{3.27}$$

At $t=t_2$, (3.20) can be expressed using (3.27) as

$$\dot{y}(t_2)=\frac{1}{\tau_1}((v_1+v_2)\;d_1\;e^{-(t_2-t_1)/\tau_1}-v_2) \tag{3.28}$$

The above equation can be rewritten as

$$d_1\;e^{-(t_2-t_1)/\tau_1}=\frac{1}{v_1+v_2}\,(v_2+\tau_1\,\dot{y}(t_2)) \tag{3.29}$$

Next, substitution of (3.27) and (3.29) in (3.21) for $t=t_2$ gives

$$v_2=-2\;\tau_1\,\dot{y}(t_2)-\tau_1^2\,\ddot{y}(t_2) \tag{3.30}$$

Putting the expression for τ_1^2 of (3.24) in (3.30), a linear equation of the following form

$$2\;\tau_1=-v_2\left(\frac{\ddot{y}(t_{p1})-\ddot{y}(t_2)}{\ddot{y}(t_{p1})\dot{y}(t_2)}\right)+\left(\frac{y(t_{p1})\ddot{y}(t_2)}{\ddot{y}(t_{p1})\dot{y}(t_2)}\right) \tag{3.31}$$

is obtained. Following the same procedure for the negative output values during input is v_1, one obtains

$$2\;\tau_1=v_1\left(\frac{\ddot{y}(t_{p2})-\ddot{y}(t_4)}{\ddot{y}(t_{p2})\dot{y}(t_4)}\right)+\left(\frac{y(t_{p2})\ddot{y}(t_4)}{\ddot{y}(t_{p2})\dot{y}(t_4)}\right) \tag{3.32}$$

Taking the ratio of (3.31) and (3.32), one gets another linear equation in terms of the measurable limit cycle data as:

$$v_1\left(\frac{\ddot{y}(t_{p2})-\ddot{y}(t_4)}{\ddot{y}(t_{p2})\dot{y}(t_4)}\right)+v_2\left(\frac{\ddot{y}(t_{p1})-\ddot{y}(t_2)}{\ddot{y}(t_{p1})\dot{y}(t_2)}\right)=\left(\frac{y(t_{p1})\ddot{y}(t_2)}{\ddot{y}(t_{p1})\dot{y}(t_2)}\right)-\left(\frac{y(t_{p2})\ddot{y}(t_4)}{\ddot{y}(t_{p2})\dot{y}(t_4)}\right) \tag{3.33}$$

Fig. 3.8 shows a typical limit cycle waveform and its first and second derivative at the end of a relay test. From one period of the limit cycle data, the two unknowns v_1 and v_2 are estimated using the expressions (3.26) and (3.33). Based on estimated outputs and corresponding inputs values, the constants of the nonlinear function (3.16) are calculated. The time constant τ_1 in $G_p(s)$ is obtained by substituting any one of the estimated value of v_1 and v_2 in (3.24) or (3.25). The second derivative plot, $\ddot{y}(t)$ gives the time delay θ as shown in Fig. 3.8.

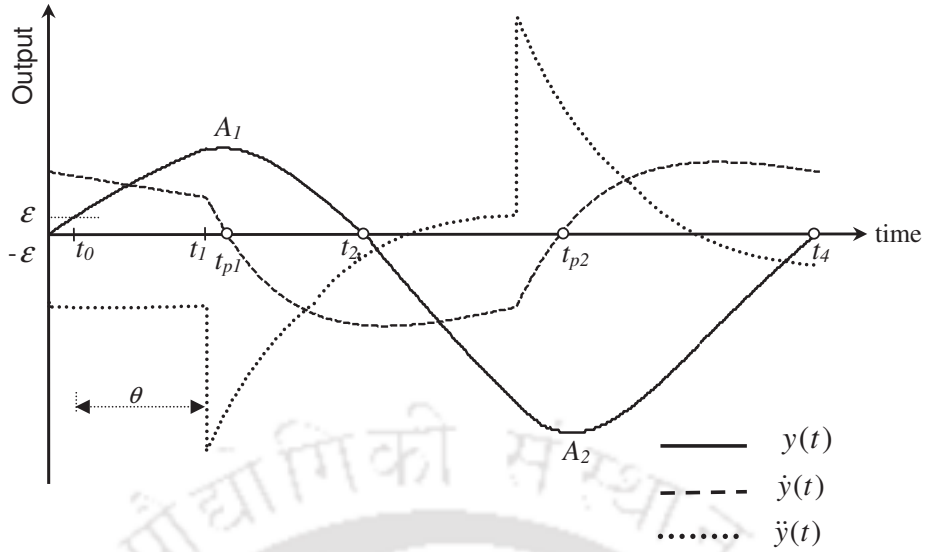

Figure 3.8: Output response and its first and second derivatives for the Hammerstein model

Finally, the steps for determining parameters of the Hammerstein-type process model are summarized below.

Step 1. Obtain the limit cycle data [T_+, T_-, t_0, t_1] and the output data [$y, \dot{y}, \ddot{y}$] at (t_{p1}, t_2, t_{p2}, t_4).

Step 2. Calculate the values of the internal signal (v_1, v_2) using (3.26) and (3.33).

Step 3. Obtain the static nonlinear function $f(u(t))$ using calculated values of $v(t)$. It is to be noted that one can obtain a higher order polynomial model for the static nonlinear function by repeating the same procedure from Step 1 with re-setting of the relay height.

Step 4. Estimate the time constant τ_1 using (3.24) or (3.25) and find the time delay from measuring t_0 and t_1 since $\theta = (t_1 - t_0)$.

3.5 Simulation study

In this section, a simulation study is conducted to verify the effectiveness of the proposed identification method. Two examples having a high order linear subsystem with two different static nonlinear gains are considered to illustrate the identification methods and compared with the reported methods. The effect of high frequency measurement noise is considered in Example

1 to demonstrate robustness of the approach. The width of the relay hysteresis is set to twice of the standard deviation of the noise to protect from the undesired relay chattering. Again the noisy limit cycle data is effectively denoised using the SG filtering technique as discussed in subsection 2.4.2.

To achieve better control performance, the overall estimation error should be small after combining both linear and nonlinear models and it is computed by an index using the integral squares error (ISE) criterion in time domain as

$$\text{ISE} = \int_0^{t_s} (y(t) - \hat{y}(t))^2 \, \mathrm{d}t \tag{3.34}$$

where, t_s is the settling time of the transient response under a step change, $y(t)$ and $\hat{y}(t)$ are the actual and estimated process outputs.

Example 1:

Consider the Wiener-type process with the higher order linear subsystem $G_1(s) = \frac{e^{-s}}{(s+1)^2(2s+1)^3}$ and the static nonlinear function, $f_1(v) = 2(1 - e^{-0.693v})$ studied by Huang et al. [28]. An autotuning test with the relay heights $h = \pm 1$ and hysteresis $\varepsilon = \pm 0.2$ results in a sustained process output as shown in Fig. 3.9.

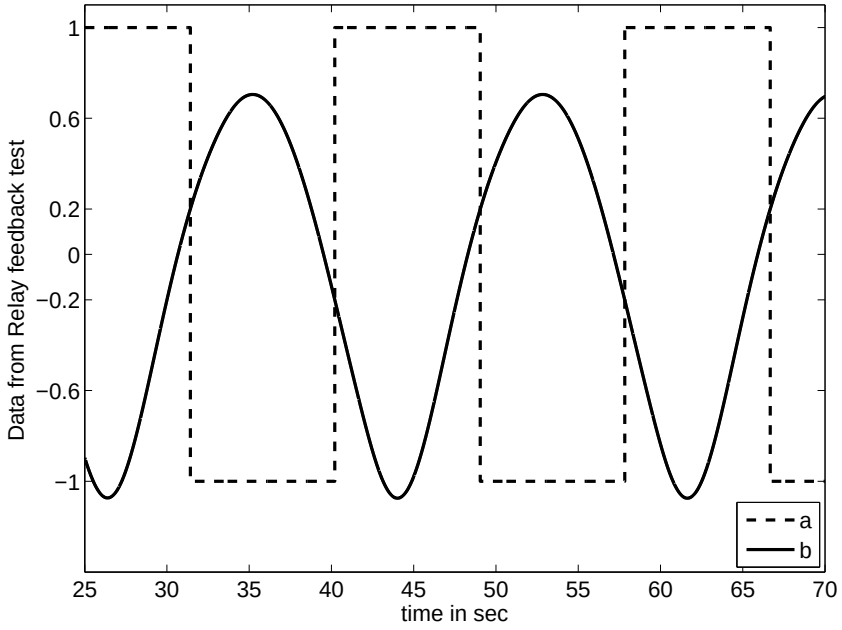

Figure 3.9: Simulation results for Example 1: (a) $u(t)$ and (b) $y(t)$

The measurements made on the limit cycle output yield $T_+ = 8.8462$, $T_- = 8.7790$, $A_1 = 0.7050$, $A_2 = -1.0747$, $t_0 = 0.6810$, $t_1 = 3.9823$ and $t_{p1} = 3.7933$. Since the criterion (3.4) gives $0.0842 < 0.2$ and $A_1 \neq A_2$, the Wiener model is estimated for the nonlinear process. Following the identification procedure described in Section 3.3, we obtain a linear subsystem model as $G_p(s) = \frac{e^{-3.3013s}}{(3.1239s+1)^2}$ and the static nonlinear function (3.9) as $y(t) = 1.4556v(t) - 0.4946v(t)^2$ using estimated intermediate values $(v_1, v_2) = (0.6114, -0.6114)$ at time t_{p1} and t_{p2}. The method reported by Huang et al. [28] uses two relay feedback tests with optimization searching problem to identify the linear model $\frac{e^{-3.780s}}{(0.308s+1)(5.295s+1)}$ and the static nonlinearity as $y(t) = 1.410v(t) - 0.464v(t)^2$. Now, the ISE by the proposed method is 0.7752 whereas that by the later method is 6.8546 for a step input change. The comparison of static nonlinearity functions and step response outputs from activated process models are shown in Figs. 3.10 and 3.11, respectively. It indicates the proposed identification method gives better results using a single relay feedback test without solving any optimization problem.

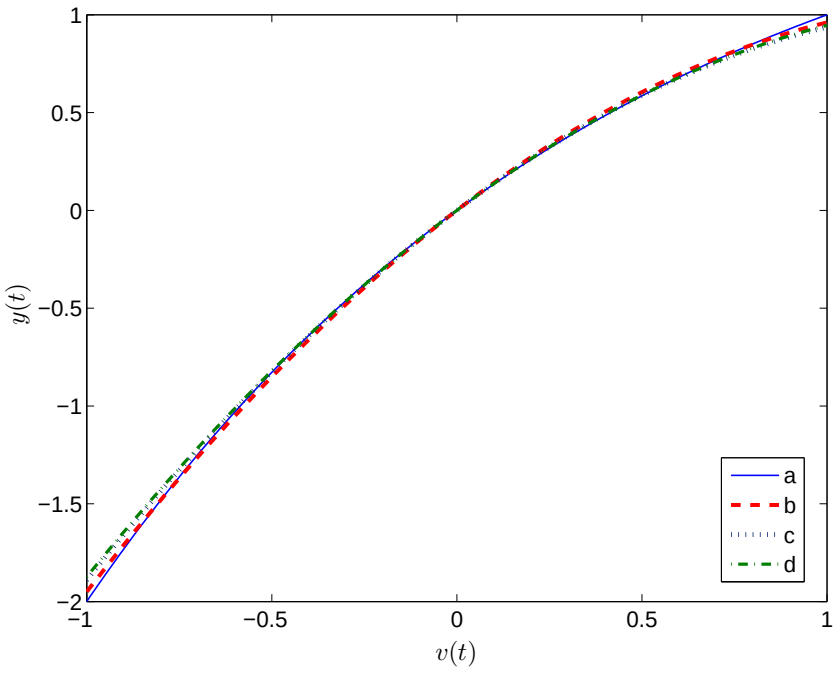

Figure 3.10: Static nonlinearity for Example 1: (a) Actual, (b) by the proposed method (no noise), (c) by the proposed method with SNR 10% and (d) by Huang et al.'s method

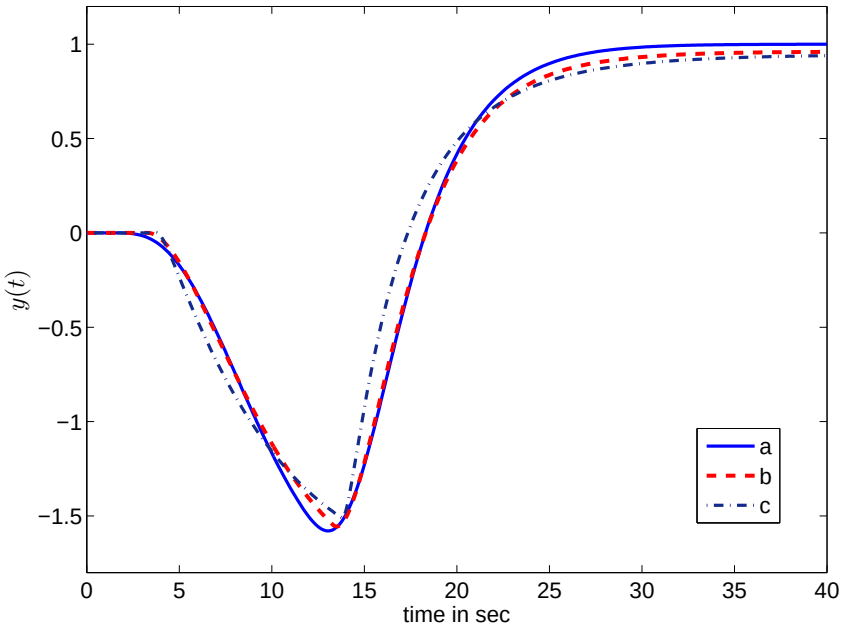

Figure 3.11: Responses under step change from -1 to 1: (a) by the actual process, (b) by the proposed method and (c) by Huang et al.'s method

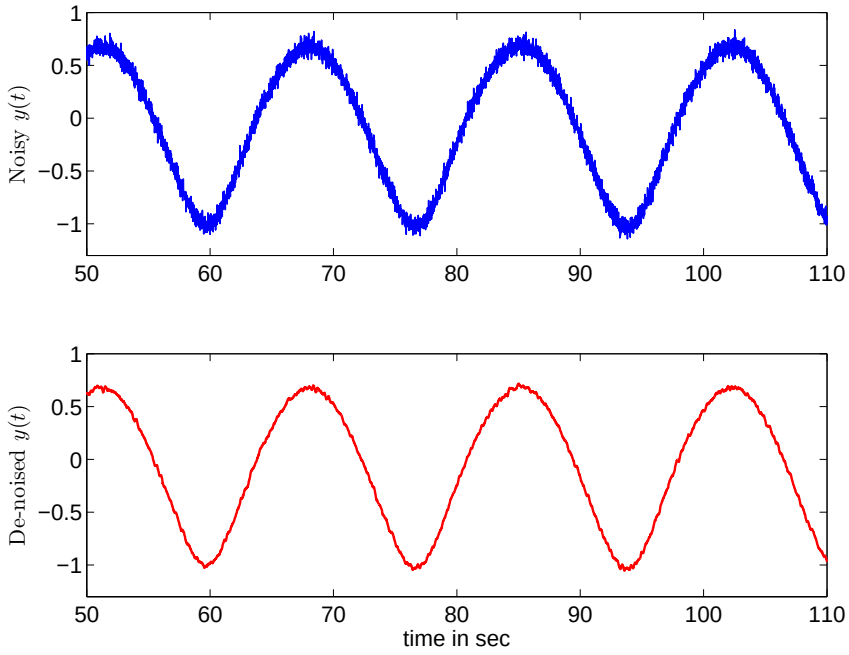

Figure 3.12: Noisy and smooth output signals

To verify usefulness of the identification method under realistic conditions, the process model parameters are estimated in the face of measurement noise. Let the process output is corrupted by Gaussian distributed random noise with 10 % SNR. The noise reduction using SG filter gives smooth output signal without attenuation of data features as shown in Fig. 3.12. The measured quantities from the de-noised output signal gives the static nonlinear model, $y(t) = 1.414v(t) - 0.477v(t)^2$ which is compared in Fig. 3.10. It is evident that the proposed identification scheme is robust against measurement noise.

Example 2:

Let us consider the Hammerstein-type process studied by Lee et al. [32] where the input nonlinearity $f_2(u) = 1.5(1 - e^{-0.5u})|u|$ and the linear subsystem $G_2(s) = \frac{e^{-s}}{(s+1)^2(2s+1)^3}$. First, from a relay settings of $h = \pm 1$ and $\varepsilon = \pm 0.1$, a sustained process output as shown in Fig. 3.13 is obtained. The output measurements give $T_+ = 7.6690$, $T_- = 9.9560$, $A_1 = 0.3753$ and $A_2 = -0.5805$. The criterion for structure identification (3.4) yields $2.2870 >> 0.1$ and since $A_1 \neq A_2$, therefore the Hammerstein model is identified.

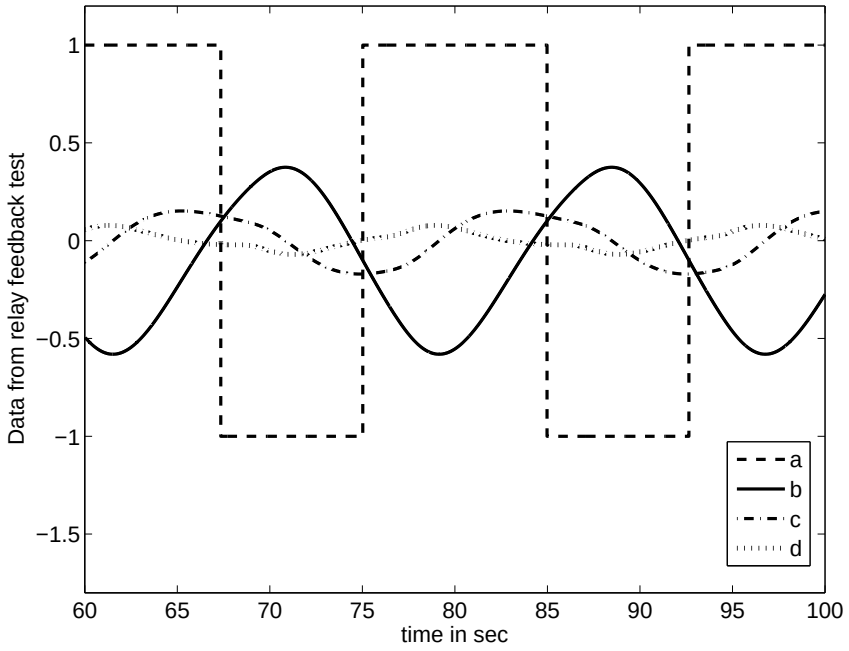

Figure 3.13: Simulation results for Example 2: (a) $u(t)$, (b) $y(t)$, (c) $\dot{y}(t)$ and (d) $\ddot{y}(t)$

Using the procedure outlined in Section 3.4, the limit cycle output data are measured at different time instances. The estimated nonlinear static function in the operation range $[-1,\ 1]$ is $v(t) = 0.2396u(t) - 0.0484u(t)^2 + 0.5425u(t)^3 - 0.1424u(t)^4$, while the linear subsystem model is $G_p(s) = \frac{1.0e^{-3.898s}}{(3.8866s+1)^2}$ with an estimation error of 0.2189. For the same nonlinear process, Lee et al.'s [32] optimization procedure using adjustable PI controller yields $v(t) = 0.266u(t) - 0.038u(t)^2 + 0.511u(t)^3 - 0.163u(t)^4$ and $G_p(s) = \frac{1.0e^{-3.82s}}{(2.74s+1)(2.63s+1)}$ with estimation error 0.2335.

It is also evident from Figs. 3.14 and 3.15 that the proposed identification scheme obtains comparable results with less efforts and time unlike their method [32] that requires one to solve an optimization problem in two different stages.

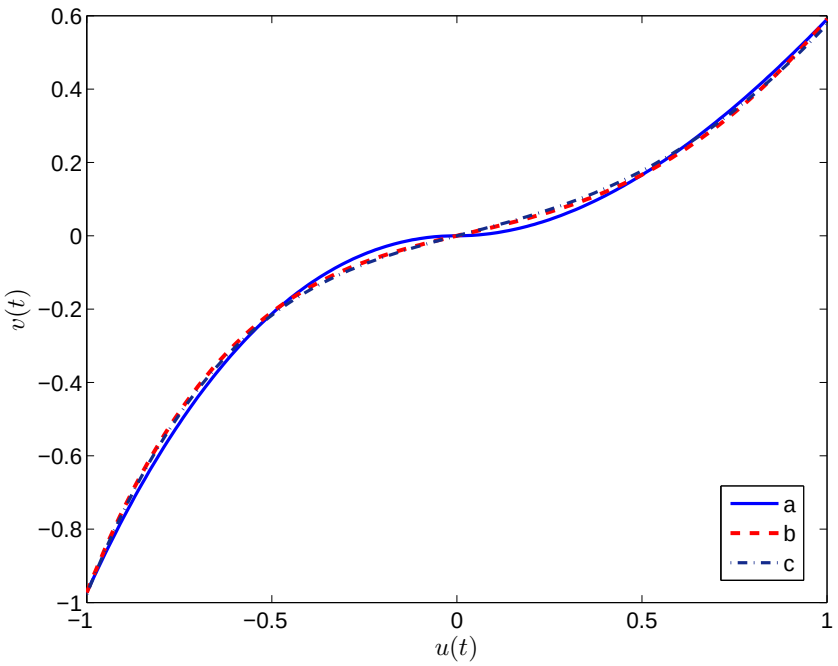

Figure 3.14: Static nonlinearity for Example 2: (a) Actual, (b) by the proposed method and (c) by Lee et al.'s method

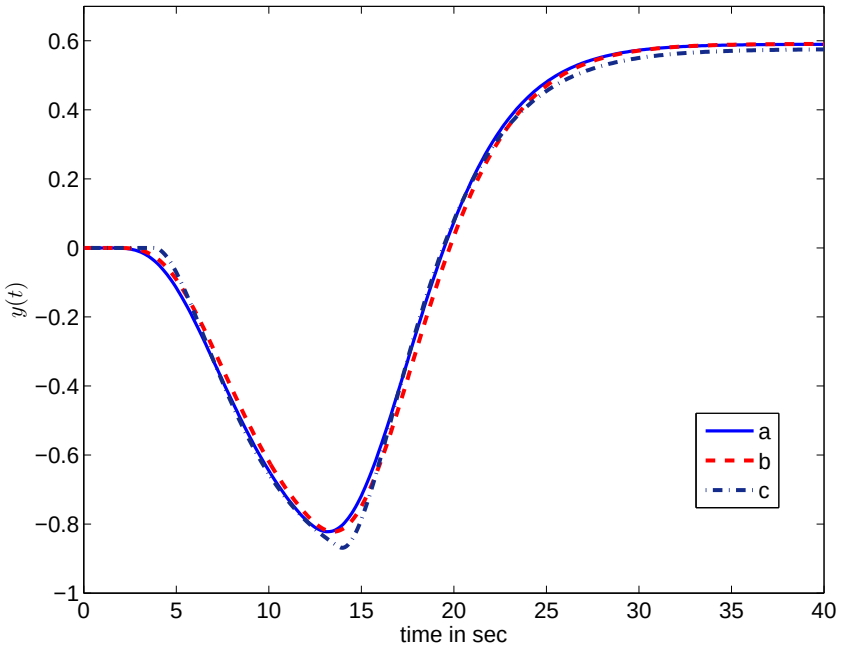

Figure 3.15: Responses under step change from -1 to 1: (a) by the actual process, (b) by the proposed method, and (c) by Lee et al.'s method

3.6 Real-time experimental study

An experimental setup using the Feedback [80] process control simulator PCS-327 and a Field Programmable Analog Arrays (FPAA) was developed to verify the efficacy of the proposed method. The setup is shown in Fig. 3.16.

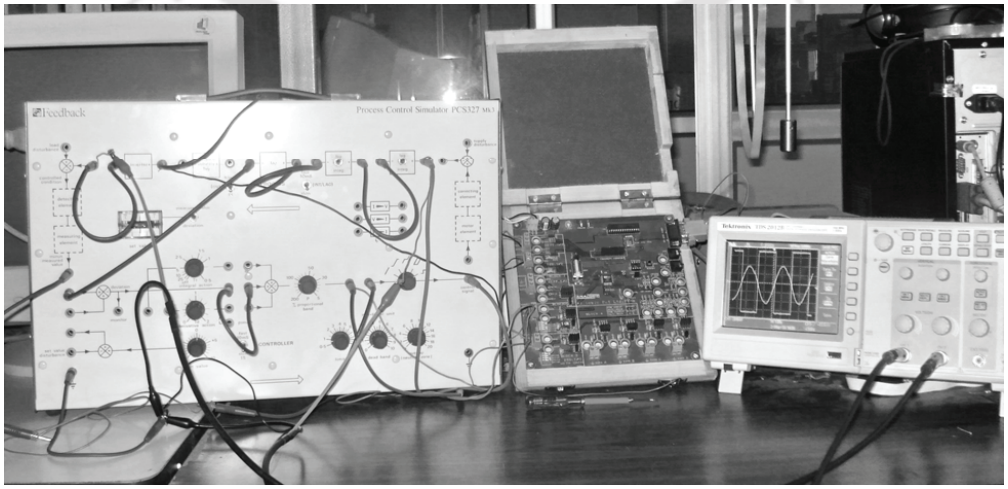

Figure 3.16: The experimental setup

The configuration was set with a transfer function $G_3(s) = \frac{1}{(s+1)^3}$ in the PCS, while a cascaded nonlinear gain of $f_3(v) = 2v(t) - v(t)^2$ in the FPAA. The sampling time was 10 msec. Fig. 3.17 shows the input and output signals obtained during a relay test with relay amplitudes ± 1 V and hysteresis 30 mV. The limit cycle data were measured as $T_+ = 1.720$ sec, $T_- = 1.731$ sec, $A_1 = 0.304$ V and $A_2 = -0.358$ V. As per the criteria in Table 3.1, the Wiener-type process is identified.

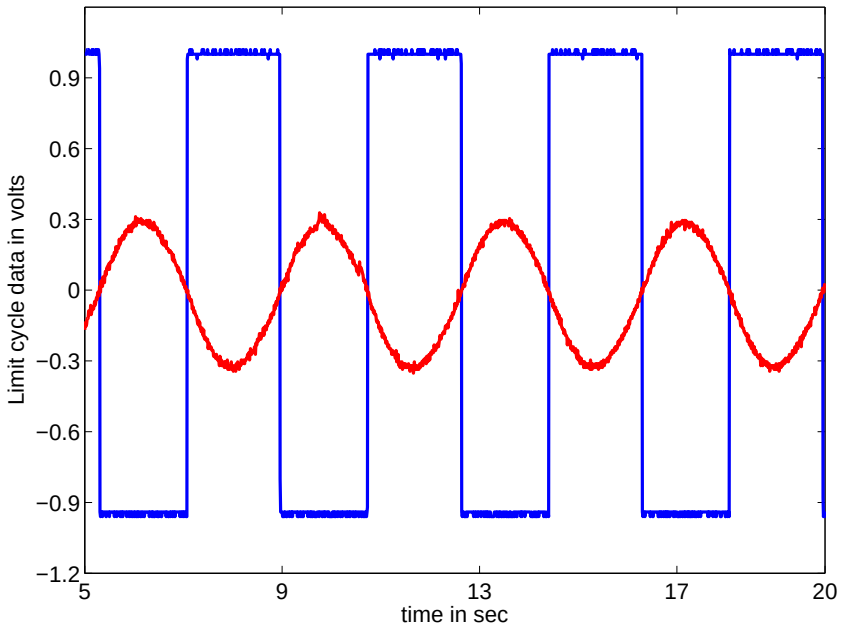

Figure 3.17: Experimental results after relay test

Following the identification procedure, a linear subsystem model $G_p(s) = \frac{e^{-1.3850s}}{(1.4097s+1)^2}$ and a nonlinear static function in the operation range $[-1,\ 1]$ V as $f(v) = 1.947v(t) - 1.005v(t)^2$ were estimated from a single relay test. The estimated process models and the actual process outputs are compared in Fig. 3.18. The identification procedure yields an estimation error of 0.9827. The good identification performance is evident from Fig. 3.18.

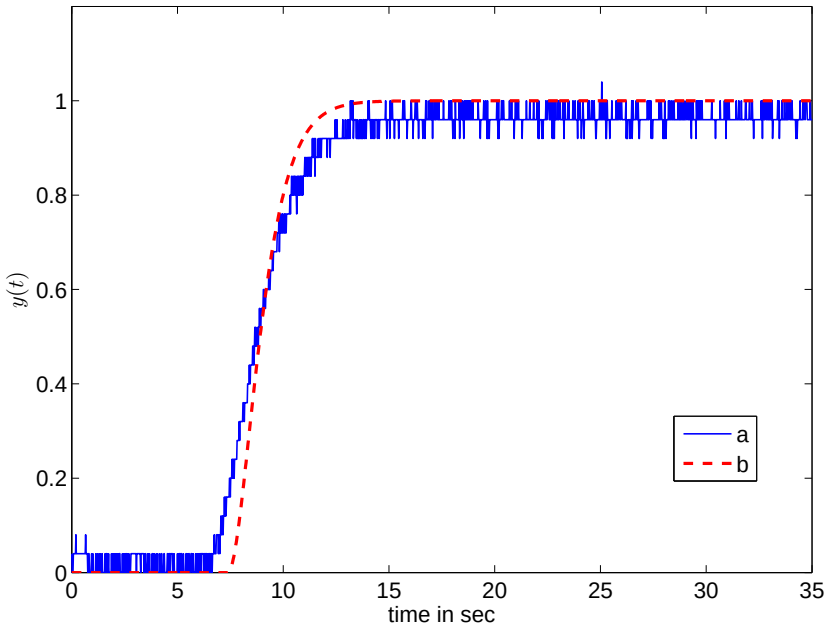

Figure 3.18: Responses under a step change: (a) by the actual process and (b) by the identified models

3.7 Summary

The basic relay autotuning method is extended for gathering more information for modelling a class of nonlinear processes. The extended method is not only non-iterative but also helps in estimating all the parameters of nonlinear process models from a single symmetrical relay test. The identification procedure having a relay with hysteresis is more acceptable in engineering practices to overcome the relay chattering problem. The procedure does not require any additional test signal, unlike some methods proposed in the literature, and is free from convergence problems. Furthermore, the simulation results show that the proposed identification method is superior to some existing methods.

CHAPTER 4

ON-LINE RELAY AUTO-TUNING FOR STABLE PROCESSES

4.1 Introduction

On-line identification for automatic tuning of controllers has received much attention during the last few years. This is mainly due to the fact that off-line tuning has associated implications like affecting operational process regulation which may not be acceptable for certain critical applications. Also, it has been reported that off-line tuning may be too expensive or dangerous when the control loop is broken for tuning purposes, and so tuning under tight continuous closed-loop control is necessary. One of the simplest and most robust auto-tuning techniques for process controllers is a relay feedback method. This has been subject of much interests in recent years and it has been field tested in a wide range of applications [3, 77]. However, the problem has not been fully solved that the loop is often opened and the process is disturbed to conduct the relay test [40].

Schei [42] proposed an on-line iterative method for closed-loop automatic tuning of the PID controller. The on-line experiment time by his method is very long which may not be acceptable in practice. Tan et al. [40] have proposed an on-line tuning method which is effective against many constraints of the basic relay auto-tuning method. The identification procedure by their direct method is not straightforward and one needs to have prior knowledge about the system to decide about the suitable frequency response prototypes. Further, their indirect controller tuning method uses the approximate describing function analysis to obtain a first order transfer function

model of the system. Some new results on auto-tuning have been presented by Tan et al. [43] for identifying an equivalent PID controller using the recursive least squares algorithm. Ho et al. [44] and Arruda et al. [81] have considered iterative methods based on specified phase margin. But, when a static load is present during the tuning experiment, their describing function based analysis may yield erroneous results. An on-line tuning method in which a relay is connected in series with a controller has been proposed by Majhi [45]. Recently, Tsay [46] has proposed on-line computing rules by introducing a relay with a pure time lag in the loop to find parameters of proportional-integral (PI) and lead compensators based on specified gain and phase margins. The method requires to initiate repetitive identification tests till an acceptable gain margin is found.

The applicability of the basic relay tuning method is extended in this chapter by an on-line method to tune PI controllers without breaking the closed-loop control. The proposed method is effective against many of the above mentioned constraints and also it retains the simplicity of the original relay based method. By placing a relay in parallel with a PI controller, to use the limit cycle oscillations induced in the steady state over a limited time span, the current process dynamics has been modelled by a low-order transfer function. Tuning formulae have been derived for the PI controller based on the parametric model such that it preserve the actuator from the large variation of control signals. Results from the simulation examples and real-time experiments are presented to show the simplicity and effectiveness of the proposed identification and control methods.

4.2 Analytical expressions for the limit cycle waveform

Departing from the conventional relay auto-tuning method where the controller is replaced by the relay, the proposed approach is to carry out on-line without breaking the closed-loop control by placing the relay in parallel with the controller. Fig. 4.1(a) shows the tuning scheme in which the relay height is increased from zero to some acceptable value when re-tuning is necessary. Based on the induced limit cycle oscillations at the process output, the process dynamics is first

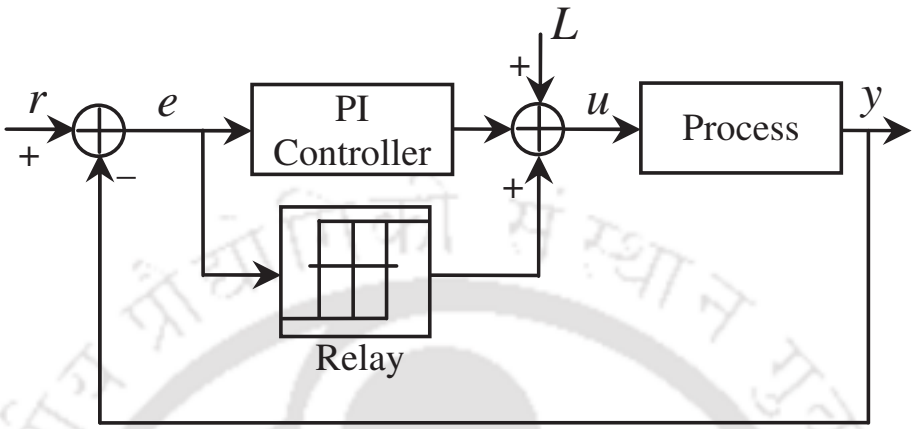

(a)

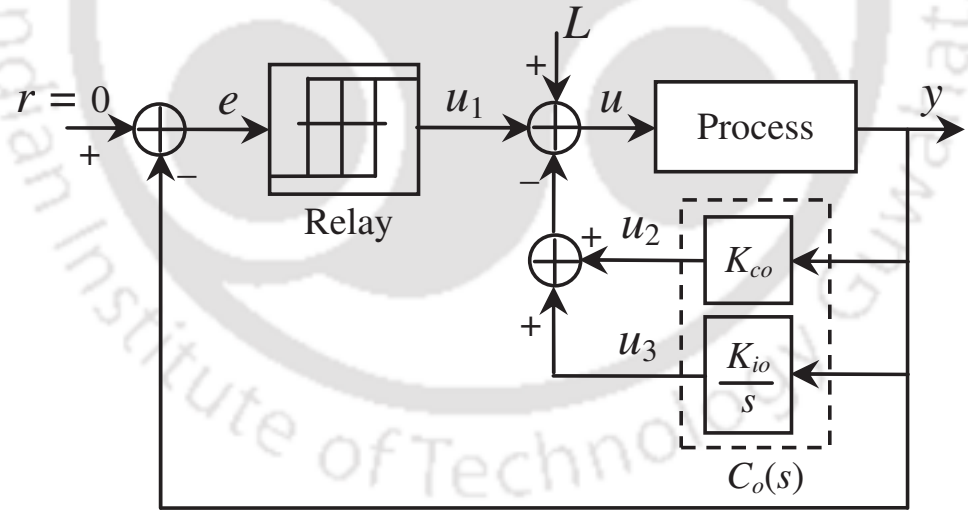

(b)

Figure 4.1: (a) Block diagram of on-line tuning scheme and (b) its equivalent form

identified by a simple transfer function model and then fine tuning of the existing PI controller is accomplished. Let us consider a first order rational transfer function model with dead time to approximate the process by

$$G_p(s) = \frac{ke^{-\theta s}}{\tau s + 1} \tag{4.1}$$

This model is simple in structure, with only three model parameters. Yet, it is one of the most common and adequate ones used, especially in the process control industries [39]. The initial PI controller at the time of relay feedback test is

$$C_o(s) = K_{co} + \frac{K_{io}}{s} \tag{4.2}$$

where K_{co} and K_{io} are its initial gains. This settings of the controller are intended primarily for the purpose of stabilizing the process and may be based on simple a priori information about the process. Practical applications of auto-tuning methods have been mainly to derive more efficient updates of current or default control settings, which are already available in many cases.

If the relay of amplitude $\pm h$ and hysteresis width $\pm\varepsilon$ is connected in parallel with $C_o(s)$ during the on-line tuning test, then the structure can be redrawn equivalently as shown in Fig. 4.1(b). The fictitious transfer function model (which the relay sees) becomes

$$\frac{y(s)}{u_1(s)} = \frac{k\, e^{-\theta s}}{\tau s + 1 + kK_{co}e^{-\theta s} + \frac{kK_{io}}{s}e^{-\theta s}} \tag{4.3}$$

It is to be noted that disturbance input L has no impact on the limit cycle output in steady state due to the integral action of the PI controller. Cross multiplication of (4.3) and inverse Laplace transform yields

$$\dot{y}(t) = -\frac{y(t)}{\tau} + \frac{k}{\tau}\left(u_1(t-\theta) - K_{co}y(t-\theta) - K_{io}\int_0^t y(t-\theta)\ \mathrm{dt} \right) \tag{4.4}$$

Assume that the autotuning test produces a symmetrical limit cycle with half period T which is obtained with the initial condition $y(t_0)$. Fig. 4.2 shows waveforms of the relay output and process output signals when the half period T is greater than the time delay, θ. For the time range $t_0 \le t \le t_1$ where the relay output $u_1(t-\theta) = h$, the analytical expression for the limit cycle output waveform is

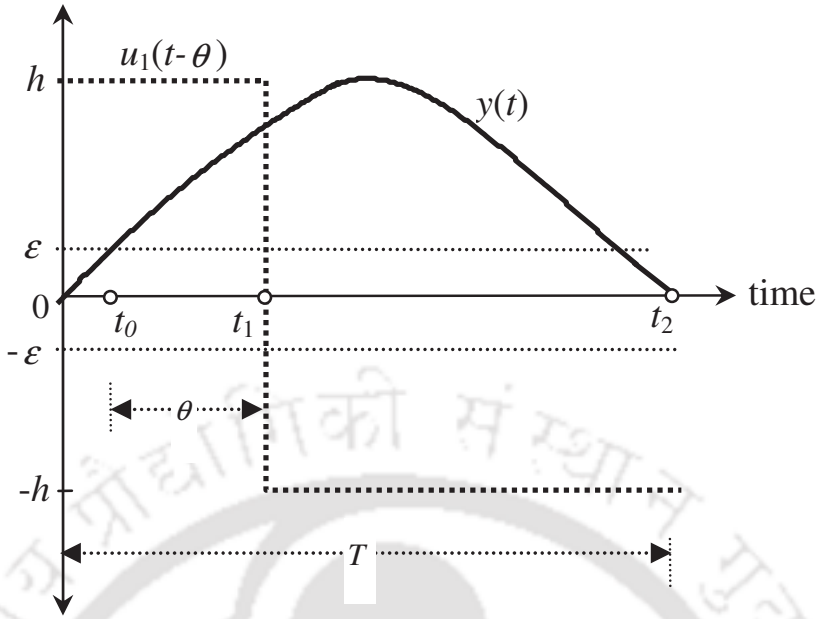

Figure 4.2: Half period of limit cycle output and relay output signals

$$y(t) = y(t_0)e^{-\frac{t-t_0}{\tau}} + k(1-e^{-\frac{t-t_0}{\tau}})\left(h - K_{co}y(t-t_0) - K_{io}\int_{t_0}^{t} y(t-t_0)\,\mathrm{dt}\right) \tag{4.5}$$

For the time range $t_1 < t \leq t_2$, where $u_1(t-\theta) = -h$ the expression becomes

$$y(t) = y(t_1)e^{-\frac{t-t_1}{\tau}} - k(e^{-\frac{t-t_1}{\tau}} - 1)\left(-h - K_{co}y(t-t_1) - K_{io}\int_{t_1}^{t} y(t-t_1)\,\mathrm{dt}\right) \tag{4.6}$$

Since the limit cycle is symmetrical, it follows that $y(t_0) = -y(t_2+t_0)$. With the help of the general method discussed in Section 2.2 for deriving the analytical expressions of the limit cycle output for the FOPDT model, one can simplify the above expressions (4.5) and (4.6). For time ranges $t_0 \leq t \leq t_1$ and $t_1 < t \leq t_2$, the output expressions are obtained as

$$\begin{aligned} y(t) = \varepsilon e^{-\frac{t-t_0}{\tau}} &+ kh(1-e^{-\frac{t-t_0}{\tau}})\left[1 - kK_{co} + kK_{io}\tau(1+e^{\theta/\tau})\right] \\ &- k^2h(t-t_0)\left[(-\frac{K_{co}}{\tau} + K_{io})e^{-\frac{t-t_1}{\tau}} + K_{io}\right] \end{aligned} \tag{4.7}$$

$$\begin{aligned} y(t) = y(t_1)e^{-\frac{t-t_1}{\tau}} - kh(1-e^{-\frac{t-t_1}{\tau}}) &+ k^2h(-\frac{K_{co}}{\tau} + K_{io})\left[(t-t_1)(2e^{-\frac{t-t_1}{\tau}} - e^{-t/\tau}) - \tau(1-e^{-\frac{t-t_1}{\tau}})\right] \\ &+ k^2K_{io}h\left[(t-t_1) - \tau(1-e^{-\frac{t-t_1}{\tau}})(2-e^{-\theta/\tau})\right] \end{aligned} \tag{4.8}$$

4.3 On-line estimation of process model parameters

In this section, the procedure to estimate the process model parameters with the controller in action is discussed. This provides a high degree of robustness to the identification procedure against external disturbances and process perturbations. Further, the approach seeks a few measurement data from the half limit cycle output. Fig. 4.2 shows a half cycle waveform of the process output under a symmetrical relay feedback test.

From the tuning test, critical instants t_0 and t_2 are measured at which the outputs become ε and zero, respectively. The time instant t_1 can also be estimated using measured half cycle data [17]. The derivative of output $y(t)$ shall have a discontinuity in the output at the time $t_1 = t_0 + \theta$, from its zero crossing due to the non-monotonic characteristics of the limit cycle data. But, we know that $y(t) = \varepsilon$ at time t_0 and this fact gives the time delay $\theta = (t_1 - t_0)$.

Now, the remaining parameters of the process model are obtained by using the limit cycle expressions (4.7) and (4.8). These expressions can further be simplified by taking values for t_0 and t_2 where $y(t)$ becomes ε and zero, respectively. If we take a first order time derivative of $y(t)$ for the time ranges $t_0 \leq t \leq t_1$ and $t_1 < t \leq t_2$, then

$$\begin{aligned}\dot{y}(t) = -\frac{\varepsilon}{\tau}\, e^{-\frac{t-t_0}{\tau}} &+ \frac{kh}{\tau} e^{-\frac{t-t_0}{\tau}} \left[1 - kK_{co} + kK_{io}\tau(1+e^{\theta/\tau})\right] \\ &+ k^2 h(-\frac{K_{co}}{\tau} + K_{io}) e^{-\frac{t-t_1}{\tau}} (\frac{t-t_0}{\tau} - 1) - k^2 K_{io} h \end{aligned} \tag{4.9}$$

$$\begin{aligned}\dot{y}(t) = -\frac{y(t_1)}{\tau} e^{-\frac{t-t_1}{\tau}} - \frac{kh}{\tau} e^{-\frac{t-t_1}{\tau}} &+ k^2 h(-\frac{K_{co}}{\tau} + K_{io}) \left[-\frac{t-t_1}{\tau}(2e^{-\frac{t-t_1}{\tau}} - e^{-t/\tau}) + (e^{-\frac{t-t_1}{\tau}} - e^{-t/\tau})\right] \\ &+ k^2 K_{io} h \left[1 - (e^{-\frac{t-t_1}{\tau}})(2 - e^{-\theta/\tau})\right] \end{aligned} \tag{4.10}$$

Setting $t = t_0$ in (4.9), a simple expression is obtained as

$$\dot{y}(t_0) = \frac{kh - \varepsilon}{\tau} + \frac{k^2 K_{co} h}{\tau}(e^{\theta/\tau} - 1) \tag{4.11}$$

Since $y(t_2) = 0$, another simplified expression is obtained using (4.10) at time t_2 as

$$\dot{y}(t_2) = -\frac{kh}{\tau} - k^2 h(-\frac{K_{co}}{\tau} + K_{io})(1 - 2e^{-\frac{t_2-t_1}{\tau}} + e^{-\frac{t_2}{\tau}}) \tag{4.12}$$

With the help of (4.11) and (4.12) the two unknown parameters k and τ of the process model are estimated. A non-linear algebraic equation solver like NESOLVE routine in MATLAB can

be used to solve these equations with suitable initial guess. In practice typical ranges for the values of the parameters are often known and it can also be obtained using simple describing function method in which case the convergence is fast.

4.4 Optimal PI controller design

When the process transfer function is known, the parameters of the PI controller may be optimised by minimising an integral performance criterion [82]. In particular, time moment weighted integral performance criteria gives a good step response with a small overshoot and short settling time [82]. But the optimal controller by this method may not be sufficient to obtain the optimum control input variations. In most PI(D) control loops valves are the only components with moving parts and more variation in control signal has high costs in terms of valve wear and maintenance programs. A quantitative analysis of how tuning affects valve costs is described in [49]. In this context, less attention has been paid, although recently a different kind of criterion in [51] has been defined to minimize the variations in $u(t)$. Their method is based on the integral time absolute error (ITAE) index and gives much smoother control by some link between the controller aggressiveness and the minimum of the ITAE performance index. However, it is shown for processes with small time delay and the relation is derived based on ITAE index, which may not be very accurate for the initial unavoidable errors during setpoint changes [82]. This is not the case with the time weighted ISE criterion. Therefore, the work of [51] is extended here using the integral squared time error (ISTE) index to achieve the overall smooth responses, which preserve actuators from untimely attrition.

The dynamics of a first order model (4.1) may be described in the normalized form by scaling the Laplace variable s to s/τ as

$$G_p(s) = \frac{ke^{-\theta_n s}}{(s+1)} \tag{4.13}$$

where $\theta_n = \theta/\tau$. Hence, if subsequently tuned $C(s)$ has the normalized transfer function

$$C(s) = K_c + \frac{K_i}{s} \tag{4.14}$$

where K_c and K_i are control gains to be determined from the tuning experiment, the velocity form of (4.14) is given by [39]

$$\dot{u}(t) = K_c\dot{e}(t) + K_i e(t) \tag{4.15}$$

where $u(t)$ and $e(t)$ are assumed to be the controller output and input, respectively. Aiming to achieve superior control performance by optimizing error signal in such a way that it gives minimum control output variations. An index has been defined to measure the total variation (TV) in $u(t)$ analytically for the controller performance [50]. If we discretize the input signal as a sequence, $[u_1, u_2, ..., u_i, ...]$, then

$$\text{TV} = \sum_{i=1}^{\infty} |u_{i+1} - u_i| \tag{4.16}$$

which should be as small as possible to minimize variations in $u(t)$. Ideally $u(t)$ should be equal to $u(\infty)$ for all $t > 0$, hence $\dot{u}(t) = 0, \forall\ t > 0$. This concept provides the following constraint using the control law (4.15) as

$$K_c^2(\dot{e}(t))^2 = K_i^2(e(t))^2 \tag{4.17}$$

If we represent the above constraint in time weighted integral of error signal, it gives a tight criterion for the initial unavoidable errors during setpoint changes. Thus, (4.17) is replaced by the following integral constraint as

$$\left(\frac{K_c}{K_i}\right)^2 \int_0^{\infty} (t\dot{e}(t))^2\,\text{dt} = \int_0^{\infty} (te(t))^2\,\text{dt} \tag{4.18}$$

First, it turns out that the right-hand side of (4.18) is the well-known ISTE performance index [82]

$$\text{ISTE} = \int_0^{\infty} (te(t))^2\,\text{dt} \tag{4.19}$$

which can be characterized with the integral control action of the PI controller. Similarly, the left-hand side of (4.18) introduces another performance index involving the derivative of the error signal to characterize the proportional control action as

$$\text{ISTD} = \left(\frac{K_c}{K_i}\right)^2 \int_0^{\infty} (t\dot{e}(t))^2\,\text{dt} \tag{4.20}$$

The index in (4.20) is defined as weighted Integral of Squared of Time Derivative of error signal (ISTD). Now, the closed-loop errors after a unit step input for the FOPDT process model (4.13) are

$$\begin{aligned} e(t) &= k, \qquad \text{for } 0 \le t < \theta_n \\ &= ke^{-(t-\theta_n)}, \text{ for } t \ge \theta_n \end{aligned} \tag{4.21}$$

The two performance indices (4.19) and (4.20) are simplified using (4.21) and an explicit design formula for K_c is obtained as

$$K_c = K_i\ \tau \left(\frac{1+2\theta_n+2\theta_n^2+(4/3)\theta_n^3}{1+2\theta_n+2\theta_n^2} \right)^{1/2} \tag{4.22}$$

To obtain another explicit relation for the controller gain, the concept of sluggishness index is used which reflects how much the closed-loop reduces the measure of response time relative to that of the open loop process [83]. If we take the average residence time of the open-loop process as $-G'(0)/G(0) = (\tau+\theta)$ [39], then for the closed-loop transfer function

$$T(s) = \frac{C(s)G_p(s)}{1+C(s)G_p(s)} = \frac{ke^{-\theta_n s}(K_c s+K_i)}{s(s+1)+ke^{-\theta_n s}(K_c s+K_i)} \tag{4.23}$$

the average residence time is calculated from $-T'(0)/T(0)$ as $\frac{1}{kK_i}$. Thus, by equating the average residence time for open-loop and close-loop transfer function, another explicit design rule for setting the integral gain K_i in terms of the parametric model values becomes

$$K_i = \frac{1}{k\tau(1+\theta_n)} \tag{4.24}$$

Using (4.22) and (4.24), the new PI controller gains are calculated based on the estimated process model parameters during the on-line relay test.

4.5 Evaluation of the tuning rules

The primary control design goal is to achieve good rejection of load disturbance effects and robustness with respect to model uncertainties. First, it is to be noted that a larger integral gain usually implies less robustness in the presence of load disturbances and it can be defined by an expression to measure the system performance [84]. This analysis is extended below for the case with input disturbance. The general closed-loop transfer function from input load

disturbance L to output y is,

$$T_{yd}(s) = G_p(s)(1+G_p(s)C(s))^{-1} \tag{4.25}$$

In industrial processes, the disturbance usually occurs at low frequency. Then the above expression can be written in the magnitude of the frequency response where ω is small as

$$\begin{aligned}\overline{M}(T_{yd}(j\omega)) &= \overline{M}[G_p(j\omega)(1+G_p(j\omega)C(j\omega))^{-1}] \\ &= \overline{M}[G_p(j\omega)(1+G_p(j\omega)K_c+G_p(j\omega)K_i/(j\omega))^{-1}] \\ &\approx \overline{M}[G_p(j\omega)(G_p(j\omega)K_i/(j\omega))^{-1}]\end{aligned} \tag{4.26}$$

For any transfer functions A and B, it is well-known that $\overline{M}(AB) \leq \overline{M}(A)\overline{M}(B)$ and $\overline{M}(A)^{-1} = \underline{M}(A)$ where, $\overline{M}(*)$ and $\underline{M}(*)$ are the maximum and minimum magnitude of transfer functions $M(*)$, respectively . So, we have

$$\overline{M}(T_{yd}(j\omega)) \leq |j\omega|\frac{\overline{M}(G_p(j\omega))}{\underline{M}(G_p(j\omega))\underline{M}(K_i)} \tag{4.27}$$

It shows that the minimum value of integral gain can play an important role in the presence of load disturbance. The relation of normalized internal gain vs time delay from the proposed tuning method and optimum tuning methods like ITAE and ISTE for setpoint based methods are plotted in Fig. 4.3(a). It is observed that the integral gains given by the proposed method are almost constant, thus the closed-loop systems are very robust while others show oscillatory responses in the presence of load disturbance since integral gains are too large specially for small time delay processes. Also, for large time delay processes the proposed method gives slightly larger K_i resulting in the best compromise between robustness and load disturbance rejection performance.

Next, the robustness is evaluated from the maximum value of the sensitivity function, $M_s = ||(1+G_p(j\omega)C(j\omega))^{-1}||$. Reasonable values of M_s are in the range from 1.2 to 2.0 [39]. The proposed tuning method has been applied to the different processes of the test batch given in [39] as representative of typical industrial processes. Fig. 4.3 (b) gives the Nyquist curves of the test processes which indicates the maximum sensitivity gain between 1.2 to 2.0. This shows that the on-line tuning method provides robust stability against modelling error and variations in process dynamics.

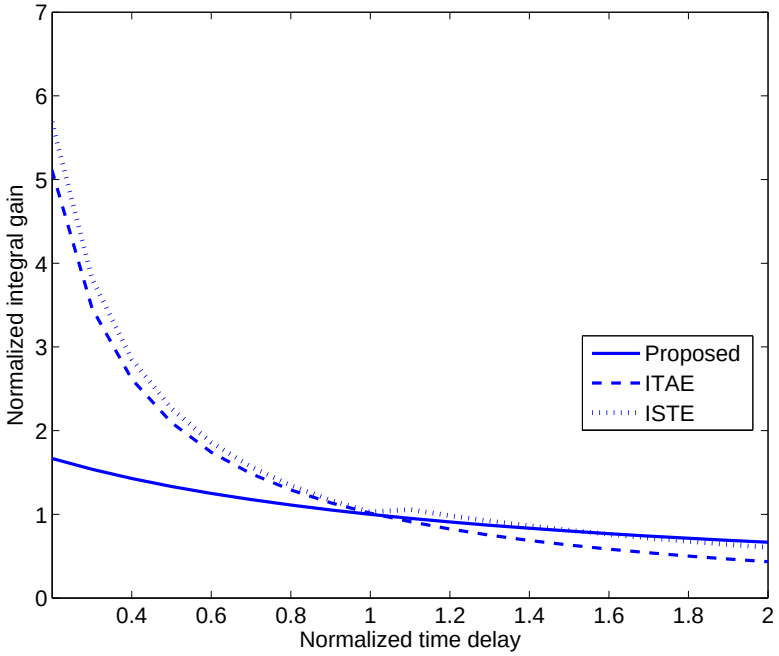

(a) Relationships between integral gains and θ_n

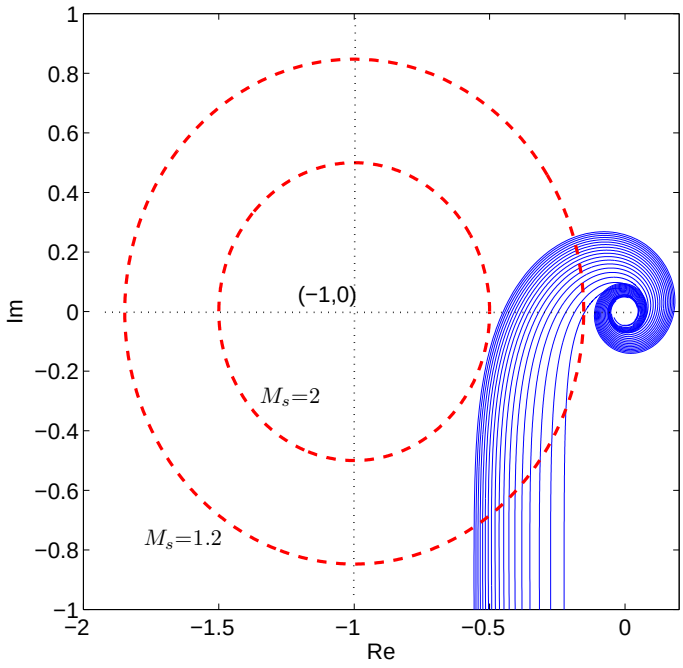

(b) M_S-circles for reasonable robustness and Open loop nyquist curves

Figure 4.3: Evaluation of the tuning method

4.6 Simulation study

The design method has been tested on three typical processes found in the literature. The effects of static load disturbance during on-line relay test is discussed in this section. Measurement noises are also introduced in Example 1 to illustrate identification robustness of the proposed method. It is important to keep the output oscillation amplitude in the prescribed limit as per the tolerable process variable swing. The process operator decides values for the relay heights that will produce a limit cycle with acceptable amplitude level. To overcome the undesirable relay chattering caused by noisy signals, the width of the hysteresis of the relay is set to twice the standard deviation of the noise. For ease in simulation study, the relay with $h = \pm 0.25$ and $\varepsilon = \pm 0.05$ are taken although fairly low values of relay height could be used. The required measurements undertaken for each process after on-line tuning experiments are tabulated in Table 4.1.

Table. 4.1: Results from a single relay test and new controller setting

Process	Initial controller, $C_o(s)$	t_0	t_1	t_2	$\dot{y}(t_0)$	$\dot{y}(t_2)$	Process model	New $C(s)$
$G_1(s)$	$0.51+\frac{0.28}{s}$	0.262	1.720	2.786	0.181	-0.193	$\frac{1.0e^{-1.458s}}{1.678s+1}$	$0.632+\frac{0.318}{s}$
$G_2(s)$	$0.2+\frac{0.02}{s}$	0.923	11.751	17.386	0.051	-0.055	$\frac{1.2001e^{-10.828s}}{7.553s+1}$	$0.446+\frac{0.045}{s}$
$G_3(s)$	$0.155+\frac{0.033}{s}$	1.021	17.359	21.777	0.047	-0.049	$\frac{1.001e^{-16.338s}}{8.120s+1}$	$0.473+\frac{0.041}{s}$

Example 1:

For a second order process $G_1(s) = \frac{e^{-s}}{(s+1)^2}$, a static load disturbance $L = 0.3$ at $t = 20$ sec enters during the relay test. Due to the presence of the PI controller during on-line test, it is noted that a stable symmetrical limit cycle is recovered after following the occurrence of the disturbance signal. Whereas the basic relay methods are sensitive to static load disturbances and need to reset the relay heights to obtain a symmetrical limit cycle. The identified transfer function model and new PI settings obtained by the proposed autotuning procedure are given in Table 4.1. For this process, Majhi [45] has proposed the PI controller $C(s) = 0.8640 + 0.3652/s$, using minimization of ISTE criterion and least-squares fitting, while Tan et al. [40] have proposed

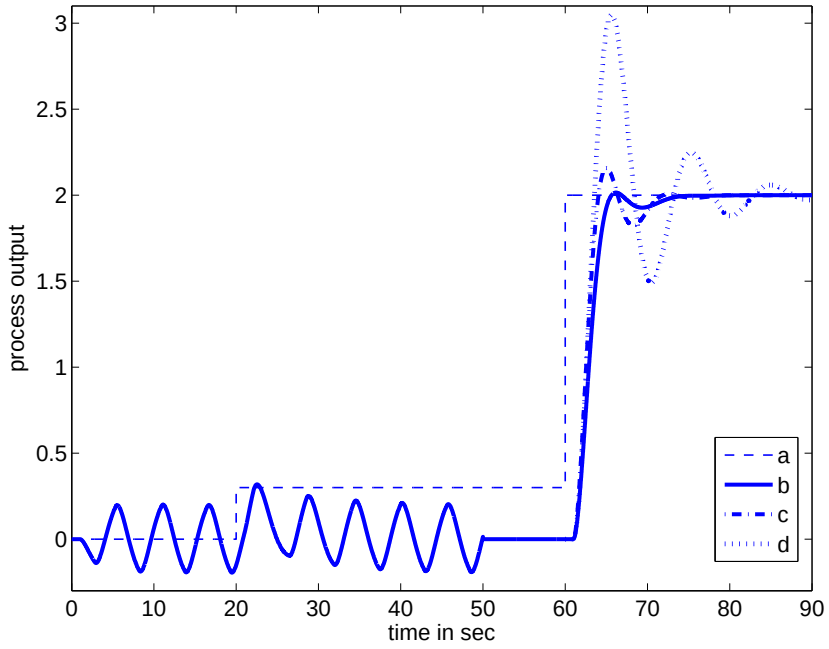

(4.4.1) Step responses

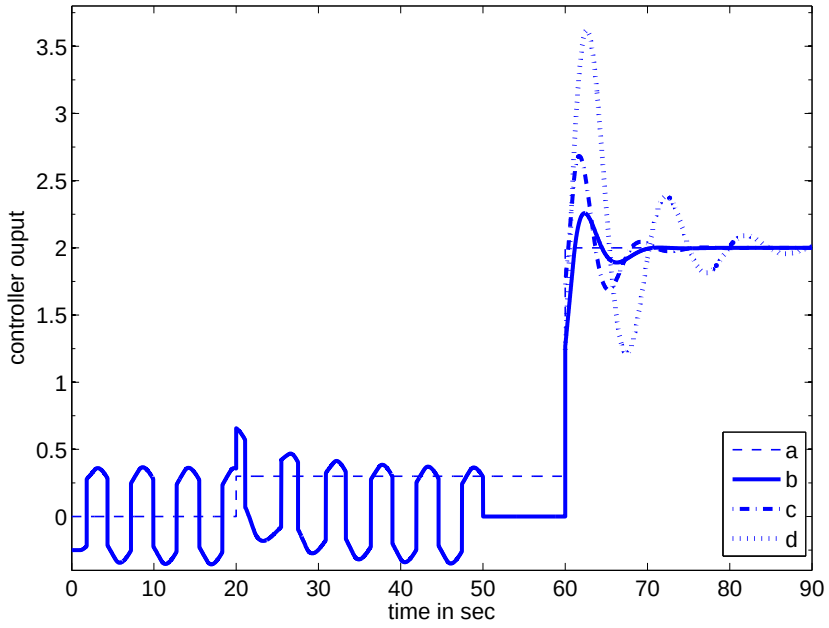

(4.4.2) Control signals

Figure 4.4: (a) Load disturbance and setpoint changes, (b) by the proposed method, (c) by Majhi's method and (d) by Tan et al.'s method

the PID controller $C(s) = 0.621(1 + 1.111/s + 0.23s)$ using their direct, multiple point on-line tuning method. Additionally, the proposed method results in the desired performance in less control signal variations with TV=1.370 while in case with Majhi and Tan et al., the values are 2.071 and 4.152, respectively. Fig. 4.4 shows the enhanced performance of the proposed on-line method with good subsequent control performance.

To show the robust performance of the control design, perturbations of $\pm 20\%$ in all the parameters k, τ and θ of the nominal process are assumed. The robust responses are compared with those of the method by Zhuang et al. [82] and robust on-line approach by Tan et al. [40] in Figs. 4.5 and 4.6 . It is observed that the closed-loop performances are very robust by the given method mainly due to the appropriate integral gain.

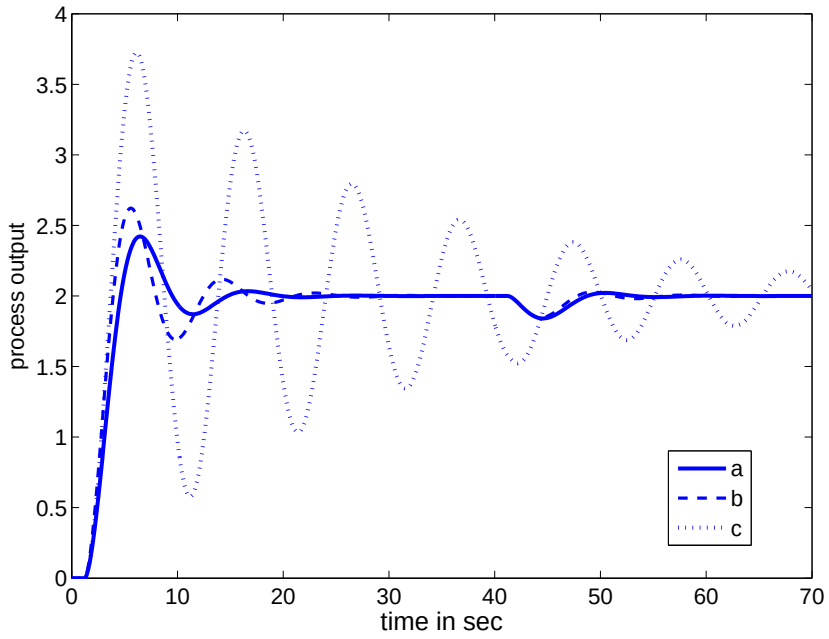

Figure 4.5: Robust responses for +20 % perturbation in k, τ and θ (a) by the proposed method, (b) by the ISTE and (c) by Tan et al.'s method

To verify the usefulness of the on-line identification method under realistic conditions, the process model parameters are estimated in the face of measurement noise. Let the process output be corrupted by Gaussian distributed random noise of several σ_N^2 such that the SNR varies from 10 dB to 20 dB. Noise reduction using the SG filter discussed in subsection 2.4.2 gives a smooth half cycle data without attenuation of data features, as shown in Fig. 4.7. The measured

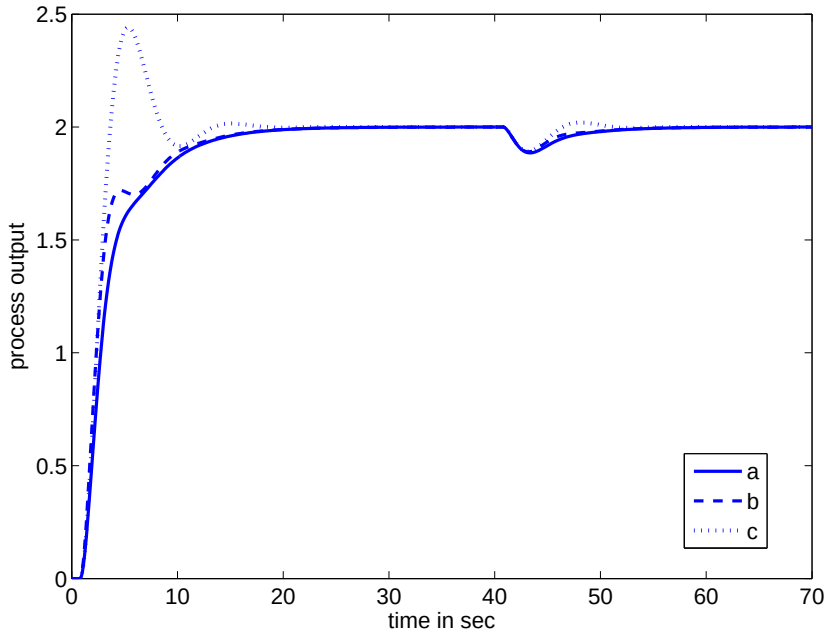

Figure 4.6: Robust responses for -20 % perturbation in k, τ and θ (a) by the proposed method, (b) by the ISTE and (c) by Tan et al.'s method

quantities from the denoised signal give the model parameters and percentage errors in these parameters due to the noise are given in Table 4.2. Interestingly, the estimated values under observation noise of various variance σ_N^2 become close to the actual values in almost all the cases. The identification, however, suffers to some extent accuracy problem when SNR is less than 10 dB. Process measurements usually contain a strong oscillation and therefore the SNR is usually high enough to warrant the use of the proposed method to estimate the model parameters in the face of output measurement noise.

Table. 4.2: Impact of measurement noise for Example 1

SNR	% Error in							
(dB)	t_0	t_1	t_2	$\dot{y}(t_0)$	$\dot{y}(t_2)$	k	θ	τ
10	-0.862	-1.212	-1.502	-0.931	-1.340	-0.391	1.282	-8.232
15	-0.541	-0.965	-1.021	-0.321	-0.789	0.652	1.028	-6.898
20	0.020	0.056	-0.053	-0.212	-0.312	0.255	-0.065	-4.342

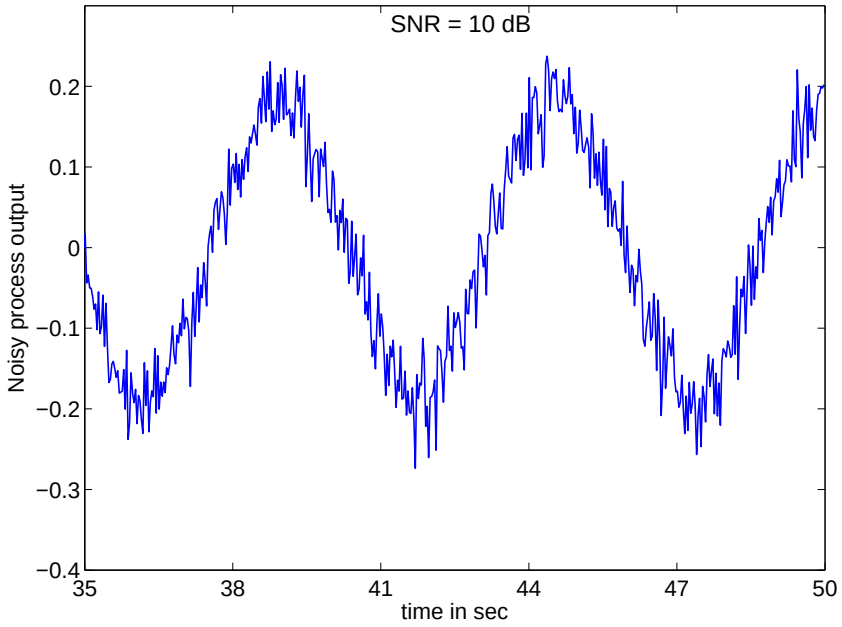

(4.7.1)

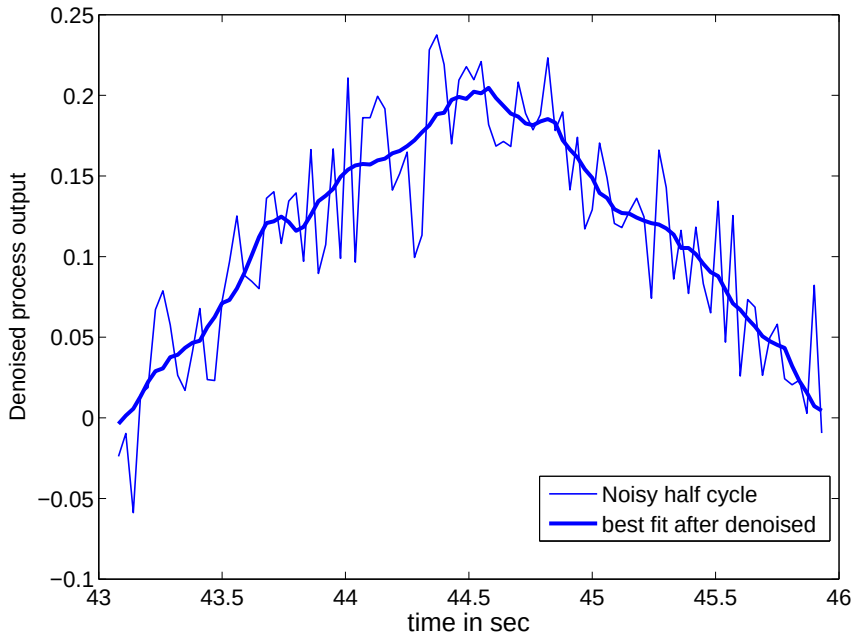

(4.7.2)

Figure 4.7: Noisy and denoised output signals

Example 2:

For the large dead time process $G_2(s) = \frac{1.2e^{-10s}}{(5s+1)(2.5s+1)}$, Zhuang et al.'s [82] basic relay autotuning method gives optimum PI parameters $K_c = 0.730$ and $K_i = 0.047$ by the ISE criterion and $K_c = 0.535$ and $K_i = 0.046$ by the ISTE criterion.

Assuming no measurement noise during identification, an FOPDT model was obtained with the use of an on-line relay test and subsequently new PI parameters estimated by the proposed method are given in the second row of Table 4.1. The new method presented gives better closed-loop responses with reasonable overshoots and short settling times for both setpoint and control signal variations as shown in Figs. 4.8 and 4.9. Due to no constraint on Zhuang et al.'s ISTE and ISE criteria, the control signal variations are measured as 1.587 and 2.474, respectively while it is less, 1.316, with the proposed method.

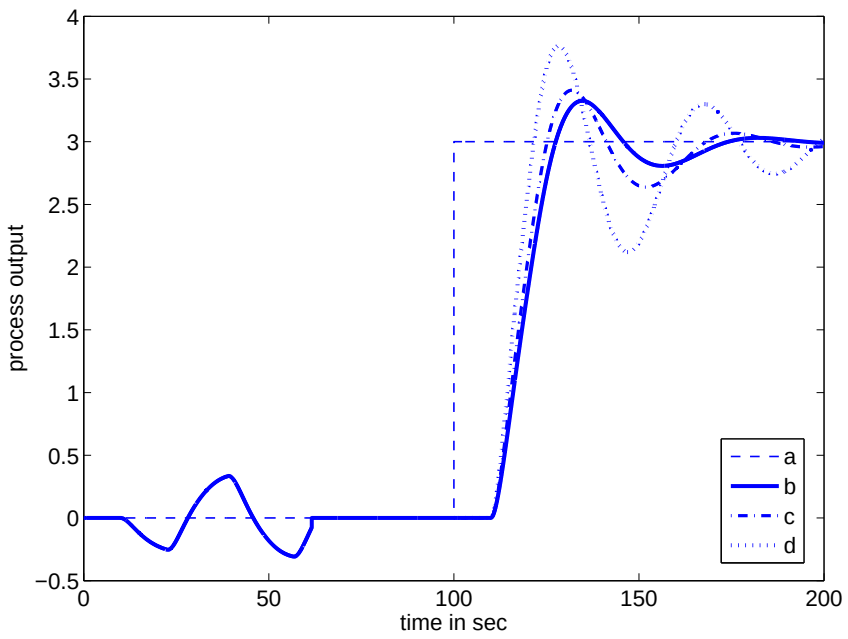

Figure 4.8: (a) Setpoint input, Step responses (b) by the proposed method, (c) by the ISTE method and (d) by the ISE method

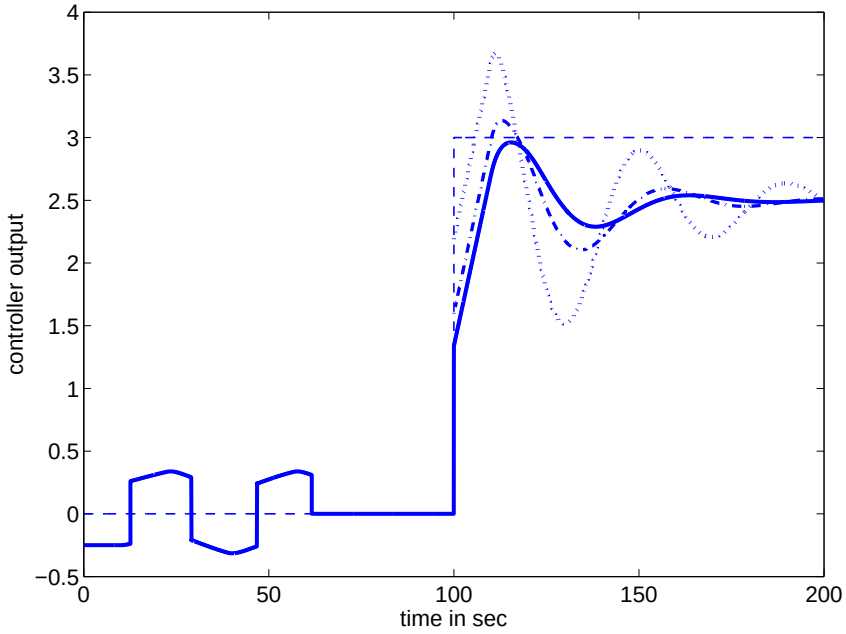

Figure 4.9: (a) Setpoint input, Control signals (b) by the proposed method, (c) by the ISTE method and (d) by the ISE method

Example 3:

Consider the very high order process, $G_3(s) = \frac{1}{(s+1)^{20}}$. In Tsay method [46], the PI+lead controller $(0.4292 + 0.0492/s)(\frac{4.7392s+1}{0.4739s+1})$ were taken for the setpoint response and for the same process, Zhuang et al.'s [82] method suggested $(0.473 + 0.058/s)$. The estimated FOPDT model and the new PI gains are given in the third row of Table 4.1. The good identification obtained by the proposed method is reflected by the superior controller performances, for both the setpoint tracking and load disturbance, are given in Fig. 4.10. It is noted that the method gives promising results with minimum experiment time of a single relay test while in the case with [46], repetitive identification tests were required to get final PI controller till an acceptable gain margin is found. The measure of control signal variations is also less, 2.672 whereas using Tsay and Zhuang et al., TVs are 3.261 and 4.387, respectively.

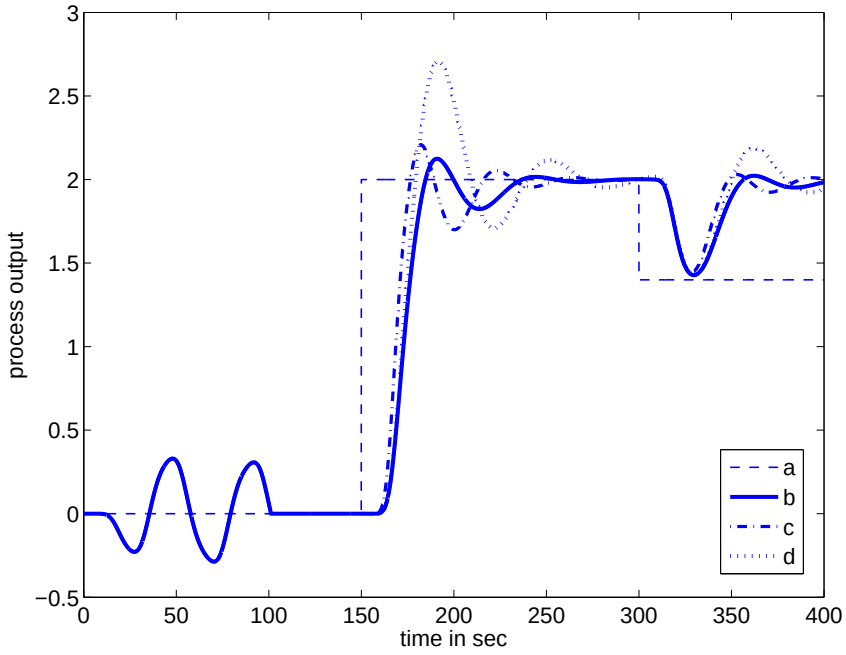

(4.10.1) Step responses

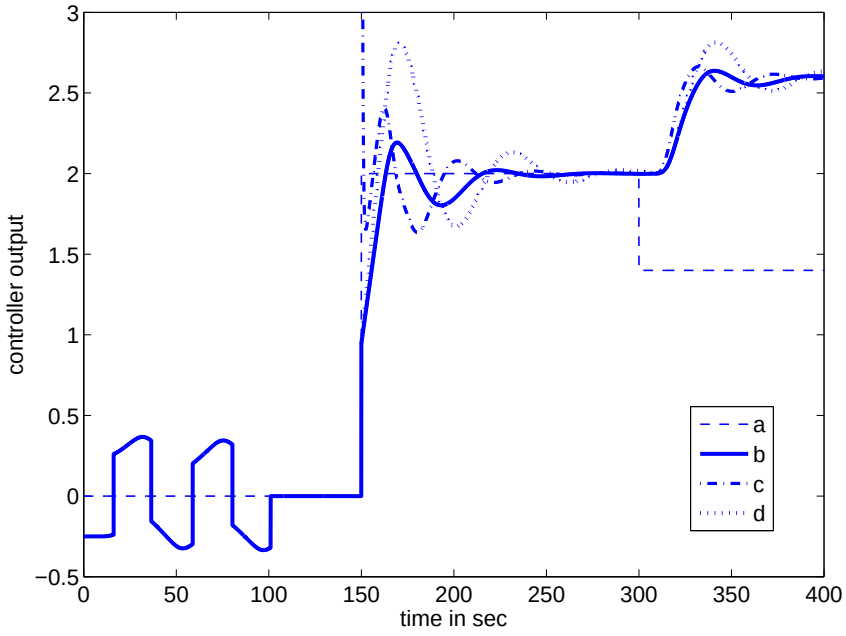

(4.10.2) Control signals

Figure 4.10: (a) Setpoint and load disturbance inputs, (b) by the proposed method, (c) by Tsay's method and (d) by Zhuang et al.'s method

4.7 Real-time experiments

4.7.1 Experiment setup with Analog programmable kit

The proposed on-line tuning method is tested with the help of an experimental setup made up of a Process Control Simulator PCS-327 from Feedback instruments [80], Anadigm AN221E04 Field Programmable Analog Array (FPAA) [85] and a personal computer. The block diagram representation of the experiment setup is given in Fig. 4.11.

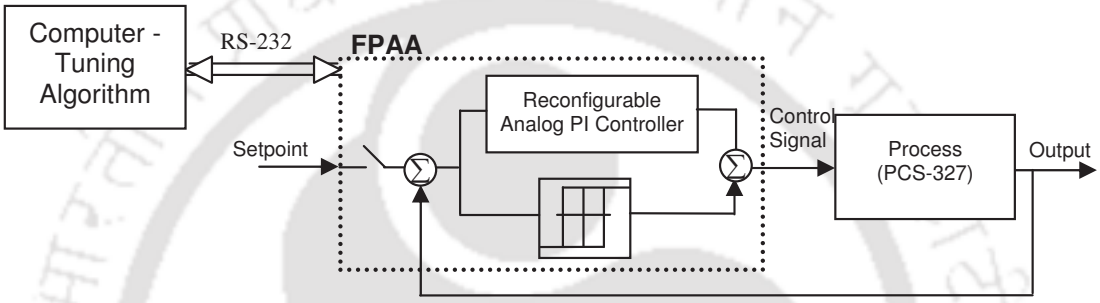

Figure 4.11: Block diagram of experimental setup

The tuning algorithm runs on a computer that also configures the FPAA dynamically using RS-232. The variety of analogue functions like amplification, summing, differentiation, integration, filtering, etc. were implemented in FPAA. The AnadigmDesigner-2 software provides a set of C functions to be used for reading current PI setting and reconfiguring the chip on-line if design parameters require to be dynamically changed. PCS-327 was configured with a transfer function $G(s) = \frac{1}{(s+1)^3}$. The sampling time, relay amplitudes and hysteresis settings were 50 msec, ± 0.2 V and 20 mV, respectively. Following the on-line tuning method, the process dynamics was modelled by $\frac{1.001e^{-0.782s}}{(2.112s+1)}$ using half cycle output data and then the new controller parameters were computed as $K_c = 0.792$ and $K_i = 0.345$. The closed-loop responses using the initial controller, limit cycle oscillations during the on-line test and then improved responses for the new step change, are shown in Fig. 4.12.

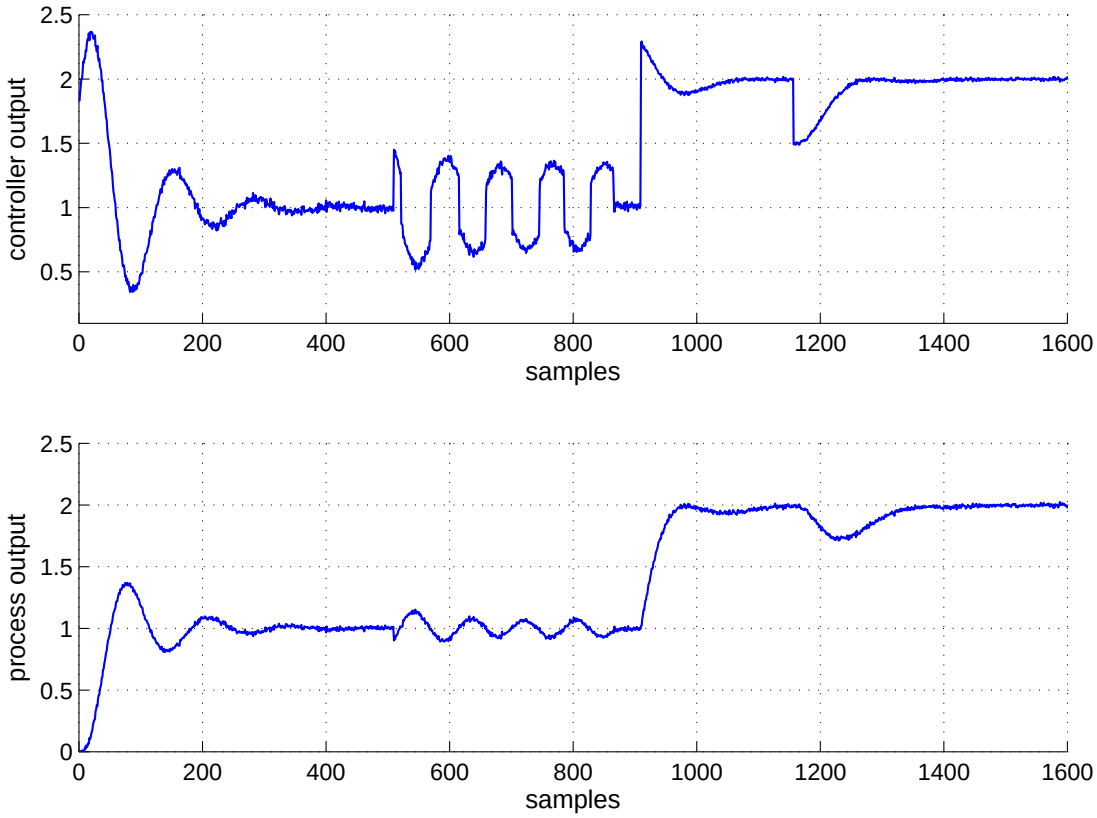

Figure 4.12: Experimental results

4.7.2 DC servo position control system

In this subsection a DC servo position control system is used to illustrate the proposed method. Setup is made up of a brush DC servo motor and Anadigm AN221E04 FPAA kit. The photograph of experimental setup is shown in Fig.4.13 .

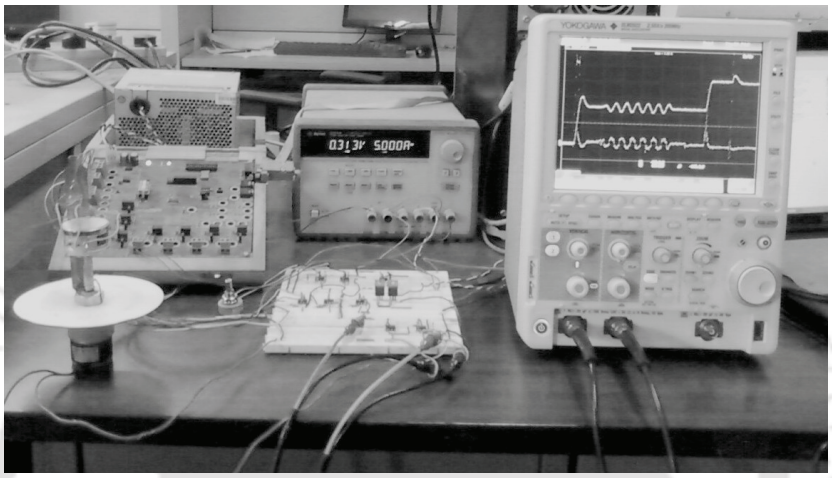

Figure 4.13: Photograph of an experimental setup

The programmable controller is designed with the help of FPAA kit and can also be dynamically configured through RS-232. The desired input references of position in degree have been calibrated with equivalent dc voltages. To perform relay test the sampling time, relay amplitudes and hysteresis settings were 16 msec, ± 0.17 V and ± 20 mV, respectively. Following the on-line tuning method, the process dynamics was modelled by $\frac{0.9937e^{-0.1990s}}{2.0926s+1}$ using initial settings $K_c = 6.3662$, $K_i = 0.550$. The new controller parameters were computed as $K_c = 0.9445$ and $K_i = 0.4391$ using the proposed tuning formulas (4.22) and (4.24). The closed-loop responses using the initial PI settings for position 90^o and using the updated PI settings for the new position of 150^o, are shown in Fig. 4.14. The tracking performance is clearly enhanced with almost no overshoot and also reduced the control efforts to obtain the desired position.

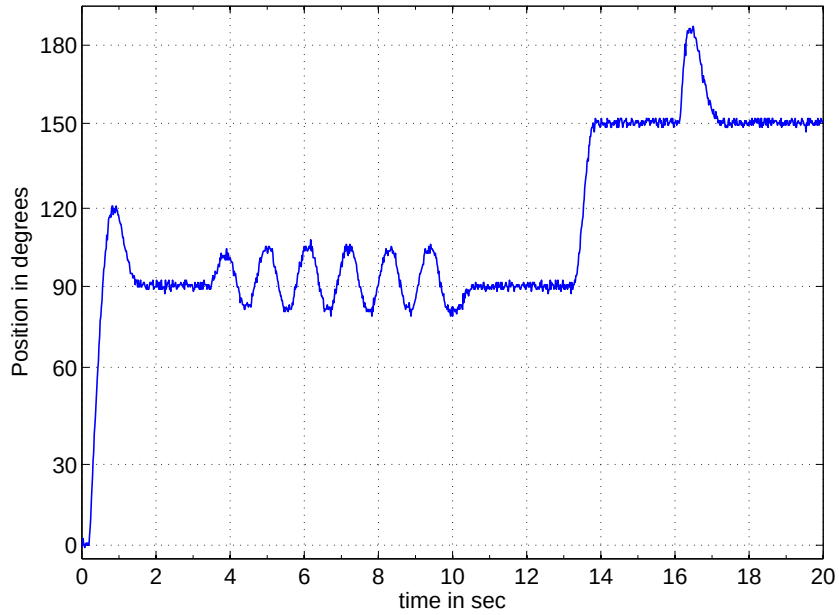

(4.14.1) Setpoint responses

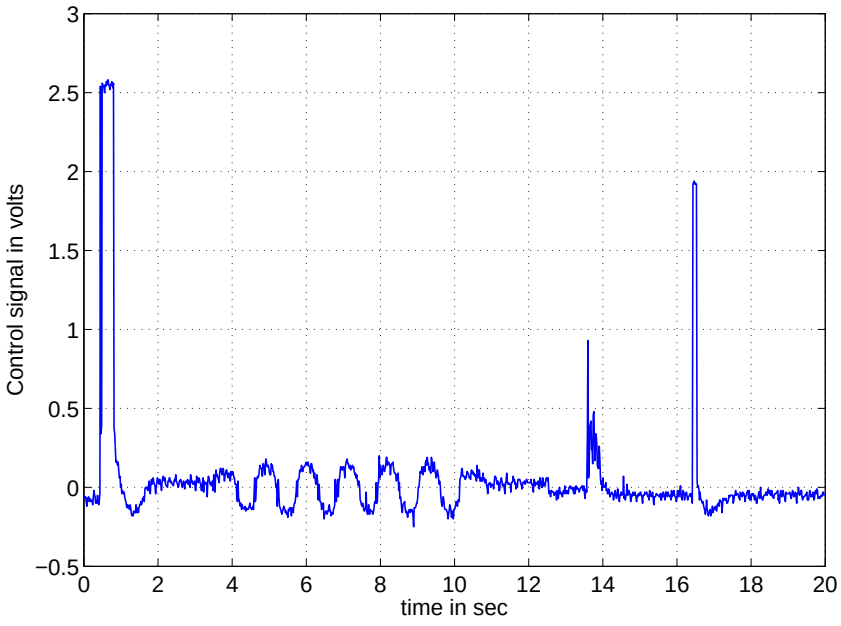

(4.14.2) Control signals

Figure 4.14: Experimental results

4.8 Summary

A simple and effective on-line technique to re-tune the PI controller has been developed. Differently from the standard relay autotuning approach, it allows the tuning of the controller in the presence of a static load disturbance without resetting the relay. Further, the identification method requires only half period of limit cycle data, which significantly reduces the time required for the autotuning test. Simulation examples and experimental study illustrate the practical applicability of the scheme to get desirable transient responses with smooth input usage.

CHAPTER 5

ON-LINE IDENTIFICATION OF CASCADE CONTROL SYSTEMS BASED ON HALF LIMIT CYCLE DATA

5.1 Introduction

Cascade control helps in eliminating the effect of load disturbance and improving the dynamic performance of a closed-loop system over a single-loop control [52]. Generally a cascade control structure is to nest one feedback loop inside another feedback loop involving the use of primary (or master) and secondary (or slave) controllers. The standard conventional approach of tuning these cascade controllers is often ineffective because it ignores strong interaction between the two loops. Also the widely used two-step approach is a fairly time consuming task due to the approach being sequential in nature and problems related to master and slave signal tracking. Thus it would be very useful to realize the automatic tuning procedure for cascade control system in which the entire tuning process is carried out in one experiment.

Today, the use of the relay feedback technique for estimation of the process dynamics has been widely adopted in the process control [3]. This is an elegant yet simple experiment design for process estimation and a large number of research work to extend its application domain and to enhance various aspects of the conventional approach has been reported. Relay based methods for cascade control strategies have been published by Hang et al. [53], Song et al. [55]

and Kaya et al. [56], however their procedures are based on the off-line relay test. Off-line tuning has associated implications in the tuning-control transfer, affecting operational process regulation which may not be acceptable for certain critical applications [54]. Although individual controller tuning has been automated in [53] and [56], the sequential nature of the tuning procedure remains unchanged. Tan et al. [54] has suggested an on-line relay tuning approach in one experiment, but the experiment requires a priori information of the process. Also, the ultimate frequency used by them for the outer-loop design is based on initial ultimate frequency without considering changes to the inner-loop control parameters. Lee et al. [57] have proposed IMC based tuning rules for the primary and secondary controllers, but it has not been specified how the procedure can be automated. Visioli and Piazzi [58] have proposed an automatic tuning method for the cascade control system but the method consists of an open-loop step test for estimation of process dynamics and command signal generator for setpoint tracking. Sadasivarao and Chidambaram [59] have presented an iterative method based on a genetic algorithm for tuning cascade controllers. The on-line experiment time by the method is very long which may not be acceptable in practice. Alfaro et al. [60] made use of a two-degrees of freedom design approach for a cascade control configuration for smooth control by introducing additional parameters that need to be tuned appropriately. Tuning methods for parallel cascade control are discussed in [61, 62] with the process information assumed to be known in the form of the FOPDT model.

This chapter discusses a new method for on-line autotuning of the cascade control system with the help of a single relay feedback test. By employing a relay in parallel to the master controller, both inner and outer process dynamics are simultaneously identified from the respective half limit cycle outputs. A set of exact and simple analytical expressions are derived which can be used for estimating process models. Then both inner and outer controllers can be tuned simultaneously based on the low order rational transfer function models. This method does not require time consuming iterative calculations and also overcomes the requirements of the sequential conventional approach for tuning the cascade control system.

5.2 On-line identification

The configuration of the cascade control system is shown in Fig. 5.1 where, C_1 and C_2 are the master and slave controllers while G_{p1} and G_{p2} are the outer and inner loop processes, respectively. Fig. 5.1 shows the on-line tuning scheme for the cascade control system by employing a relay in parallel with the master controller without disturbing the closed-loop control. The relay height is increased from zero to some acceptable value when re-tuning is necessary. Based on the induced limit cycle oscillations y_1 and y_2, the process dynamics are first identified and then fine tuning of the existing controllers are accomplished.

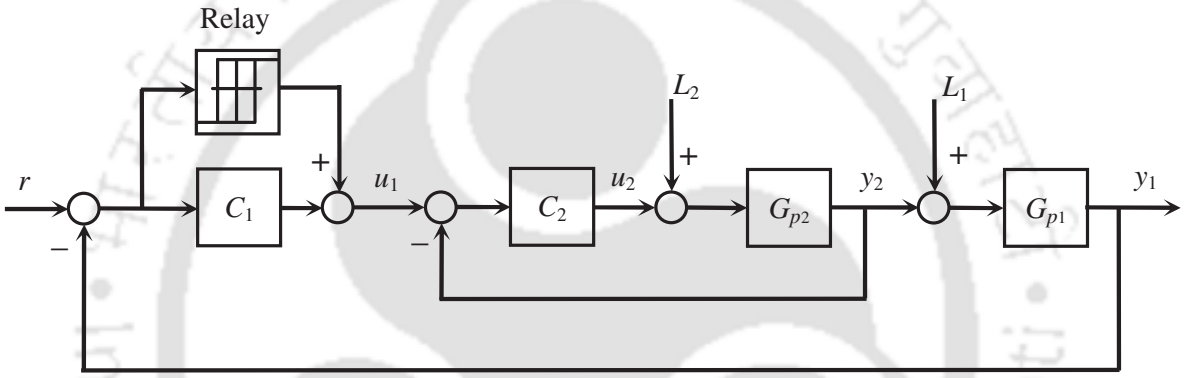

Figure 5.1: Structure for on-line tuning of the cascade control system

To make the cascade control effective, the following guidelines are to be incorporated.

- The inner loop should be faster than the outer loop at least by five times and it should be possible to have a high gain in order to regulate disturbances more effectively [39].
- In the absence of default control settings, C_1 and C_2 are proportional-integral (PI) and proportional (P) type controllers, respectively. These settings are intended primarily for the purpose of stabilizing the process during the tuning procedure. Practical applications of autotuning methods have been mainly to derive more efficient updates of current or default control settings, which are already available in many cases.

Let the process dynamics be represented by the first order rational transfer function model with

dead time

$$G_{pi}(s) = \frac{k_i e^{-\theta_i s}}{\tau_i s + 1} \tag{5.1}$$

where, $i = 1$ for the outer and $i = 2$ for the inner process model. Although, the transfer function model is simple with only three model parameters, yet it is most commonly used, especially in the process control industries [39].

5.2.1 Estimation of inner process model

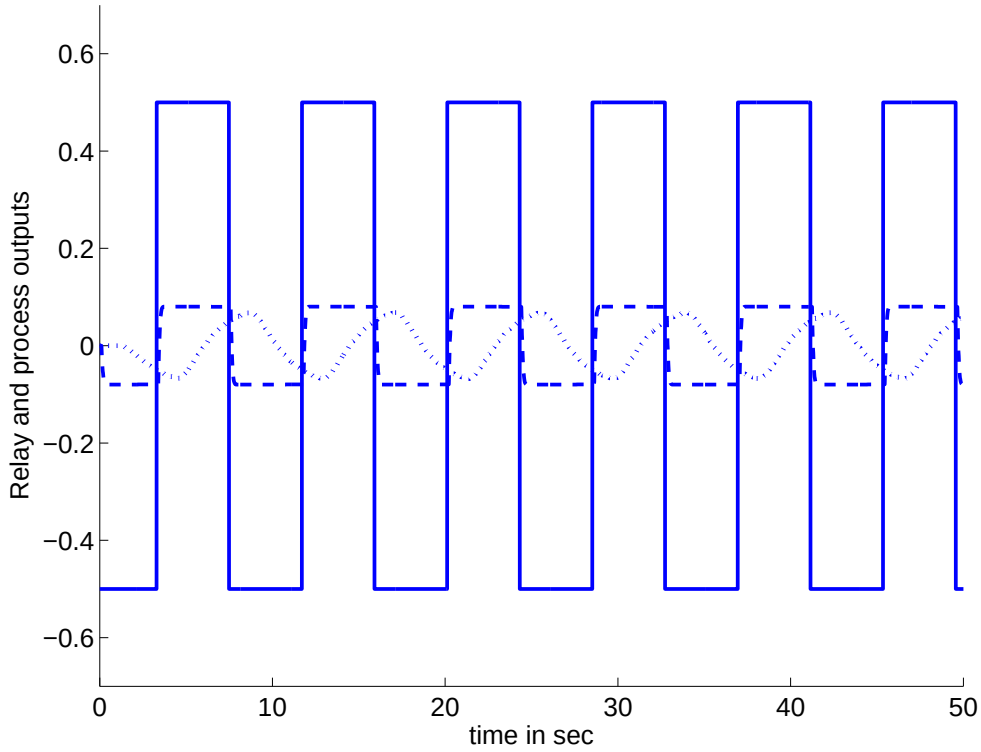

Figure 5.2: Responses from the relay test, – relay output, – – $y_2(t)$ and $\cdots y_1(t)$

A relay autotuning test yields interesting results as shown Fig. 5.2 due to faster dynamics and higher gain of the inner loop compared to the outer loop. The output y_2 is constant at least over a half period and acts as a constant input for the outer process during that period. Therefore, it is possible to obtain the analytical expressions for half limit cycles y_1 and y_2 (Fig. 5.3) from a single relay test.

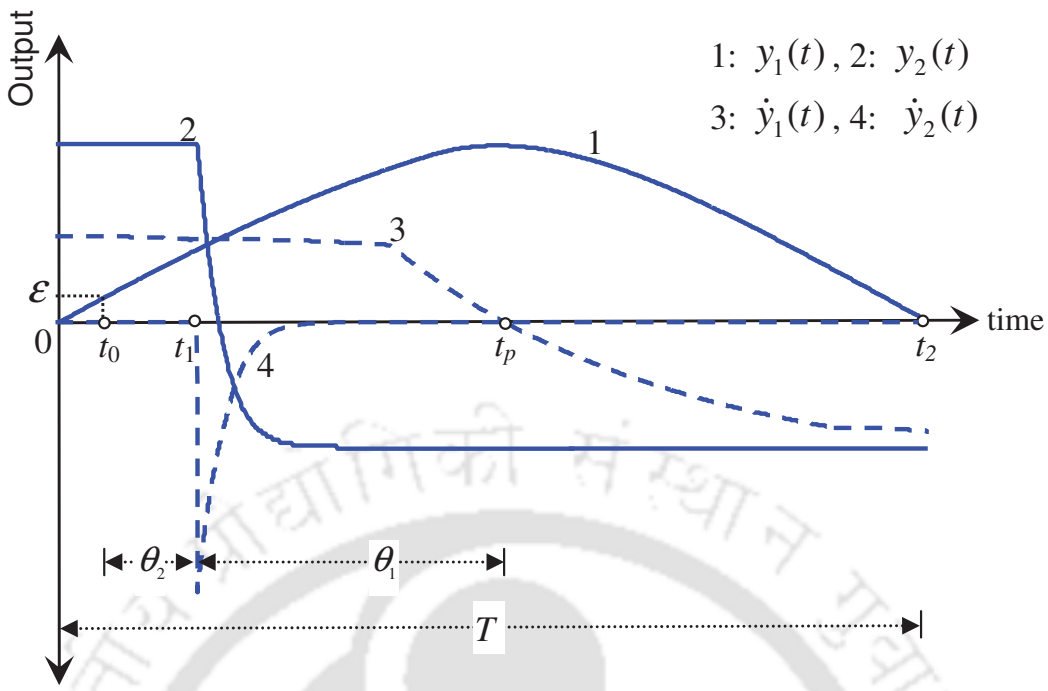

Figure 5.3: Half cycle of the limit cycle outputs

Let the relay amplitudes and hysteresis widths be $\pm h$ and $\pm\varepsilon$, respectively. The method to obtain the analytical expression of a limit cycle waveform as given in Section 4.2 is used here. The state and output expressions for $G_{p2}(s)$ in (5.1) are written in the time domain controllable canonical form as

$$\begin{aligned} \dot{x}_2(t) &= \lambda x_2(t) - k_2\lambda u_2(t-\theta_2) \\ y_2(t) &= x_2(t) \end{aligned} \tag{5.2}$$

where, $\lambda = -1/\tau_2$. The relay switches from h to $-h$ at time $t = t_0$ due to hysteresis and provides two different piecewise constant input signals during a half period of the inner process output. The solution of (5.2) for $t \geq t_1$ where the input signal $u_2(t-t_1) = -h$ can simply be

$$y_2(t) = y_2(t_1)e^{\lambda(t-t_1)} - k_2h(1-e^{\lambda(t-t_1)}) \tag{5.3}$$

Similarly, the solution for the inner loop transfer function

$$T_2(s) = \frac{Y_2(s)}{U_1(s)} = G_{p2}C_2(s)[1+G_{p2}C_2(s)]^{-1} \tag{5.4}$$

is obtained for the inner process output. During an on-line relay test $C_2(s) = K_{c2}$ and substitution

of $G_{p2}(s)$ in (5.4) gives

$$T_2(s) = \frac{k_2 K_{c2} e^{-\theta_2 s}}{\tau_2 s + 1 + k_2 K_{c2} e^{-\theta_2 s}} \tag{5.5}$$

The static load disturbance is neglected during the analysis. With the help of (5.3) and using the limit cycle analysis given in Section 4.2, the output expression from $T_2(s)$ is derived. The expression of y_2 for $t \geq t_1$ is obtained as

$$y_2(t) = y_2(t_1)e^{\lambda(t-t_1)} - k_2K_{c2}h(1-e^{\lambda(t-t_1)}) + (k_2K_{c2})^2 h\lambda \left[(t-t_1)(2e^{\lambda(t-t_1)} - e^{\lambda(t-t_0)}) + \lambda^{-1}(1-e^{\lambda(t-t_1)})\right] \tag{5.6}$$

The first order time derivative of $y_2(t)$ becomes

$$\dot{y}_2(t) = y_2(t_1)e^{\lambda(t-t_1)}\lambda + k_2K_{c2}he^{\lambda(t-t_1)}\lambda + (k_2K_{c2})^2 h\lambda \left[e^{\lambda(t-t_1)} - e^{\lambda(t-t_0)} + (t-t_1)(2e^{\lambda(t-t_1)}\lambda - e^{\lambda(t-t_0)}\lambda)\right] \tag{5.7}$$

It is straightforward to calculate the steady state gain k_2, since $T_2(0) = k_2K_{c2}/(1+k_2K_{c2})$ from (5.5). This can be simplified for k_2 as

$$k_2 = \frac{T_2(0)}{(1-T_2(0))K_{c2}} \tag{5.8}$$

If the constant amplitude of y_2 is denoted by h_{y2}, then the inner loop gain $T_2(0) = h_{y2}/h$. Then, (5.8) becomes

$$k_2 = \frac{1}{K_{c2}}\left(\frac{h_{y2}}{h-h_{y2}}\right) \tag{5.9}$$

It is evident from Fig. 5.3 that the time derivative of y_2 shows an abrupt change in slope at $t = t_1$ (time is measured from the beginning of the positive half cycle output) due to non-monotonic characteristics of the limit cycle waveform [17]. But, the relay switches at time t_0 due to the hysteresis and this fact is used to find the time delay $\theta_2 = (t_1 - t_0)$.

Next, substitution of $t = t_1$ and $\theta_2 = (t_1 - t_0)$ in (5.7) results in

$$\dot{y}_2(t_1) = \lambda y_2(t_1) + k_2K_{c2}h\lambda + (k_2K_{c2})^2 h\lambda(1-e^{\lambda\theta_2}) \tag{5.10}$$

Using the Pade approximation of $e^{\lambda\theta_2} = (2+\lambda\theta_2)/(2-\lambda\theta_2)$, (5.10) can be written in a polynomial equation form as

$$a\lambda^2 + b\lambda + c = 0 \tag{5.11}$$

where,

$$a = y_2(t_1)\theta_2 + k_2K_{c2}h\theta_2 + 2(k_2K_{c2})^2h\theta_2$$
$$b = -2y_2(t_1) - 2k_2K_{c2}h - \dot{y}_2(t_1)\theta_2 \tag{5.12}$$
$$c = 2\dot{y}_2(t_1)$$

Because of $a > 0$ and $c < 0$ for the positive half period, there exists only one solution for $\tau_2 > 0$ and that is

$$\tau_2 = \frac{2a}{b + \sqrt{(b^2 - 4ac)}} \tag{5.13}$$

Thus, all the parameters of the inner process model $G_{p2}(s)$ can be estimated using the explicit expressions (5.9) and (5.13) and the measurements of t_0, t_1, h_{y2}, $y_2(t_1)$ and $\dot{y}_2(t_1)$.

5.2.2 Estimation of outer process model

If the peak amplitude of y_1 occurs at time $t = t_p$, the expression for the limit cycle output for $G_{p1}(s)$ with a constant input of h_{y2} can be written for $t \geq t_p$ as

$$y_1(t) = y_1(t_p)e^{\lambda_1(t-t_p)} - k_1h_{y2}(1 - e^{\lambda_1(t-t_p)}) \tag{5.14}$$

where, $\lambda_1 = -1/\tau_1$. First derivative of the above expression gives

$$\dot{y}_1(t) = \lambda_1 y_1(t_p)e^{\lambda_1(t-t_p)} + \lambda_1 k_1 h_{y2} e^{\lambda_1(t-t_p)} \tag{5.15}$$

Since $y_1(t_2) = 0$, (5.14) becomes

$$\frac{k_1h_{y2}}{y_1(t_p) + k_1h_{y2}} = e^{\lambda_1(t_2-t_p)} \tag{5.16}$$

which upon simplification yields

$$\tau_1 = -\frac{t_2 - t_p}{\ln\left(\frac{k_1h_{y2}}{y_1(t_p)+k_1h_{y2}}\right)} \tag{5.17}$$

Next, substitution of $t = t_2$ in (5.15) and the use of (5.16) gives

$$k_1 = -\frac{\tau_1\dot{y}_1(t_2)}{h_{y2}} \tag{5.18}$$

In principle, (5.17) and (5.18) explicit expressions can be used for estimation of the unknowns τ_1 and k_1 from the measurements of t_p, t_2, $y_1(t_p)$ and $\dot{y}_1(t_2)$.

The time delay θ_1 is estimated using the half cycle output for y_1 and its first derivative data as was done for the inner process model. It should be noted that the measurement of peak time t_p for y_1 gives an effective total delay with respect to the time t_0 as shown in Fig. 5.3. Thus, θ_1 is calculated as $\theta_1 = t_p - t_1 = t_p - t_0 - \theta_2$.

In practice, the estimation of $\dot{y}_2(t_1)$ and $\dot{y}_1(t_2)$ by taking numerical derivatives will be sensitive to measuring noise. Therefore, the data to compute $\dot{y}_2(t_1)$ and $\dot{y}_1(t_2)$, are denoised first by using the Savitzky-Golay smoothing filter discussed in subsection 2.4.2. Then $\dot{y}_2$ at $t = t_1$ is estimated by taking three or more values of y_2 starting from the time instant t_1, separated by a small sampling interval, from the half limit cycle database during a relay test. These data are then fitted to a straight line. The slope of this line is then taken as the estimate of $\dot{y}_2$ at $t = t_1$. Similarly, $\dot{y}_1(t_2)$ is estimated using the database of y_1.

5.3 Tuning of controllers

After estimating the parametric models of inner and outer processes from a single relay test, the tuning rules are employed to update the current settings of C_1 and C_2 without any additional test. Unlike the traditional sequential approach, the proposed method is to tune the primary and secondary controllers simultaneously. It is also necessary to consider the effect of new secondary controller while designing the primary controller. Let the subsequently tuned controllers C_2 and C_1 have the transfer function form

$$C_2(s) = K_{c2}(1 + 1/T_{i2}s) \tag{5.19}$$

$$C_1(s) = K_{c1}(1 + 1/T_{i1}s + T_{d1}s) \tag{5.20}$$

The objective of simultaneous parameter tuning for C_1 and C_2 is to achieve widespread industrial acceptance for good disturbance rejections. As per the ultimate transfer function models of inner and outer processes, the tuning rules are tabulated in Table 5.1. Detailed procedures for development of the tuning rules are available in [50]. With the current setting of the secondary

Table. 5.1: Tuning rules for cascade controllers

C_2		C_1		
K_{c2}	T_{i2}	K_{c1}	T_{i1}	T_{d1}
$\frac{0.5\tau_2}{k_2\theta_2}$	τ_2	$\frac{0.5\tau_1}{k_1(\theta_1+\theta_2)}$	τ_1	θ_2

controller $C_2(s)$, the inner closed-loop transfer function $T_2(s)$ becomes

$$T_2(s) = \frac{0.5e^{-\theta_2 s}}{\theta_2 s + 0.5e^{-\theta_2 s}} \tag{5.21}$$

$T_{i2} = \tau_2$ due to fast dynamics of the inner loop. When the delay $e^{-\theta_2 s}$ is approximated with $1 - \theta_2 s$ without loss of generality, then

$$T_2(s) = \frac{e^{-\theta_2 s}}{\theta_2 s + 1} \tag{5.22}$$

An apparent controlled process seen by the primary (master) controller C_1 is

$$G_{11}(s) = \frac{k_1 e^{-(\theta_1+\theta_2)s}}{(\tau_1 s + 1)(\theta_2 s + 1)} \tag{5.23}$$

Now, $C_1(s)$ is tuned using this apparent second order process model $G_{11}(s)$ instead of $G_{p1}(s)$ while taking into account the updated inner loop control parameters. Thus, simultaneous tuning of the primary and secondary controllers are done with the PID setting of C_1 given in Table 5.1. The tuning rules are designed to effect damped responses by the cascade controllers.

5.4 Simulation study

The proposed method has been tested on typical processes available in the relevant literature. The effects of noise and disturbance are also discussed. It is important to keep the output oscillation amplitude in the prescribed limit as per the tolerable process variable swing and to decide values for the relay heights that produce a limit cycle with acceptable amplitude level. The choice of h is dictated by the physical constraints on the manipulated variable, as well as

Table. 5.2: Identified models and controller settings from half limit cycle data

Example	Loop	Initial controllers	Identified models	Index I_G	New controllers
1	Inner	0.19	$\frac{0.997e^{-0.104s}}{0.101s+1}$	2.8×10^{-3}	$0.487(1+\frac{1}{0.101s})$
	Outer	$0.02(1+\frac{1}{2s})$	$\frac{0.999e^{-1.481s}}{1.635s+1}$	2.0×10^{-2}	$0.516(1+\frac{1}{1.633s}+0.105s)$
2	Inner	0.01	$\frac{3.05e^{-3.057s}}{13.108s+1}$	3.5×10^{-4}	$0.703(1+\frac{1}{13.108s})$
	Outer	$0.1(1+\frac{1}{100s})$	$\frac{10.01e^{-72.444s}}{68.814s+1}$	3.0×10^{-3}	$0.046(1+\frac{1}{68.810s}+3.057s)$

the allowed deviation in the measured output. The choice of ε depends on the measurement noise level. With a large ε, the adverse effect of noise for a relay feedback is avoided, generally ε is set to twice the standard deviation of the noise. For ease in simulation study, a relay of amplitude $h=\pm0.5$ and $\varepsilon=\pm0.05$ is used although fairly low values of relay height could be used. The estimated models and controller settings for both the examples are tabulated in Table 5.2.

Again, the performance is evaluated by measuring an estimation error index using the integral of absolute error (IAE) criterion for each of the process models by

$$I_G=\int_0^{\omega_c}\left|\frac{G_p(j\omega)-G(j\omega)}{G_p(j\omega)}\right|d\omega \tag{5.24}$$

where $G(j\omega)$ is the actual process and $G_p(j\omega)$ is the identified model. Only $\omega\in[0,\omega_c]$, where ω_c is the phase crossover frequency of the process, are considered since that is most important for controller design.

Example 1:

Consider the cascade system discussed in [53] and [55] with $G_1(s)=\frac{e^{-s}}{(s+1)^2}$ and $G_2(s)=\frac{e^{-0.1s}}{0.1s+1}$. A step load disturbance $L_1=0.1$ at $t=20$ sec enters during the relay test. Due to the presence of the PI controller during the on-line test, a stable symmetrical limit cycle appears automatically after an initial transient following the occurrence of the disturbance signal. But the basic relay

methods [53, 55] are sensitive to static load disturbance and need to reset the relay height to obtain a symmetrical limit cycle output.

From the on-line relay test, the half cycle output signals are obtained as shown Fig. 5.4 and the required measurements (t_0, t_1, t_p, t_2)=$(1.418, 1.519, 3.001, 4.206)$ and $(h_{y2} = y_2(t_1), y_1(t_p), \dot{y}_2(t_1), \dot{y}_1(t_2)) = (0.079, 0.069, -1.876, -0.049)$ are performed from a single relay experiment.

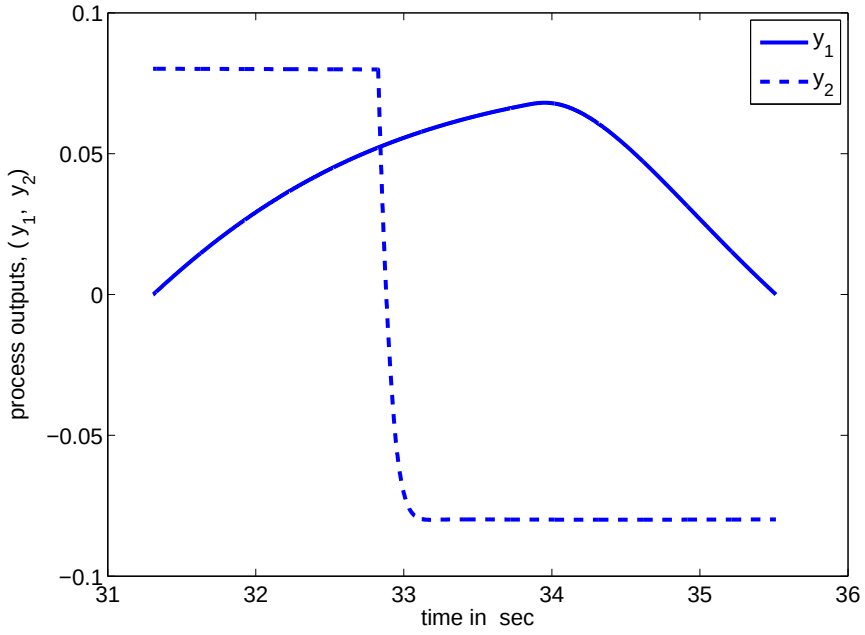

Figure 5.4: Half cycle outputs

The identified transfer function models, estimation errors and new PI/PID settings for the system are given in Table 5.2. A new setpoint change follows at $t = 60$ sec and an inverse load disturbance of 0.5 occurs in the intermediate process output at $t = 90$ sec. For this system, the setpoint performances are compared with that obtained by the method proposed by Hang [53] and Song [55]. Fig. 5.5 shows the enhanced performance of the proposed on-line method even in the presence of the static load disturbance.

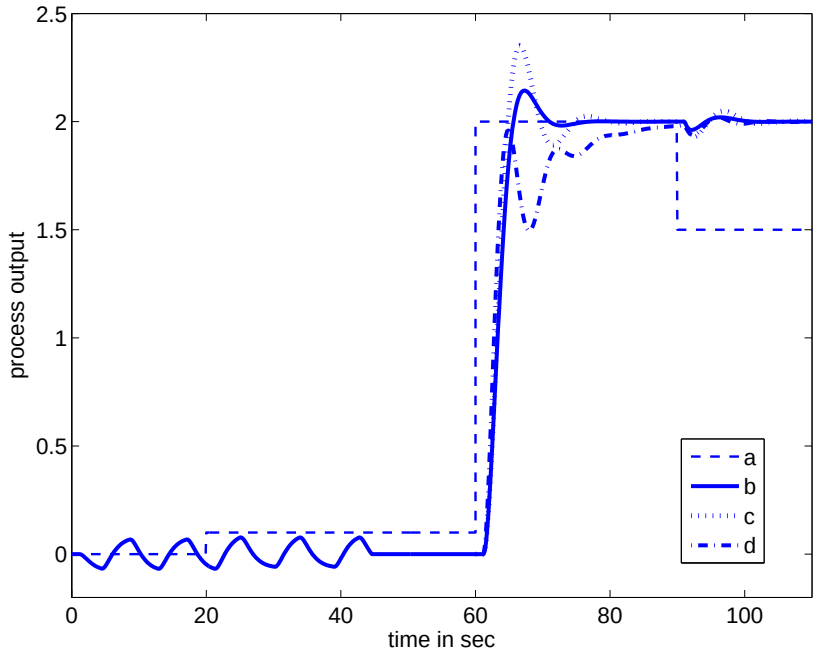

Figure 5.5: (a) Load disturbance and setpoint changes, Process output by (b) proposed method, (c) Song et al.'s method and (d) Hang et al.'s method

To verify the usefulness of the on-line identification method under realistic conditions, the process model parameters are estimated in the face of measurement noise. Let the process output be corrupted by Gaussian distributed random noise of variance 0.02 which give approximately absolute SNR value of 20 dB. Then, the noise reduction using the Saviztky-Golay filtering gives a smooth half cycle data without attenuation of data features, as shown in Fig. 5.6. The measured quantities from the denoised signal give the estimated models $G_{p1}(s) = \frac{1.01e^{-1.472s}}{1.586s+1}$ and $G_{p2}(s) = \frac{0.992e^{-0.106s}}{0.109s+1}$ with estimation errors of 6.3×10^{-2} and 7.0×10^{-3}, respectively. The small values indicates the proposed on-line identification scheme is robust against the measurement noise.

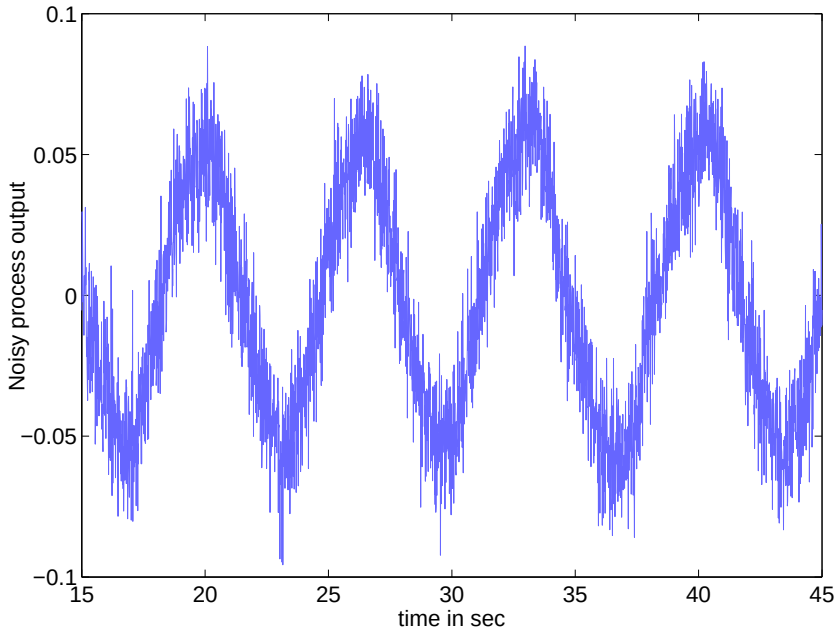

(5.6.1)

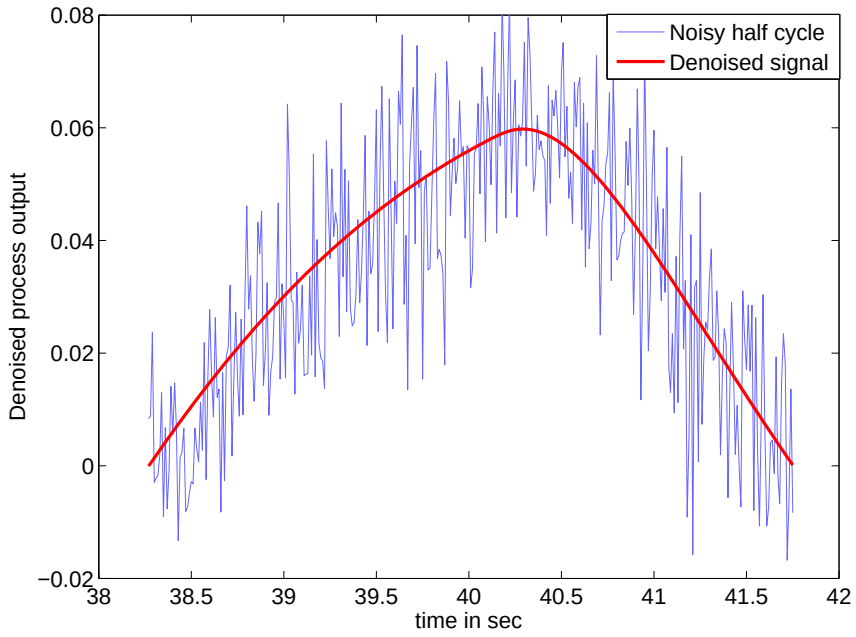

(5.6.2)

Figure 5.6: Noisy and denoised output signals

Example 2:

Let us consider the cascade system [58,59] that exhibits a significant high-order and nonminimum-phase dynamics with $G_1(s) = \frac{10(-5s+1)}{(30s+1)^3(10s+1)^2}e^{-5s}$ and $G_2(s) = \frac{3}{13.3s+1}e^{-3s}$. The measurements of $(t_0, t_1, t_p, t_2) = (25.078, 28.135, 100.578, 149.734)$ and $(h_{y2} = y_2(t_1), y_1(t_p), \dot{y}_2(t_1), \dot{y}_1(t_2)) = (0.0148, 0.0963, -0.0023, -0.0022)$ are obtained from a single relay experiment. The estimated process models, estimation errors and new PI/PID settings for the system are given in Table 5.2. Using Visioli et al.'s method [58], both the primary and secondary controllers $C_1(s)$=$0.11(1+\frac{1}{0.162.8s})$ and $C_2(s)$=$1.52(1+\frac{1}{9.41s}+2.18s)$, respectively are obtained from the open-loop step test and command signal generator for setpoint tracking. Sadasivarao and Chidambaram's method [59] suggests $C_1(s)$=$0.126(1+\frac{1}{84.595s}+31.811s)$ and $C_2(s)$=$1.516(1+\frac{1}{5.44s}+0.055s)$ for the cascade control system. The good identification with less computational efforts obtained by the proposed method is reflected by the superior controller performances, as shown in Fig. 5.7.

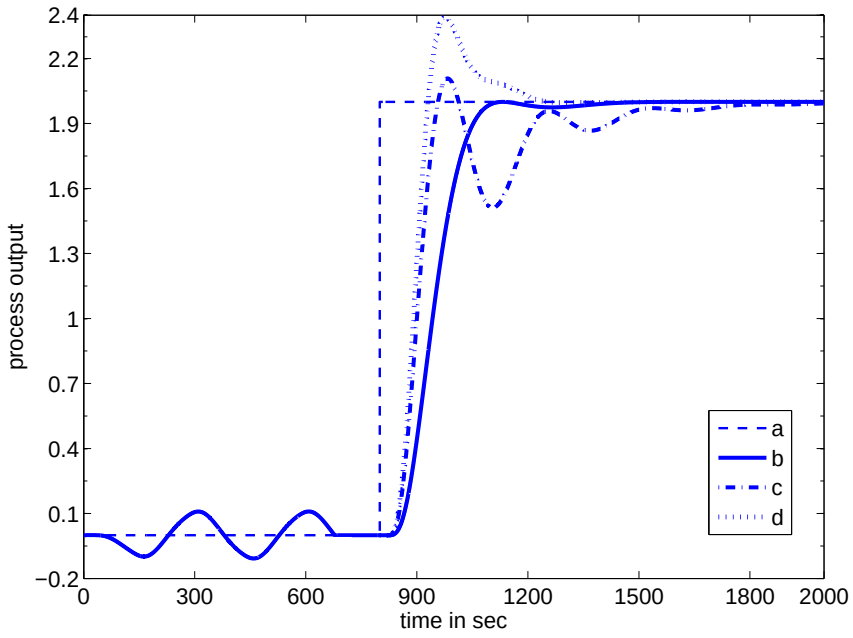

Figure 5.7: (a) Setpoint input, Process output by (b) proposed method, (c) Visioli et al.'s method and (d) Sadasivarao et al.'s method

To illustrate the robustness to parameter variations, assume that the time delay of the inner process is actually 20% larger and its time constant 20% smaller, i.e. $G_2(s) = \frac{3e^{-3.6s}}{10.6s+1}$. Visioli

et al.'s method cannot yield a bounded output and similarly Sadasivarao and Chidambaram's method is highly sensitive to the modelling errors which makes the system unstable. However, the responses by the proposed method as given in Fig. 5.8 show robust performances for the perturbed system.

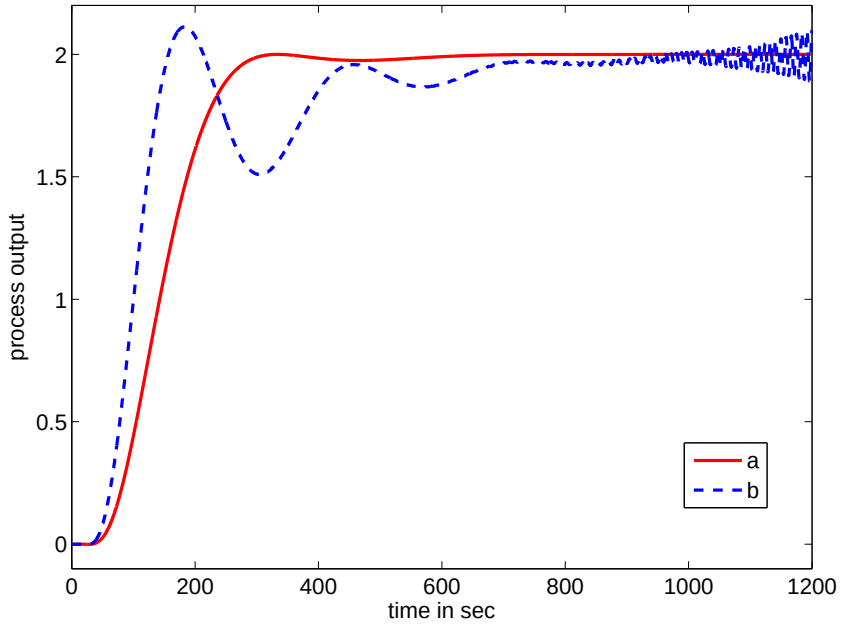

Figure 5.8: Perturbed system responses by (a) proposed method and (b) Visioli et al.'s method

5.5 Summary

A simple on-line technique for the automatic tuning of the cascade control systems has been developed to tune both the controllers simultaneously. Exact analytical expressions are derived for estimating process model parameters in terms of a few measurements made on half limit cycle outputs. This significantly reduces the time required for the relay test. The method gives the robustness against static load disturbances during the relay experiment, unlike the basic relay methods that requires to reset the relay height to obtain a symmetrical limit cycle output. Low estimation errors and the satisfactory performances shown in simulation study indicate the usefulness of the proposed technique.

CHAPTER 6

EXTENSION OF RELAY FEEDBACK TECHNIQUE FOR UNSTABLE PROCESSES WITH LARGE TIME DELAY

6.1 Introduction

The conventional relay feedback has become a widely accepted approach to system identification in process control. However, it has been shown that unlike stable processes, unstable FOPDT process under relay feedback produces limit cycle only when the ratio of time delay (θ) to unstable time constant (τ_1) is less than 0.693 [63, 86]. Many relay based techniques for stable processes have been presented in the literature, but a few methods have been discussed for an unstable FOPDT process. Kavdia and Chidambaram [65] have proposed an identification method for an unstable FOPDT process, but they did not suggest a satisfactory method for choosing the gain of the forward proportional (P) controller to make the system stable. Park et al. [66] have suggested an improved relay feedback method to obtain the ultimate data set using the describing function approach, but this yields erroneous results as the normalized dead time $\theta_n (= \theta/\tau_1)$ approaches 0.693. Ananth and Chidambaram [67] presented a step response based identification method for unstable processes using the PID controller. Majhi and Atherton [69] proposed an exact analytical method based on a single relay feedback test and the constraint was relaxed up to $\theta_n < 1.2$ by adding an internal proportional-derivative (PD) feedback. Marchetti et al. [8] have proposed a modified autotune variation method for unstable processes by using two

different unbiased relay tests. By using a single biased/unbiased relay feedback test, Liu and Gao [87] have presented an iterative algorithm for identifying the FOPDT model parameters. However, the constraint of their method is still the same as $\theta_n < 0.693$.

It is often desirable to extend the applicability of the relay feedback test for unstable processes with large time delay. This chapter presents: (i) the necessary conditions for the existence of limit cycles when a relay with hysteresis test is performed, (ii) a strategy to induce a sustained oscillation of the process output for $\theta_n < 2$, and (iii) a non-iterative method to estimate process dynamics information. The proposed stabilization concept is simple and also it retains the simplicity of the original relay feedback method. Again, a relay with hysteresis instead of an ideal relay is used to give the robust solution from a practical point of view so that the resultant system is less sensitive to measurement noise.

6.2 Necessary condition for existence of limit cycles

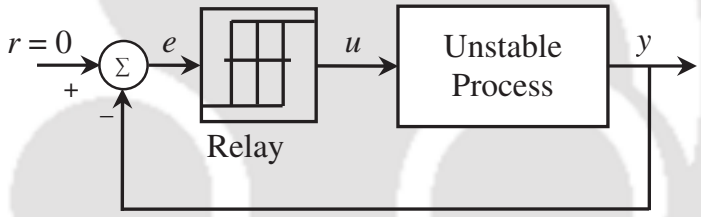

Figure 6.1: Conventional relay feedback structure

In this section, the conditions under which relay control can stabilize an open-loop unstable process are obtained using the exact analytical state-space method discussed in Chapter 2. We consider the process to be relay-stabilized if the output of the feedback process is bounded for all $t > 0$. Let the relay amplitudes be $\pm h$ and hysteresis widths be $\pm\varepsilon$ during a relay feedback test. Consider an unstable first order model as

$$G_p(s) = \frac{ke^{-\theta s}}{\tau_1 s - 1} \tag{6.1}$$

where $\tau_1 > 0$. Using the analytical expression derived in Section 2.3, the explicit state equation at time $t = t_1$ is written as

$$y(t_1) = A_1 = \varepsilon e^{\frac{\theta}{\tau_1}} - kh(1 - e^{\frac{\theta}{\tau_1}}) \tag{6.2}$$

where A_1 is the positive peak amplitude. It can be expressed as

$$e^{\frac{\theta}{\tau_1}} = \left(\frac{kh + A_1}{kh + \varepsilon}\right) \tag{6.3}$$

This gives a boundary condition as

$$\frac{\theta}{\tau_1} = \ln\left(\frac{kh + A_1}{kh + \varepsilon}\right) \tag{6.4}$$

Similarly, the expression of $y(t)$ can also be written for time range $t_1 \leq t \leq T$ as

$$y(t) = kh(1 - c_1 e^{\frac{t-t_1}{\tau_1}}) \tag{6.5}$$

using the analysis given in Section 2.2. At $t = t_1$ we obtain the peak amplitude

$$A_1 = kh(1 - c_1) = kh - 2kh/(1 + e^{\frac{T}{\tau_1}}) \tag{6.6}$$

After simplification we obtain

$$\tau_1 = T \ln\left(\frac{kh + A_1}{kh - A_1}\right)^{-1} \tag{6.7}$$

which gives one of the necessary condition for the limit cycle

$$kh > A_1 \tag{6.8}$$

Using the relations (6.8) and (6.4), the condition for the existence of a limit cycle can be written as

$$\theta_n < \ln\left(\frac{2kh}{kh + \varepsilon}\right) \tag{6.9}$$

This result is consistent with the findings for first order processes in [88] using the graphical and bifurcation analysis. When we substitute $\varepsilon = 0$ for an ideal relay case, the condition is

$$\theta_n < \ln(2) \quad \text{or} \quad \theta_n < 0.693 \tag{6.10}$$

which is the similar condition given in [16]. The relation (6.9) depends on the parameters h and ε and plotted in Fig. 6.2 assuming $k = 1$, giving $\theta_n < 0.693$. It is the maximum value of θ_n for a limit cycle exist as ε decreases to zero. The range of θ_n is enlarged maximum up to 0.693 for any value of h, as indicated by Fig. 6.2.

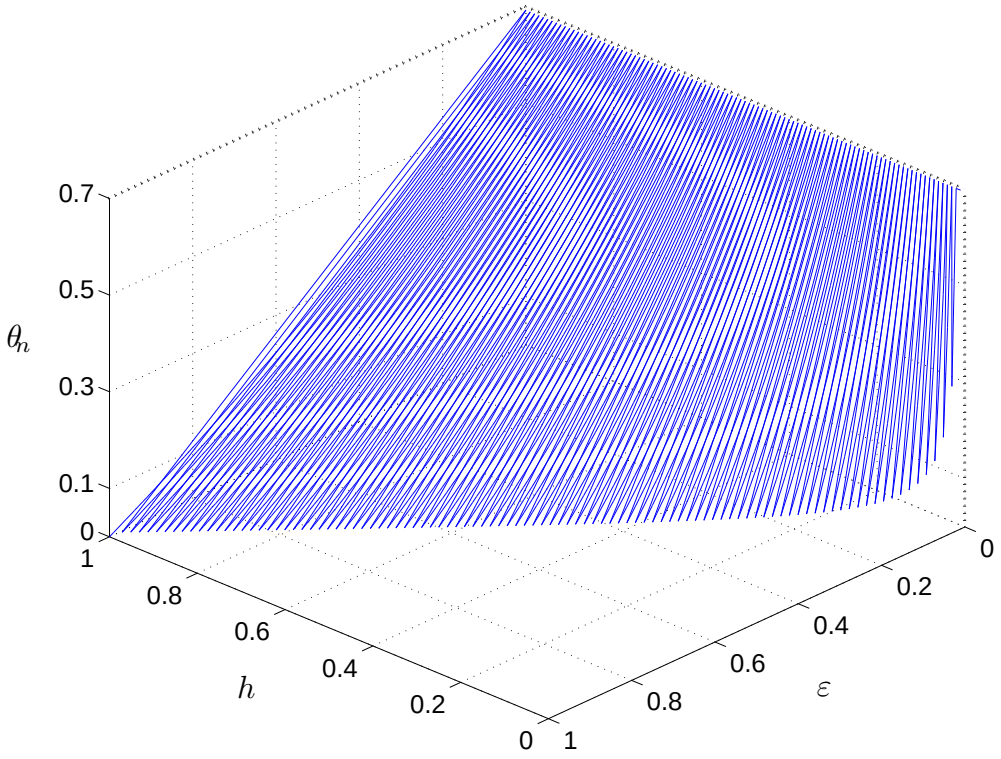

Figure 6.2: Relation of h, ε and θ_n for an unstable process

Similarly, the necessary condition for an unstable SOPDT process model can also be obtained using the state space analysis. Let us take an unstable SOPDT model by

$$G_p(s) = \frac{ke^{-\theta s}}{(\tau_1 s - 1)(\tau_2 s + 1)} \tag{6.11}$$

The state and output equation constants are

$$\mathbf{A} = \begin{bmatrix} \lambda_1 & 0 \\ 0 & \lambda_2 \end{bmatrix}; \quad \mathbf{b} = \begin{bmatrix} 1 \\ 1 \end{bmatrix}; \quad \mathbf{c} = \frac{k\lambda_1\lambda_2}{\lambda_1 - \lambda_2}[1 \quad -1] \tag{6.12}$$

where $\lambda_1 = 1/\tau_1$ and $\lambda_2 = -1/\tau_2$ are the eigenvalues of $\mathbf{A}$. If the amplitude of the output at time t_1 is A_1, then the expression of A_1 using (2.7) can be shown to be

$$A_1 = \mathbf{c}e^{\mathbf{A}\theta}\mathbf{x}(t_0) + \mathbf{c}\mathbf{A}^{-1}(e^{\mathbf{A}\theta} - \mathbf{I})\mathbf{b}h \tag{6.13}$$

When we determine the condition for existence of a limit cycle, the solution for $T \to \infty$ is examined. Also the constraint includes the case with an unstable time constant λ_1, a positive

constant and λ_2 a negative one and then (6.13) is solved by taking the value of T. (6.13) becomes

$$A_1 = \varepsilon e^{\lambda_1 \theta} - \frac{\lambda_1}{\lambda_2}(kh+\varepsilon)e^{\lambda_1 \theta} + (e^{\lambda_1 \theta} - 1)kh \tag{6.14}$$

Further simplification of (6.14) gives

$$kh + A_1 = (kh+\varepsilon)\left(1 - \frac{\lambda_1}{\lambda_2}\right)e^{\lambda_1 \theta} \tag{6.15}$$

But we know the condition $kh > A_1$ and by adding inequalities one gets the constraint for the existence of a limit cycle for the SOPDT model as

$$e^{\lambda_1 \theta} < a\left(\frac{2kh}{kh+\varepsilon}\right) \tag{6.16}$$

where $a = \tau_1/(\tau_1+\tau_2)$. Simplification of (6.16) gives

$$\theta_n < \ln\left(a\frac{2kh}{kh+\varepsilon}\right) \tag{6.17}$$

(6.17) is the necessary condition for existence of limit cycles for second order unstable processes.

6.3 Relay feedback system with PD controller

We have seen that under relay control the unstable process does not always experience a limit cycle, only exists for $\theta_n < 0.693$. This constraint can be relaxed by incorporating an additional PD controller [69] as illustrated in Fig. 6.3. Also it has been shown that a PI-PD controller design can provide excellent control performances for unstable processes. Let us derive the limit cycle equation when the PD controller is connected in an inner feedback loop during a relay feedback experiment. The dynamics of an unstable process may be described by the normalised form transfer function model

$$G_p(s) = \frac{ke^{-\theta_n s}}{s-1} \tag{6.18}$$

Hence, if the PD controller in Fig. 6.3 has the normalised transfer function

$$C(s) = K_c + K_d s \tag{6.19}$$

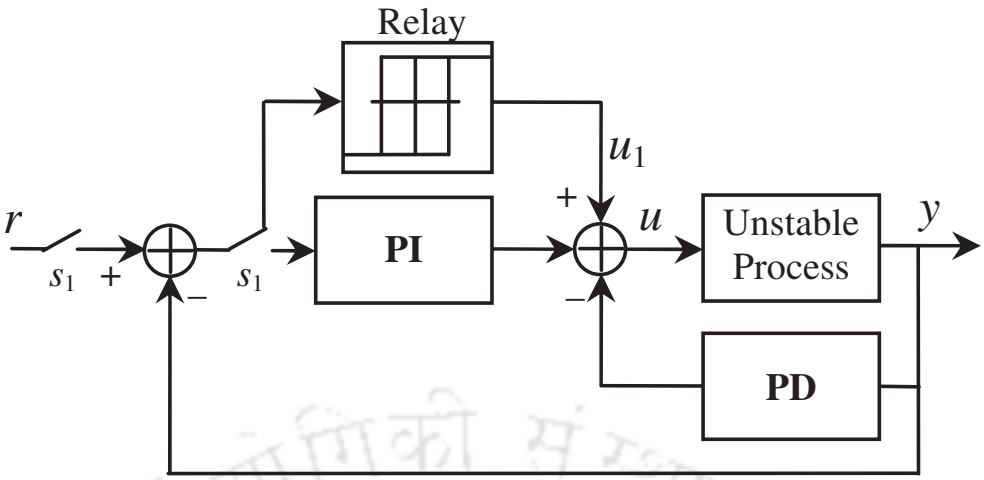

Figure 6.3: Relay feedback system with inner PD controller

where K_c and K_d denote the proportional and derivative gains of the controller, the closed-loop transfer function of the feedback control system (which the relay sees) is given by

$$\frac{y(s)}{u_1(s)} = \frac{k\, e^{-\theta_n s}}{s - 1 + k(K_c + K_d s)e^{-\theta_n s}} \tag{6.20}$$

Assume that the relay test induces a limit cycle output with a half period T by use of suitable choice of PD gains and the relay amplitude and hysteresis width of $\pm h$ and $\pm\varepsilon$, respectively. With hysteresis, relay switches at time $t = t_0$ when $y(t_0) = \varepsilon$. The state and output expressions for (6.20) in the time domain controllable canonical form can be written as

$$\begin{aligned} \dot{\mathrm{x}}(\mathrm{t}) &= \mathrm{x}(t) - k(u_1(t-\theta_n) - K_c y(t-\theta_n) - K_d \dot{y}(t-\theta_n)) \\ y(t) &= \mathrm{x}(t) \end{aligned} \tag{6.21}$$

The method explained in Section 4.2 is used to derive the solution of the state equation (6.21). At time $t = \theta_n + t_0$ the peak amplitude of the output is A_1 and the solution is obtained as

$$A_1 = \varepsilon e^{\theta_n} - kh + khe^{\theta_n} + k^2 hK_c e^{\theta_n} - k^2 hK_c\theta_n - k^2 hK_d\theta_n \tag{6.22}$$

Now, (6.22) can be expressed as

$$\theta_n = \log\left(\frac{A_1 + kh + k^2 hK_c\theta_n + k^2 hK_d\theta_n}{kh + \varepsilon + k^2 hK_c}\right) \tag{6.23}$$

(6.23) shows that θ_n is a function of (K_c, K_d) and vice versa. However, the process model parameters τ_1 and θ may not be known a priori for setting initial PD gains. Guidelines for initial settings of PD gains is discussed in the following section which considers guaranteed stability of the closed-loop relay control system.

6.4 Existence of sustained oscillations

The closed-loop characteristic equation from (6.20) becomes

$$F(s) = (s-1) + (k_c + k_d s)e^{-\theta_n s} = 0 \tag{6.24}$$

where $k_c = kK_c$ and $k_d = kK_d$ are assumed to be nonnegative. Aim is to obtain a pair (k_c, k_d) such that it gives a sustain oscillation during relay feedback test. If the process is delay-free i.e. $\theta_n = 0$; the characteristic function $F(s)$ is an algebraic polynomial which has a finite number of zeros. For $\theta_n > 0$; the characteristic function $F(s)$ is a quasi polynomial which has an infinite number of zeros. In [89], it has been shown that $F(s)$ can be represented by independent of θ_n using the D-partition technique which gives

$$F'(s) = (k_d^2 - 1)s^2 + (1 - k_c^2) = 0 \tag{6.25}$$

Detailed procedure for D-partition boundary technique is available in [89]. By solving (6.25), a pair of complex conjugate pure-imaginary zeros can be written as

$$s = \pm\omega, \quad \omega = \sqrt{-\frac{(1-k_c^2)}{(1-k_d^2)}} \tag{6.26}$$

and the D-partition boundaries at $\omega = 0$ and ∞ give $k_c = 1$ and $k_d = 1$, respectively. Now, (6.24) must satisfy following two equations simultaneously:

$$\begin{aligned} -1 + k_c\cos(\theta_n\omega) + \omega k_d \sin(\theta_n\omega) &= 0 \\ \omega - k_c\sin(\theta_n\omega) + \omega k_d \cos(\theta_n\omega) &= 0 \end{aligned} \tag{6.27}$$

The simple empirical relationship for θ_n obtained using (6.27) is

$$\theta_n = \omega^{-1}\tan^{-1}\left(\frac{\omega(k_c + k_d)}{k_c - k_d\omega^2}\right) \tag{6.28}$$

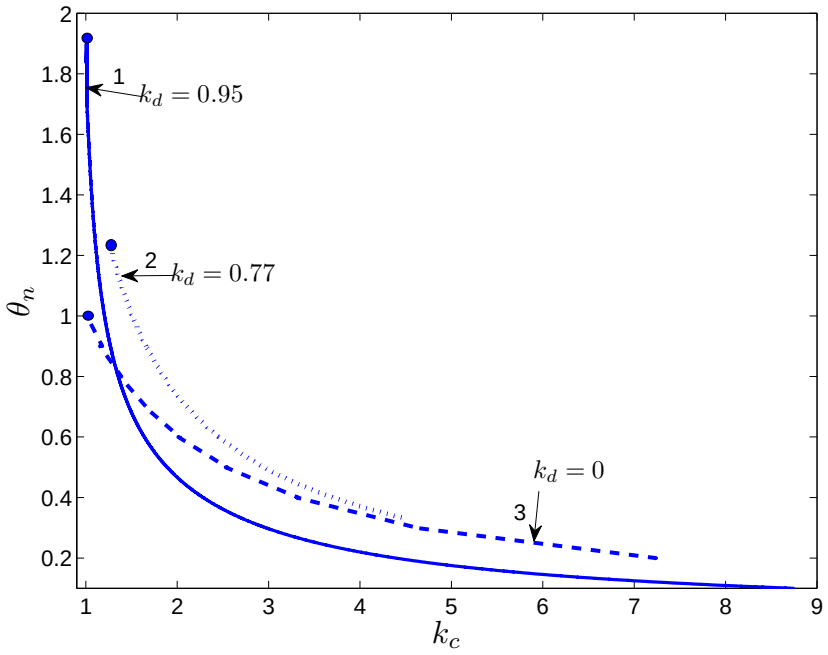

Figure 6.4: Maximum stability boundaries by: 1. Proposed method, 2. Majhi's method and 3. Park's method

Analysis of (6.23) and (6.28) for the existence of a sustained oscillation results in the stability boundaries as shown in Fig. 6.4 which are obtained with the help of extensive simulation study and [89]. It is observed that the initial PD setting of $(kc, k_d) = (1, 0.95)$ can stabilize the relay control system up to $\theta_n \leq 1.95$. Fig. 6.4 also shows the limitation of other reported methods. The stability condition of $k_c \geq 1$ and $\theta_n - 1 < k_d < 1$ for given arbitrary $\theta_n < 2$ is in agreement with [90].

6.5 Improved identification

In this section, to show the usefulness of the proposed stabilization technique, simple describing function (DF) analysis is used for identifying the process model parameters. We place the relay in tandem with the unstable process with inner PD controller to generate limit cycle output. The relay induces a permanent oscillation of the process output and the frequency and amplitude of the oscillation are used to identify an equivalent transfer function model of the processes using

the DF analysis [86]. The describing function specifies the change in the amplitude and phase of the fundamental component of the relay output with respects to its input assumed to be a pure sine wave. In DF analysis, the self-oscillation of the overall feedback system is of interest for estimation of the critical point (ultimate gain and ultimate frequency). Further, the relay is replaced with its equivalent DF and a self-sustained oscillation of amplitude, A_1 and frequency, ω_c are measured from the output. It is assumed that k is known a priori and initial setting of PD controller is $(K_c, K_d) = (1/k, 0.95/k)$. For Fig. 6.3, a relay with hysteresis induces the limit cycle output at frequency ω_c when

$$G_p(j\omega_c)[D_r + C(j\omega_c)] = -1 \tag{6.29}$$

where

$$D_r = \frac{4h}{\pi A_1^2}(\sqrt{A_1^2 - \varepsilon^2} - j\varepsilon) \tag{6.30}$$

is the DF of the relay with hysteresis. The proof of the above expression is given in the Appendix A.3.

Now, substitution of $G_p(j\omega_c)$ and $C(j\omega_c)$ in (6.29) gives

$$\frac{ke^{-j\omega_c\theta}}{j\omega_c\tau_1 - 1}(\alpha + j\beta) = -1 \tag{6.31}$$

where

$$\begin{aligned} \alpha &= \frac{4h}{\pi A_1^2}(\sqrt{A_1^2 - \varepsilon^2}) + K_c \\ \beta &= \omega_c K_d - \frac{4h\varepsilon}{\pi A_1^2} \\ \omega_c &= \pi/T \end{aligned} \tag{6.32}$$

By equating the real and imaginary parts of both side of (6.31), one obtains explicit expressions for τ_1 and θ as

$$\begin{aligned} \tau_1 &= \frac{\sqrt{k^2(\alpha^2+\beta^2) - 1}}{\omega_c} \\ \theta &= \frac{\tan^{-1}(\beta/\alpha) + \tan^{-1}(\omega_c\tau_1)}{\omega_c} \end{aligned} \tag{6.33}$$

6.6 Simulation study

Five processes, as tabulated in Table 6.1, are considered here. Assuming k is known or obtained by the method in [16]. Initially, setting an inner PD controller $(K_c, K_d) = (1/k, 0.95/k)$ the relay experiment is performed to obtain the limit cycle parameters like half period T and positive peak amplitude of the output A_1. Then, the unknown process model parameters τ_1 and θ are estimated using the explicit expressions in (6.33). As shown in Figs. 6.5 and 6.6, the Nyquist plots for the second order unstable processes in Examples 1 and 2 and the corresponding identified models illustrate the accuracy of the method near to the critical point. From the third example the conventional relay feedback method does not yield a limit cycle oscillation. It can be observed from Table 6.1 that the method not only yields a limit cycle for $\theta_n \geq 1.2$ but also helps to estimate accurate model parameters.

Table. 6.1: Results with the relay setting $(h, \varepsilon) = (0.1, 0.01)$

Example	Process	Measured values (T, A_1)	Estimated (τ_1, θ)
1	$\frac{e^{-0.1s}}{0.1s^2+0.9s-1}$	$(0.572, 0.017)$	$(1.281, 0.281)$
2	$\frac{e^{-0.5s}}{(0.5s+1)(2s-1)}$	$(2.089, 0.044)$	$(2.499, 1.005)$
3	$\frac{e^{-0.8s}}{s-1}$	$(1.065, 0.345)$	$(0.999, 0.799)$
4	$\frac{e^{-1.2s}}{s-1}$	$(1.914, 1.017)$	$(0.999, 1.199)$
5	$\frac{e^{-1.9s}}{s-1}$	$(11.208, 33.338)$	$(1.000, 1.900)$

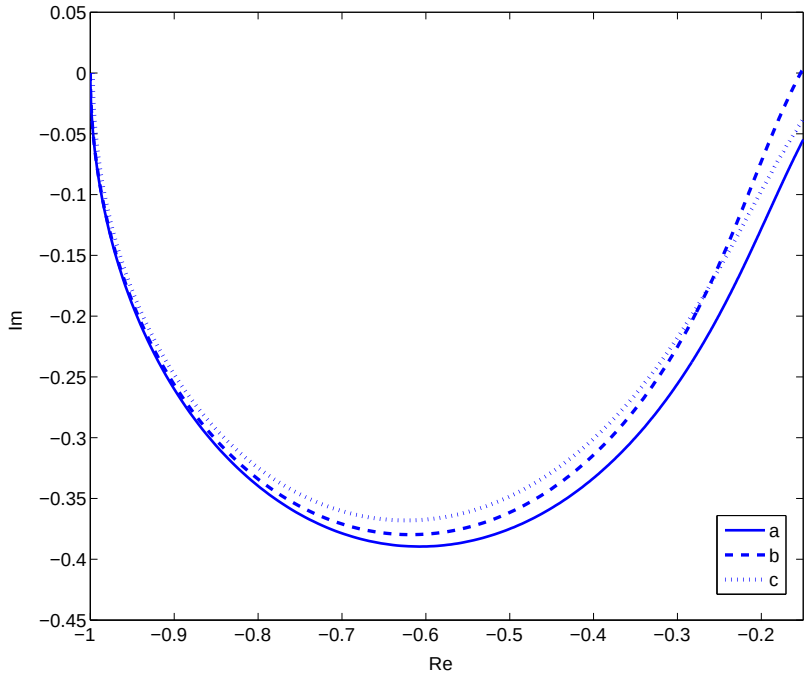

Figure 6.5: Nyquist plots for the process in Example 1 : (a) actual process, (b) proposed method and (c) Marchetti et al.'s method [8]

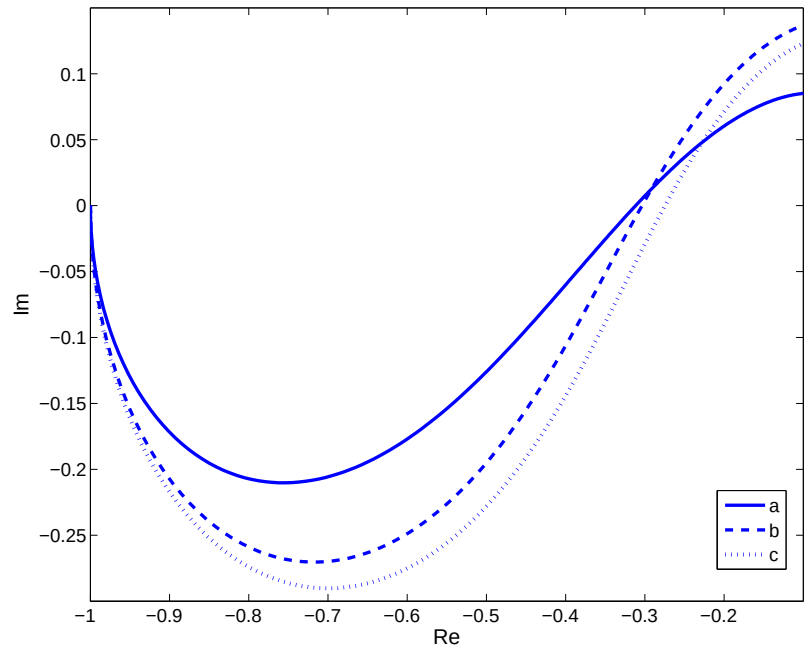

Figure 6.6: Nyquist plots for the process in Example 2 : (a) actual process, (b) proposed method and (c) Majhi's method [86]

6.7 Summary

General conditions are given for the existence of limit cycle for the unstable time delay processes under relay control. The proposed control strategy helps stabilise relay control system for unstable processes having θ_n up to 1.95. In addition, a relay with hysteresis is used to reduce chattering problem in the event of measurement noise unlike the reported methods that are based on an ideal relay and where applicability is restricted to $\theta_n < 1.2$. The non-iterative algorithm estimates exact model parameters (τ_1, θ) using only half cycle data of limit cycle output.

CHAPTER 7

CONCLUSIONS AND FUTURE WORK

7.1 Conclusions

Many research work on modifying the relay feedback auto-tuning method have been reported in recent years. Still there is much room for further improvement and extensions of such methods. In this thesis, several new results are obtained that improve the accuracy of identification, relay analysis, auto-tuning and cascade control. Briefly, the results are summarized as follows:

A. Identification of linear processes from the half limit cycle data

A class of processes with time delay is analyzed under relay feedback. The time-domain based explicit expressions for output limit cycle waveform are derived to identify the unknown process model parameters accurately. The method acquires more information about the process dynamics from only half limit cycle data. The procedure is not only simple but also obtains the process model parameters without solving any nonlinear equation or optimization problem unlike many relay based methods reported in the literature.

B. Identification of nonlinear processes with monotonic static gains

Apart from linear processes, the relay feedback approach can also be used for identifying nonlinear processes having static nonlinear gain. The extended approach can be used successfully to estimate the structure of nonlinear model and its parameters from a single symmetrical relay test. The analysis of a limit cycle waveform is shown by considering a hysteresis in the relay test, which may prevent the relay control from oscillating at high frequency and relay switching at wrong instants. The real-time laboratory experiment shows the practical applicability of the proposed method.

C. On-line relay auto-tuning for stable processes

The on-line relay method is presented to remove the effects of static load disturbances by the continuous action of the integral controller in the loop. The procedure allows the relay auto-tuning under tight continuous closed-loop control and estimates the process dynamics from the measured half cycle output. The PI controller can then be tuned based on the parametric model such that it preserves the actuator from the large variation of control signals and gives robustness with respect to process parameter variations. The application of a DC servo position control is experimentally tested by the proposed method. The experiment time for the auto-tuning test and performance of the transient response with less control signal variation prove its effectiveness.

D. On-line identification of cascade control systems based on half limit cycle data

The on-line relay method is extended for the auto-tuning of the cascade control system. The time-domain analysis for half cycle outputs is given to estimate the process model parameters. The approach reduces the time required for the relay test by simultaneously identifying both the inner and outer process dynamics. The improved results of the procedure is also proved with respect to measurement noise and process perturbation.

E. Extension of relay feedback technique for unstable processes with large time delay

The necessary condition for the existence of a limit cycle, when a relay with hysteresis test is performed, is developed. A simple control strategy using an inner PD loop is given with a suitable choice of PD gains such that the relay test produces a sustained oscillation for unstable processes with large time delay. The method not only stabilizes relay control systems for the normalize time delay up to 1.95 but also estimates the model parameters accurately.

7.2 Suggestions for Further Work

Following the design methods described in this thesis, a number of possible directions for extensions to this work are discussed below:

- It is natural and interesting at this point to see if the proposed relay analysis can be extended to other class of processes like underdamped and nonminimum phase. In addition, the limit cycle analysis with residual motion is important to be addressed in the design aspect.

- In the presented work, a relay with hysteresis is considered to overcome the problem due to measurement noise in a relay control system. Again the measured noisy limit cycle is successfully denoised using the described filtering technique. The results may be improved by inserting a low-pass filter in the feedback path. The analysis of the relay feedback together with the filter dynamics needs further investigation.

- The relay method is used to identify nonlinear processes with static nonlinearity. Study of nonlinear processes with other kind of nonlinearities such as discontinuous, dead zone and memory type, will be an interesting and useful area of research.

- It will be interesting if a general method for the on-line automatic tuning of stable, integrating and unstable processes can be proposed.

- Using the proposed on-line approach for the series cascade structure, the analysis for the parallel cascade structure may be carried out.

- There has been some work in the thesis about the existence and stability of limit cycles for unstable processes in relay feedback systems. Similar investigations may be carried out for processes with more than one integrator.

- Exact analytical methods for identification may be carried out for a multivariable system.

APPENDIX A

SUPPLEMENTARY MATERIALS

A.1 Detailed derivation of the expression (3.19)

A set of exact expressions of limit cycle output is derived to evaluate the process model parameters from measurements performed on a stable cycle under an asymmetrical relay test [16]. Let the Hammerstein-type process be subjected to an asymmetrical relay feedback when the input amplitudes are v_1 and $-v_2$. Fig. A.1 shows waveforms of the input and output signals of $G_p(s)$ under the relay control.

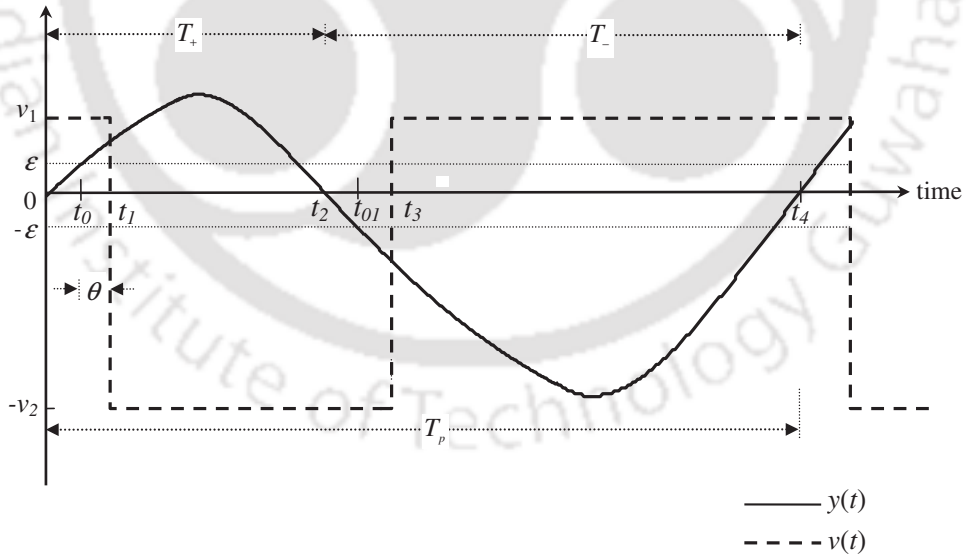

Figure A.1: Hammerstein model: Input and output signals of $G_p(s)$ under relay control

For the time range $t_0 \leq t \leq t_1$, where input is v_1, the state equation becomes

$$\mathbf{x}(t) = e^{\mathbf{A}(t-t_0)}\mathbf{x}(t_0) + \mathbf{A}^{-1}(e^{\mathbf{A}(t-t_0)} - \mathbf{I})\mathbf{b}v_1 \tag{A.1}$$

For the time range $t_1 < t \leq t_{01}$, where input is $-v_2$, the state equation is

$$\mathbf{x}(t) = e^{\mathbf{A}(t-t_1)}\mathbf{x}(t_1) - \mathbf{A}^{-1}(e^{\mathbf{A}(t-t_1)} - \mathbf{I})\mathbf{b}v_2 \tag{A.2}$$

For the time range $t_{01} < t \leq t_3$, where input is $-v_2$, the state equation is

$$\mathbf{x}(t) = e^{\mathbf{A}(t-t_{01})}\mathbf{x}(t_{01}) - \mathbf{A}^{-1}(e^{\mathbf{A}(t-t_{01})} - \mathbf{I})\mathbf{b}v_2 \tag{A.3}$$

For the time range $t_3 < t \leq t_4$, where input is v_1, the state equation is

$$\mathbf{x}(t) = e^{\mathbf{A}(t-T_+-t_1)}\mathbf{x}(t_3) + \mathbf{A}^{-1}(e^{\mathbf{A}(t-T_+-t_1)} - \mathbf{I})\mathbf{b}v_1 \tag{A.4}$$

Since $\mathbf{x}(T_p + t_0) = \mathbf{x}(t_0)$ for a selfoscillation condition, use of Eqs. (A.1 to A.4) yields an expression for the initial state

$$\mathbf{x}(t_0) = (\mathbf{I} - e^{\mathbf{A}T_p})^{-1}(e^{\mathbf{A}(T_p-t_1)}\mathbf{g_1}v_1 - e^{\mathbf{A}(T_p-T_+)}\mathbf{g_2}v_2 - e^{\mathbf{A}(T_p-T_+-t_1)}\mathbf{g_3}v_2 + \mathbf{g_4}v_1) \tag{A.5}$$

where

$$\mathbf{g_1} = \mathbf{A}^{-1}(e^{\mathbf{A}(t_1-t_0)} - \mathbf{I})\mathbf{b} \tag{A.6}$$

$$\mathbf{g_2} = \mathbf{A}^{-1}(e^{\mathbf{A}(T_+-t_1)} - \mathbf{I})\mathbf{b} \tag{A.7}$$

$$\mathbf{g_3} = \mathbf{A}^{-1}(e^{\mathbf{A}(t_3-t_{01})} - \mathbf{I})\mathbf{b} \tag{A.8}$$

$$\mathbf{g_4} = \mathbf{A}^{-1}(e^{\mathbf{A}(T_p-T_+-t_1)} - \mathbf{I})\mathbf{b} \tag{A.9}$$

The conditions for limit cycle require $y(t_0) = -y(t_{01}) = \varepsilon$; which can be written as

$$\mathbf{c}\mathbf{x}(t_0) = -\mathbf{c}\mathbf{x}(t_{01}) = \varepsilon \tag{A.10}$$

The state equation $\mathbf{x}(t_1)$ is obtained by putting $t = t_1$ in (A.1) and then using (A.5). Finally, the output expression for an asymmetrical limit cycle waveform during $t_1 < t \leq t_{01}$ using (3.18) and (A.2) becomes

$$y(t) = (v_1 + v_2)\, e^{-\frac{(t-t_1)}{\tau_1}}(d_1 + \frac{d_1(t-t_1)}{\tau_1} + \frac{d_2}{\tau_1}) - v_2 \tag{A.11}$$

where $d_1 = \frac{1-e^{-\frac{T_p-T_+}{\tau_1}}}{1-e^{-\frac{T_p}{\tau_1}}}$ and $d_2 = \frac{T_p\, e^{-\frac{T_p}{\tau_1}}\,(1-e^{-\frac{T_p-T_+}{\tau_1}})}{\left(1-e^{-\frac{T_p}{\tau_1}}\right)^2} - \frac{(T_p-T_+)\, e^{-\frac{T_p-T_+}{\tau_1}}}{\left(1-e^{-\frac{T_p}{\tau_1}}\right)}$. Likewise, the output expression for the time range $t_3 < t \leq t_4$ when the input is v_1 becomes

$$y(t) = v_1 - (v_1+v_2)\, e^{-\frac{(t-t_1)}{\tau_1}}(e_1 + \frac{e_1(t-t_1)}{\tau_1} + \frac{e_2}{\tau_1}) \tag{A.12}$$

where $e_1 = \frac{1-e^{-\frac{T_+}{\tau_1}}}{1-e^{-\frac{T_p}{\tau_1}}}$ and $e_2 = \frac{T_p\, e^{-\frac{T_p}{\tau_1}}\,(1-e^{-\frac{T_+}{\tau_1}})}{\left(1-e^{-\frac{T_p}{\tau_1}}\right)^2} - \frac{T_+\, e^{-\frac{T_+}{\tau_1}}}{\left(1-e^{-\frac{T_p}{\tau_1}}\right)}$.

A.2 Shape characteristics of function $f(v)$

It is assumed that the static nonlinear function $f(v)$ is continuous and monotone and therefore it can be illustrated by two possible shapes: concave up and concave down as shown in Fig. A.2. By definition, $f(v)$ is concave up if all of the tangents to the curve are below the graph of $f(v)$ and similarly, $f(v)$ is concave down if all of the tangents to the curve are above the graph of $f(v)$. The function can be approximated by second order polynomial if it is either concave up or concave down and so all the tangent lines appear on one of the side of $f(v)$ curve. In case of function having both type of shapes like concave up and down (Fig. A.2.3), the approximation is carried out with minimum fourth order of polynomial since tangents appear on both sides of $f(v)$.

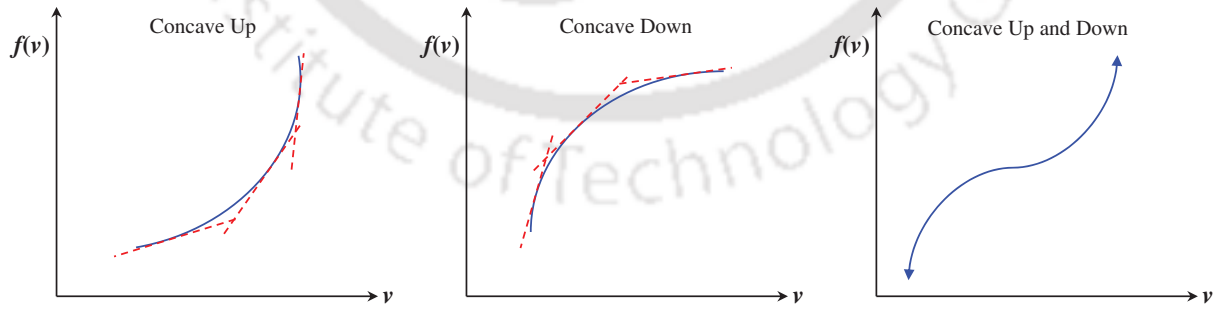

(A.2.1) (A.2.2) (A.2.3)

Figure A.2: Shape characteristics of function $f(v)$

A.3 Detailed derivation of the expression (6.30)

Let $e(t) = A_1 \sin(\omega t) = A_1 \sin(\varphi)$, where A_1 is the peak amplitude and ω is the fundamental frequency of the relay input signal. Due to hysteresis in a relay, the output of a relay $u(t)$ takes the value $+h$ or $-h$ according to whether e was greater than ε or less than $-\varepsilon$ on the last occasion when $|e| > \varepsilon$. The output of the relay is then

$$u(\varphi) = \begin{cases} -h & 0 < \varphi < \varphi_0 \\ h & \varphi_0 < \varphi < \pi + \varphi_0 \\ -h & \pi + \varphi_0 < \varphi < 2\pi \end{cases} \tag{A.13}$$

where $\varphi_0 = \sin^{-1}(\varepsilon/A_1)$. The describing function is obtained by considering only the principal harmonic of the relay output signal. Therefore, the relay is approximated by a gain of

$$D_r = \frac{1}{\pi A_1} \int_0^{2\pi} u(\varphi)(\sin\varphi + j\cos\varphi)\, d\varphi = \frac{1}{\pi A_1}(b_1 + j a_1) \tag{A.14}$$

where $a_1 = \int_0^{2\pi} u(\varphi)\cos\varphi\, d\varphi$ and $b_1 = \int_0^{2\pi} u(\varphi)\sin\varphi\, d\varphi$. The solution of these constants are obtained using (A.13).

$$\begin{aligned} a_1 &= \int_0^{\varphi_0} -h\cos\varphi\, d\varphi + \int_{\varphi_0}^{\pi+\varphi_0} h\cos\varphi\, d\varphi + \int_{\pi+\varphi_0}^{2\pi} -h\cos\varphi\, d\varphi \\ &= -4h\sin\varphi_0 \end{aligned} \tag{A.15}$$

Similarly,

$$\begin{aligned} b_1 &= \int_0^{\varphi_0} -h\sin\varphi\, d\varphi + \int_{\varphi_0}^{\pi+\varphi_0} h\sin\varphi\, d\varphi + \int_{\pi+\varphi_0}^{2\pi} -h\sin\varphi\, d\varphi \\ &= 4h\cos\varphi_0 \end{aligned} \tag{A.16}$$

Substituting a_1 and b_1 in (A.14) one gets

$$\begin{aligned} D_r &= \frac{4h}{\pi A_1}[\cos\varphi_0 - j\sin\varphi_0] \\ &= \frac{4h}{\pi A_1}[\cos(\sin^{-1}\varepsilon/A_1) - j\sin(\sin^{-1}\varepsilon/A_1)] \\ &= \frac{4h}{\pi A_1}[\sqrt{1-(\varepsilon/A_1)^2} - j\varepsilon/A_1] \end{aligned} \tag{A.17}$$

The simplification gives the DF of a relay with hysteresis as (6.30).

REFERENCES

[1] C. C. Yu, *Autotuning of PID Controllers: Relay Feedback Approach*. London: Springer-Verlag, 1999.

[2] Q. G. Wang, T. H. Lee, and C. Lin, *Relay feedback: Analysis, Identification and control*. London: Springer-Verlag, 2003.

[3] D. P. Atherton, "Relay autotuning: An overview and alternative approach," *Ind. Eng. Chem. Res.*, vol. 45, pp. 4075–4080, 2006.

[4] K. J. Åström and T. Hägglund, "Automatic tuning of simple regulators with specifications on phase and amplitude margins," *Automatica*, vol. 20, pp. 645–651, 1984.

[5] W. L. Luyben, "Derivation of transfer functions for highly nonlinear distillation columns," *Ind. Eng. Chem. Res.*, vol. 26, pp. 2490–2495, 1987.

[6] R. C. Chang, S. H. Shen, and C. C. Yu, "Derivation of transfer function from relay feedback systems," *Ind. Eng. Chem. Res.*, vol. 30, pp. 1530–1541, 1991.

[7] S. H. Shen, J. H. Wu, and C. C. Yu, "Use of biased-relay feedback for system identification," *AIChE*, vol. 42, pp. 1174–1180, 1996.

[8] G. Marchetti, C. Scali, and D. R. Lewin, "Identification and control of open loop unstable processes by relay methods," *Automatica*, vol. 37, pp. 2049–2055, 2001.

[9] K. Srinivasan and M. Chidambaram, "Modified relay feedback method for improved system identification," *Comp. Chem. Eng.*, vol. 27, pp. 727– 732, 2003.

[10] I. Kaya and D. P. Atherton, "Parameter estimation from relay autotuning with asymmetric limitcycle data," *J. Proc. Contr.*, vol. 11, pp. 429–439, 2001.

[11] I. Kaya, "Parameter estimation for integrating processes using relay feedback control under static load disturbances," *Ind. Eng. Chem. Res.*, vol. 45, pp. 4726–4731, 2006.

[12] K. K. Tan, T. H. Lee, S. Huang, K. Y. Chua, and R. Ferdous, "Improved critical point estimation using a preload relay," *J. Proc. Contr.*, vol. 16, pp. 445–455, 2006.

[13] P. K. Padhy and S. Majhi, "Relay based PI-PD design for stable and unstable FOPDT processes," *J. Comp. Chem. Eng.*, vol. 30, pp. 790–796, 2006.

[14] Q. G. Wang, C. C. Hang, and B. Zou, "Low order modeling from relay feedback systems," *Ind. Eng. Chem. Res.*, vol. 36, pp. 375–281, 1997.

[15] L. Wang, M. Desarmo, and W. R. Cluett, "Recursive estimation of process frequency response and step response from relay feedback experiments," *Automatica*, vol. 35, pp. 1427–1436, 1999.

[16] S. Majhi and D. P. Atherton, "Autotuning and controller design for processes with small time delay," *IEE Proc.-Contr. Theory Appl.*, vol. 146, pp. 415–424, 1999.

[17] S. Majhi, "Relay based identification of processes with time delay," *J. Proc. Contr.*, vol. 17, pp. 93–101, 2007.

[18] ——, "Relay-based identification of a class of nonminimum phase SISO processes," *IEEE Trans. Automatic Contr.*, vol. 52, pp. 134–139, 2007.

[19] S. Vivek and M. Chidambaram, "Identification using single symmetrical relay feedback test," *Comp. Chem. Eng.*, vol. 29, pp. 1625–1630, 2005.

[20] R. C. Panda and C. C. Yu, "Analytical expressions for relay feedback responses," *J. Proc. Contr.*, vol. 13, pp. 489–501, 2003.

[21] ——, "Shape factor of relay response curves and its use in autotuning," *J. Proc. Contr.*, vol. 15, pp. 893 –906, 2005.

[22] J. Lee, S. W. Sung, and T. F. Edgar, "Integrals of relay feedback responses for extracting process information," *AIChE*, vol. 53(9), pp. 2329 – 2338, 2007.

[23] T. Liu, F. Gao, and Y. Wang, "A systematic approach for on-line identification of second-order process model from relay feedback test," *AIChE*, vol. 54(6), pp. 1560–1578, 2008.

[24] T. Liu and F. Gao, "A generalized relay identification method for time delay and non-minimum phase processes," *Automatica*, vol. 45, pp. 1072–1079, 2009.

[25] H. C. Park, S. W. Sung, and J. Lee, "Modeling of hammerstein-wiener processes with special input test signals," *Ind. Eng. Chem. Res.*, vol. 45, pp. 1029–1038, 2006.

[26] W. L. Luyben and E. Eskinat, "Nonlinear auto-tune identification," *Int. J. Control*, vol. 59, pp. 595–626, 1994.

[27] M. W. Lee and H. P. Huang, "Identification and control of hammerstein-type nonlinear process," *J. Chin. Inst. Chem. Engrs.*, vol. 32(4), pp. 361–370, 2001.

[28] H. P. Huang, M. W. Lee, and Y. T. Tang, "Identification of wiener model using relay feedback test," *J. Chem. Eng. Japan*, vol. 31, pp. 604–612, 1998.

[29] H. P. Huang, M. W. Lee, and C. Y. Tasi, "Structure identification for block-oriented non-linear models using relay feedback tests," *J. Chem. Eng. Japan*, vol. 34, pp. 748–756, 2001.

[30] S. Sung and J. Lee, "Modeling and control of wiener type processes," *Chem. Eng. Sci.*, vol. 59, pp. 1515–1521, 2004.

[31] H. C. Park, D. G. Koo, J. H. Youn, J. Lee, and S. W. Sung, "Relay feedback approaches for the identification of hammerstein-type nonlinear processes," *Ind. Eng. Chem. Res.*, vol. 43, pp. 735–740, 2004.

[32] W. Lee, H. P. Haung, and J. C. Jeng, "Identification and controller design for nonlinear processes using relay feedback," *J. Chem. Eng. Japan*, vol. 37, pp. 1194–1206, 2004.

[33] S. W. Sung, "System identification method for hammerstein processes," *Ind. Eng. Chem. Res.*, vol. 41, pp. 4295–4302, 2002.

[34] J. C. Jeng, M. W. Lee, and H. P. Huang, "Identification of block-oriented nonlinear processes using designed relay feedback tests," *Ind. Eng. Chem. Res.*, vol. 44, pp. 2145–2155, 2005.

[35] S. W. Sung and J. Lee, "Relay feedback method under nonlinearity and static disturbance conditions," *Ind. Eng. Chem. Res.*, vol. 45, pp. 4028–4031, 2006.

[36] H. C. Park and J. Lee, "Step and pulse response methods for identification of wiener processes," *AIChE*, vol. 52(2), pp. 668–677, 2006.

[37] C. H. Je, J. Lee, S. W. Sung, and D. H. Lee, "Enhanced process activation method to remove harmonics and input nonlinearity," *J. Proc. Contr.*, vol. 19(2), pp. 353–357, 2009.

[38] A. Yoneya, "Identification of linear part of a plant having input nonlinearity using a limit cycle test," *J. Chem. Eng. Japan*, vol. 38(3), pp. 202–207, 2005.

[39] K. J. Åström and T. Hägglund, *PID Controllers: Theory, Design and Tuning*, NC, Ed. Instrument Society of America, Research Triangle Park, 1995.

[40] K. K. Tan, T. H. Lee, and X. Jiang, "Robust on-line relay automatic tuning of PID control system," *ISA Trans.*, vol. 39 (2), pp. 219–232, 2000.

[41] C. C. Hang, K. J. Åström, and W. K. Ho, "Relay auto-tuning in the presence of static load disturbance," *Automatica*, vol. 29(2), pp. 563–564, 1993.

[42] T. S. Schei, "A method for closed loop automatic tuning of PID controllers," *Automatica*, vol. 28 (3), pp. 587–591, 1992.

[43] K. K. Tan, R. Ferdous, and S. Huang, "Closed-loop automatic tuning of PID controller for nonlinear systems," *Chem. Eng. Sci.*, vol. 57, pp. 3005–3011, 2002.

[44] W. K. Ho, Y. Honga, A. Hanssonb, H. Hjalmarssonc, and J. W. Denga, "Relay auto-tuning of PID controllers using iterative feedback tuning," *Automatica*, vol. 39, pp. 149–157, 2003.

[45] S. Majhi, "On-line PI control of stable processes," *J. Proc. Contr.*, vol. 15, pp. 859–867, 2005.

[46] T.-S. Tsay, "On-line computing of PI/lead compensators for industry processes with gain and phase specifications," *Comp. Chem. Eng.*, vol. 33, pp. 1468–1474, 2009.

[47] A. O'Dwyer, *Handbook of PI and PID Controller Tuning Rules*. Imperial College Press, 2003.

[48] M. Kano and M. Ogawa, "The state of art in advanced process control in japan," in *IFAC Symposium ADCHEM2009*, Istanbul, Turkey, 2009.

[49] G. Buckbee, "Poor controller tuning drives up valve costs," *Control Magazine*, vol. 15, pp. 47–51, 2002.

[50] S. Skogestad, "Simple analytic rules for model reduction and PID controller tuning," *J. Proc. Contr.*, vol. 13, pp. 291–309, 2003.

[51] P. Klan and R. Gorez, "On aggressiveness of PI control," in *16-th IFAC World Congress, Praha*, 2005.

[52] L. W. Luyben, *Process Modeling, Simulation, and Control For Chemical Engineers*, 2nd Edition, Ed. McGraw-Hill, 1996.

[53] C. C. Hang, A. P. Loh, and V. U. Vasani, "Relay feedback auto-tuning of cascade controllers," *IEEE Trans. Control Syst. Tech.*, vol. 2 (1), pp. 42–45, 1994.

[54] K. K. Tan, T. H. Lee, and R. Ferdous, "Simultaneous online automatic tuning of cascade control for open loop stable process." *ISA Trans.*, vol. 39, pp. 233–243, 2000.

[55] S. H. Song, W. J. Cai, and Y. G. Wang, "Auto-tuning of cascade control systems," *ISA Tran.*, vol. 42 (1), pp. 63–72, 2003.

[56] I. Kaya, N. Tan, and D. Atherton, "Improved cascade control structure for enhanced performance," *J. Proc. Contr.*, vol. 17 (1), pp. 3 – 16, 2007.

[57] Y. Lee, S. Oh, and S. Park, "Enhanced control with a general cascade control structure," *Ind. Eng. Chem. Res.*, vol. 41, pp. 2679 – 2688, 2002.

[58] A. Visioli and A. Piazzi, "An automatic tuning method for cascade control systems," in *Proceedings of the 2006 IEEE International Conference on Control Applications, Munich, Germany*, 2006, pp. 2968 - 2973.

[59] M. V. Sadasivarao and M. Chidambaram, "PID controller tuning of cascade control systems using genetic algorithm," *J. Indian Inst. Sci.*, vol. 86, pp. 343–354, 2006.

[60] V. M. Alfaro, R. Vilanova, and O. Arrieta, "Robust tuning of two-degree-of-freedom (2-DoF) PI/PID based cascade control systems," *J. Proc. Contr.*, vol. 19, pp. 1658–1670, 2009.

[61] Y. Lee, M. Skliar, and M. Lee, "Analytical method of PID controller design for parallel cascade control," *J. Proc. Contr.*, vol. 16, pp. 809–818, 2006.

[62] A. S. Rao, S. Seethaladevi, S. Uma, and M. Chidambaram, "Enhancing the performance of parallel cascade control using Smith predictor," *ISA Trans.*, vol. 48, pp. 220–227, 2009.

[63] D. P. Atherton, "Improving accuracy of autotuning parameter estimation," in *Proc. IEEE Int. Conference. on Control Applications*, Hartford, USA, 1997, pp. 51 – 56.

[64] S. Majhi and D. P. Atherton, "Autotuning and controller design for unstable time delay processes," in *Proceedings of IEE Conference CONTROL'98, UKACC, UK*, 1998, pp. 769–774.

[65] M. Kavdia and M. Chidambaram, "On-line controller tuning for unstable systems," *Comp. Chem. Eng.*, vol. 20(3), pp. 301–305, 1996.

[66] J. H. Park, S. W. Sung, and I. Lee, "An enhanced PID control strategy for unstable processes," *Automatica*, vol. 34(6), pp. 751–756, 1998.

[67] I. Ananth and Chidambaram, "Closed loop identification of transfer function model for unstable process," *J. Franklin Inst.*, vol. 336(7), pp. 1055–1061, 1999.

[68] R. P. Sree and M. Chidambaram, "Improved closed loop identification of transfer function model for unstable systems," *J. Franklin Inst.*, vol. 342(2), pp. 152–160, 2006.

[69] S. Majhi and D. P. Atherton, "Online tuning of controllers for an unstable FOPDT process," *IEE Proc. - Contr. Theory Appl*, vol. 147(4), pp. 421–427, 2000.

[70] T. Liu and F. Gao, "Identification of integrating and unstable processes from relay feedback," *Comp. Chem. Eng.*, vol. 32, pp. 3038–3056, 2008.

[71] W. Li, E. Eskinat, and W. L. Luyben, "An improved autotune identification method," *Ind. Eng. Chem. Res.*, vol. 30, pp. 1530–1541, 1991.

[72] W. L. Luyben, "Getting more information from relay feedback tests," *Ind. Eng. Chem. Res.*, vol. 40, pp. 4391–4402, 2001.

[73] V. Ramakrishnan and M. Chidambaram, "Estimation of a SOPTD transfer function model using a single asymmetrical relay feedback test," *Comp. Chem. Eng.*, vol. 27, pp. 1779–1784, 2003.

[74] A. Savitzky and M. J. E. Golay, "Smoothing and differentiation of data by simplified least squares procedures," *Analytical Chemistry*, vol. 36(2), pp. 16–27, 1964.

[75] S. J. Orfanidis, *Introduction to Signal Processing*, N. Englewood Cliffs, Ed. Prentice-Hall, 1996.

[76] I. Boiko, "Autotune identification via the locus of a perturbed relay system approach," *IEEE Trans. Control Syst. Tech.*, vol. 16(1), pp. 182–185, 2008.

[77] C. C. Hang, K. J. Åström, and Q. G. Wang, "Relay feedback autotuning of process controllers - a tutorial review," *J. Proc. Contr.*, vol. 12, pp. 143–162, 2002.

[78] E. Eskinat, S. H. Johnson, and W. L. Luyben, "Use of hammerstein models in identification of nonlinear systems," *AIChE*, vol. 37(2), pp. 255–268, 2002.

[79] A. Balestrino, A. Landi, M. Zmirli, and L. Sani, "Automatic nonlinear auto-tuning method for hammerstein modeling of electrical drives," *IEEE Trans. Ind. Elect.*, vol. 48(3), pp. 645–655, 2001.

[80] "Feedback Instruments Ltd., Process Control Simulator PCS327," FI Ltd., Crowborough, England., Tech. Rep.

[81] G. H. M. Arruda and P. R. Barros, "Relay-based gain and phase margins PI controller design," *IEEE Trans. Instrum. Meas.*, vol. 52 (5), pp. 1548–1553, 2003.

[82] M. Zhuang and D. P. Atherton, "Automatic tuning of optimum PID controllers," *IEE Proc.-Contr. Theory Appl.*, vol. 140, pp. 216–224, 1993.

[83] T. Hägglund, "Automatic detection of sluggish control loops," *Control Eng. Pract.*, vol. 7, pp. 1505 – 1511, 1999.

[84] W. Tan, J. Liu, T. Chenb, and H. J. Marquez, "Comparison of some well-known pid tuning formulas," *Comp. Chem. Eng.*, vol. 30, pp. 1416–1423, 2006.

[85] AN221E04, *Datasheet, "Dynamically Reconfigurable FPAA", http://www.anadigm.com*, FPAA.

[86] S. Majhi, *Advance Control Theory - A Relay Feedback Approach*. Cengage Learning, 2009.

[87] T. Liu and F. Gao, "Alternative identification algorithms for obtaining a first-order stable/unstable process model from a single relay feedback test," *Ind. Eng. Chem. Res.*, vol. 47, pp. 1140–1149, 2008.

[88] T. Co, "Relay-stabilization and bifurcations of unstable SISO processes with time delay," *IEEE Trans. Automatic Contr.*, vol. 55(5), pp. 1131–1141, 2010.

[89] C. Hwang and J. H. Hwang, "Stabilisation of first-order plus dead-time unstable processes using PID controllers," *IEE Proc.-Contr. Theory Appl.*, vol. 151(1), pp. 89–94, 2004.

[90] C. Xiang, Q. G. Wang, X. Lu, L. A. Nguyen, and T. H. Lee, “Stabilization of second-order unstable delay processes by simple controllers,” *J. Proc. Contr.*, vol. 17, pp. 675–682, 2007.